UNIVERSITY OF SOUTHAMPTON

FACULTY OF NATURAL AND ENVIRONMENTAL SCIENCES

School of Ocean and Earth Science

Coccolithophores in high latitude and Polar regions: Relationships between community composition, calcification and environmental factors

by

Anastasia Charalampopoulou

Thesis for the degree of Doctor of Philosophy

July 2011

UNIVERSITY OF SOUTHAMPTON

ABSTRACT

FACULTY OF NATURAL AND ENVIRONMENTAL SCIENCES
SCHOOL OF OCEAN AND EARTH SCIENCE

Doctor of Philosophy

COCCOLITHOPHORES IN HIGH LATITUDE AND POLAR REGIONS: RELATIONSHIPS BETWEEN COMMUNITY COMPOSITION, CALCIFICATION AND ENVIRONMENTAL FACTORS

by Anastasia Charalampopoulou

Coccolithophores are a unique group of calcifying phytoplankton that dominate pelagic biogenic calcification and facilitate carbon export. Changes in coccolithophore calcite production through changes in their abundance, species distribution or cellular calcification could affect the oceanic carbon cycle. Ocean acidification, global warming and future changes in nutrient and light conditions might affect coccolithophore populations. This study investigated the relationships between coccolithophore distribution and calcification and environmental factors, between the North Sea and the Arctic Ocean and in the Southern Ocean. Large gradients in carbonate chemistry and other variables provided insights into coccolithophore response to concurrent changes in the future ocean.

Freshwater inputs and biological processes were driving the carbonate chemistry changes in the surface waters of the North Sea, the Norwegian Sea and the Svalbard Arctic region. Even though biological processes seemed to play a major role in shaping the saturation state ($\Omega_{calcite}$) and pH of these regions, the carbonate chemistry of the freshwater sources (Baltic Sea, sea-ice melt, riverine input/ terrestrial runoff) was also important and had accentuated the effects of biological activity.

A multivariate approach showed that changes in pH and mixed layer irradiance explained most of the variation in coccolithophore distribution and community composition between the North Sea and Svalbard. Differences between the Svalbard population (dominated by the family Papposphaeraceae) and those from other regions were mostly explained by pH, whereas mixed layer irradiance explained most of the variation between the North Sea, Norwegian Sea and Arctic water assemblages. Estimates of cell specific calcification rates showed that species composition can considerably affect community calcification.

At Drake Passage, the coccolithophore community was dominated by *Emiliania huxleyi* B/C. Diversity and abundance were highest in the Subantarctic and Polar Frontal Zones, respectively, where temperature and mixed layer irradiance were high. Community and cell specific calcification, as well as coccolith production rates, showed an overall decreasing trend towards Antarctica and were correlated with the strong latitudinal gradients in temperature and $\Omega_{calcite}$ and anti-correlated with nutrient concentrations. Additionally, coccolith production rates and cell specific calcification were also correlated with mixed layer irradiance.

Coccolithophore calcification rates at Svalbard and at Drake Passage were low compared to other oceanic regions. At Svalbard, the low calcification rates were the result of very low abundances of species that have both a low (e.g. Papposphaeraceae) and high (e.g. *Coccolithus pelagicus*) calcite content. At Drake Passage low calcification rates were the result of low to moderate abundances of *E. huxleyi* B/C, which has a low calcite content.

The results of this study suggest that changes in future pelagic calcite production may result from physiological changes acting on single species and/or from shifts in the species composition of coccolithophore assemblages, as well as poleward biome migrations induced by ocean acidification, sea surface warming and stratification.

Table of contents

List of figures

List of Tables

DECLARATION OF AUTHORSHIP

I, Anastasia Charalampopoulou, declare that the thesis entitled:

'Coccolithophores in high latitude and Polar regions: Relationships between community composition, calcification and environmental factors'

and the work presented in the thesis are both my own, and have been generated by me as the result of my own original research. I confirm that:

- this work was done wholly or mainly while in candidature for a research degree at this University;
- where any part of this thesis has previously been submitted for a degree or any other qualification at this University or any other institution, this has been clearly stated;
- where I have consulted the published work of others, this is always clearly attributed;
- where I have quoted from the work of others, the source is always given. With the exception of such quotations, this thesis is entirely my own work;
- I have acknowledged all main sources of help;
- where the thesis is based on work done by myself jointly with others, I have made clear exactly what was done by others and what I have contributed myself;
- Part of this work (Chapter 3) has been published as:

  Charalampopoulou A, Poulton AJ, Tyrrell T, Lucas MI (2011) Irradiance and pH affect coccolithophore community composition on a transect between the North Sea and the Arctic Ocean. Marine Ecology Progress Series 431:25-43

Signed: ……..

Date:…….

Acknowledgments

Firstly, I would like to thank my supervisors Toby Tyrrell, Alex Poulton and Mike Lucas for making this work possible and providing helpful advice and guidance during the course of my PhD. Additional thanks go to Mike Lucas, my sea-going supervisor, for his invaluable help during the research cruises.

I would also like to acknowledge the help of all the people involved in the ICE-CHASER cruise. The captain, officers and crew of the RRS *James Clark Ross*; the principal scientist Ray Leakey; Estelle Dumont and Colin Griffiths for the CTD and underway data; Tim Brand for the nutrient data.

Also, I would like to thank the people involved in the JC31 cruise. The captain, officers and crew of the RRS *James Cook*, the principal scientist Elaine McDonagh; Dave Hamersley for the CTD data; Mark Stinchcombe and the nutrients team (Glaucia Berbel and Maria Salta) for the nutrient data; Dorothee Bakker and the CO_2 team (Elizabeth Jones and Jennifer Riley) for the carbonate chemistry data; Sally Close and Gavin Evans for their help with the determination of frontal positions; Louise Darroch from BODC for helping out with data calibrations.

There is a number of people at NOC that I would also like to thank. Stephanie Henson and Mark Moore for their advice on irradiance calculations; Richard Pearce for his help with the scanning electron microscope; Duncan Purdie for his help with chl-a analysis; Patrick Holligan, Sinhue Torres-Valdes and Stuart Painter for useful discussions. Also my friends Jen Riley, Cynthia Dumousseaud, Ibrahim Mohammed and many others for their support and their willingness to listen!

Finally, I would like to thank my parents, Agathoklis and Niki, and my family for their unconditional love and support throughout the course of my studies. Special thanks go to Rob, for his love, support and patience, without which this thesis would not have been possible.

List of abbreviations

ACC	Antarctic Circumpolar Current
ARCT	Arctic influenced waters
AZ	Antarctic Zone
cell-CF	Cell specific calcification
CF	Calcification
CNS	central North Sea
CTD	Conductivity Temperature Depth
CZ	Continental Zone
DIC	Dissolved Inorganic Carbon
DSL	Distal Shield Length
E_0	Instantaneous PAR irradiance just below the sea surface
$E_{\text{above surface}}$	Instantaneous PAR irradiance above the sea surface
EC	English Channel
ECcast	CTD station at the English Channel
E_{MLD}	Average mixed layer irradiance
E_z	Downward PAR irradiance at depth z
HOL	Holococcolithophore
ICE	Ice station
k_{490}	light attenuation coefficient at 490 nm wavelength
k_d	vertical attenuation coefficient for PAR for downward irradiance
LOF	CTD station off Lofoten Islands
MDS	Non-metric Multi-Dimensional Scaling analysis
MIZ	Marginal Ice Zone station
MLD	Mixed Layer Depth
NNS	Northern North Sea
NNScast	CTD station at the northern North Sea
NORW	Norwegian Sea
PAR	Photosynthetically Active Radiation
PC	Principal Component
PCA	Principal Component Analysis

pCO_2	Partial pressure of CO_2
PF	Polar Front
PFZ	Polar Frontal Zone
PIC	Particulate Inorganic Carbon
POC	Particulate Organic Carbon
PP	Primary Production
PS	Photosynthesis
RIP	Rijpfjorden station
SACCF	Southern Antarctic Circumpolar Current Front
SAF	Subantarctic Front
SAZ	Subantarctic Zone
SB	Southern Boundary of the Antarctic Circumpolar Current
SNS	Southern North Sea
SNScast	CTD station at the southern North Sea
SS1	Shelf Station 1
STF	Subtropical Front
SVAL	Svalbard
TA	Total Alkalinity
VINDTA 3C	Versatile Instrument for the Determination of Titration Alkalinity
z	Depth (m)
Z_{eu}	Euphotic zone depth
ΔDIC_{CaCO3}	Deficit in DIC attributed to calcium carbonate precipitation or dissolution
$\Delta DIC_{deficit}$	Deficit in DIC
ΔDIC_{org}	Deficit in DIC attributed to organic matter production
$\Delta DIC_{residual}$	Residual of the DIC deficit
$\Delta DIC_{salinity}$	Deficit in DIC attributed to salinity changes
$\Delta TA_{deficit}$	Deficit in TA
ΔTA_{org}	Deficit in TA attributed to organic matter production
$\Delta TA_{residual}$	Residual of the TA deficit
$\Delta TA_{salinity}$	Deficit in TA attributed to salinity changes
$\Delta\sigma_t$	Difference in sigma density
$\Omega_{aragonite}$	Aragonite saturation state
$\Omega_{calcite}$	Calcite saturation state

Chapter 1: General Introduction

1.1 Biogeochemical role of coccolithophores

Coccolithophores are a unique group of phytoplankton that secrete calcite scales (coccoliths) to form a shell (coccosphere) around their cell. They contribute to both the organic carbon pump via photosynthesis and to the carbonate counter pump via calcification, and thus they may act as a smaller sink or even a source of CO_2 (Purdie & Finch 1994). Moreover, coccolithophores may facilitate the transfer of organic carbon from the surface to the deep ocean as a result of the "ballast effect" imparted by their coccoliths (Klaas & Archer 2002). They can contribute up to 20% of total primary production in selected oceanic regions (Poulton et al. 2007, 2010) and produce high numbers of coccoliths, thus dominating (50 – 80%) pelagic biogenic calcification (Milliman 1993, Broecker & Clark 2009). Therefore, coccolithophores have a significant role in carbon export and changes in coccolithophore calcite production through changes in their abundance or cellular calcification could affect the oceanic carbon cycle. Global warming and the resulting increased stratification is expected to reduce future nutrient concentrations and increase light availability, which may modify phytoplankton biogeography with biomes extending polewards (Sarmiento et al. 2004) and a poleward shift of marine export production (Bopp et al. 2001). Direct chlorophyll measurements of over 70 years, also suggest a declining trend in phytoplankton associated with global warming (Boyce et al. 2010). Ocean acidification is also expected to have an impact on phytoplankton (see review by Boyd et al. 2010) and many research studies have focused on the effect on coccolithophores, due to the potential vulnerability of calcifying organisms to changes in carbonate chemistry (Orr et al. 2005).

1.2 Carbonate chemistry changes

Since the industrial revolution atmospheric CO_2 has increased from a pre-industrial level of 280 ppm to the present level of 390 ppm (Figure 1.1). The rise in atmospheric CO_2 would have been even greater had it not been buffered by the oceans

that have absorbed about 25% of this fossil-fuel effluent (Zeebe et al. 2008), resulting in a decrease in oceanic pH (Figure 1.1; Doney et al. 2009).

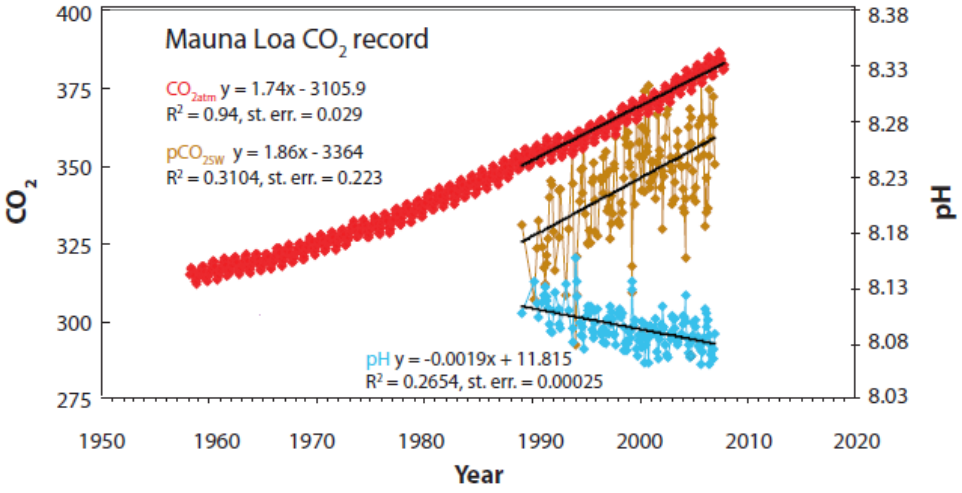

Figure 1.1 Time series of atmospheric CO_2 at Mauna Loa (ppmv) and surface ocean pH and pCO_2 (µatm) at Ocean Station ALOHA in the subtropical North Pacific Ocean. Adapted from Doney et al. (2009).

1.2.1 The carbonate system

Dissolved carbon exists in the ocean in three different inorganic forms: as aqueous carbon dioxide, CO_2 (aq), as bicarbonate ions, HCO_3^-, and as carbonate ions, CO_3^{2-}. When CO_2 reacts with seawater it initially forms carbonic acid (H_2CO_3), however its concentration is much lower than that of CO_2, and is usually ignored because it is quantitatively insignificant. These species are in thermodynamic equilibrium in seawater and, to some extent, with the atmospheric gaseous carbon dioxide, CO_2 (g):

$$\begin{array}{l} CO_2\ (g) \\ \Updownarrow \\ H_2O + CO_2\ (aq) \leftrightarrow H_2CO_3\ (aq) \leftrightarrow H^+\ (aq) + HCO_3^-\ (aq) \\ \qquad\qquad\qquad\qquad\qquad\qquad\qquad\qquad \Updownarrow \\ \qquad\qquad\qquad\qquad\qquad\qquad\qquad\qquad H^+\ (aq) + CO_3^{2-}\ (aq) \end{array} \qquad (1.1)$$

The sum of the dissolved forms CO_2 (aq), HCO_3^- and CO_3^{2-} is the total dissolved inorganic carbon (DIC). In seawater, ~91% of DIC is HCO_3^-, ~8% is CO_3^{2-} and only ~1% is CO_2.

Three other variables of the carbonate system are total alkalinity (TA), pH and partial pressure of CO_2 (pCO_2). TA is defined by Dickson (1981) as:

'The number of moles of hydrogen ion equivalent to the excess of proton acceptors (bases formed from weak acids with a dissociation constant $K \leq 10^{-4.5}$ at 25°C and zero ionic strength) over proton donors (acids with $K \geq 10^{-4.5}$) in 1 kg of seawater'

$$TA = [HCO_3^-] + 2[CO_3^{2-}] + [B(OH)_4^-] + [OH^-] + [HPO_4^{2-}] + 2[PO_4^{3-}] + [SiO(OH)_3^-] + [NH_3] + [HS^-] - [H^+]_F - [HSO_4^-] - [HF] - [H_3PO_4] \quad (1.2)$$

The brackets represent total concentrations of these constituents in solution and $[H^+]_F$ represents the free hydrogen ion concentration.

By the term pH the acidity of a liquid is described as the negative common logarithm of the concentration of hydrogen ions:

$$pH = -\log [H^+]_F \quad (1.3)$$

Finally, pCO_2 is the partial pressure of CO_2 in equilibrium with seawater (Zeebe & Wolf-Gladrow 2001).

Any two of the carbonate system quantities, together with temperature, salinity and pressure, are sufficient to calculate all other quantities of the carbonate system. TA and DIC are conserved quantities, when temperature and/or pressure are changed.

1.2.2 Processes affecting the carbonate system

Several processes affect the carbonate system, including biological (e.g. calcium carbonate formation and dissolution, photosynthesis and respiration), physical (e.g. mixing, evaporation, river inputs) and chemical (e.g. CO_2 uptake and release) processes. The effect of these processes on the carbonate system can be described considering the changes in DIC and TA that are associated with them (Figure 1.2). CO_2 release or invasion in the ocean has an effect on DIC but not on TA, whereas biological processes affect both DIC and TA. Calcium carbonate formation decreases both DIC and TA in a

ratio 1:2, as for each mole of $CaCO_3$ precipitated one mole of carbon and one mole of double positively charged Ca^{2+} ions are taken up:

$$Ca^{2+} + 2\ HCO_3^- \leftrightarrow CaCO_3 + H_2O + CO_2 \quad (1.4)$$

As a result, the system shifts to higher CO_2 levels and lower pH. Dissolution of $CaCO_3$ has the opposite effect. On the other hand photosynthesis reduces DIC, as a result of CO_2 consumption, but slightly increases TA because of the simultaneous consumption of nitrate and the system shifts to lower CO_2 levels and higher pH (Figure 1.2):

$$6\ CO_2 + 12\ H_2O \leftrightarrow C_6H_{12}O_6 + 6\ O_2 + 6\ H_2O \quad (1.5)$$

Respiration, which returns CO_2 to the water column, has the opposite effect (Zeebe & Wolf-Gladrow 2001). Complete remineralisation of organic matter returns both CO_2 and nitrate to the water column and hence increases DIC while slightly decreasing TA.

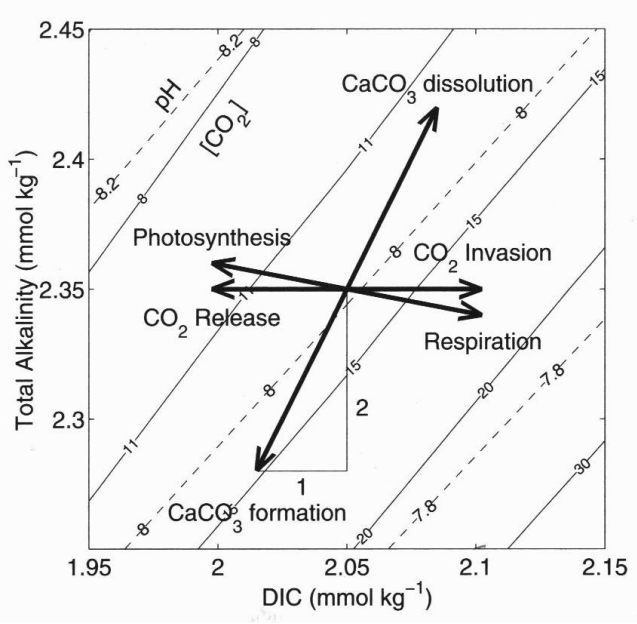

Figure 1.2 Effects of various processes on DIC and TA (arrows). Solid and dashed lines indicate levels of dissolved CO_2 (in μmol kg^{-1}) and pH, respectively. From Zeebe & Wolf-Gladrow (2001).

1.2.3 Ocean acidification

The buffering capacity of the oceans, due to interconversion between the carbonate system constituents, is not unlimited. A significant increase in atmospheric CO_2, like the increase since the industrial revolution, eventually results in noticeable changes in the speciation of DIC in seawater: the increase of pCO_2 in the surface ocean increases bicarbonate ion concentration ($[HCO_3^-]$), decreases carbonate ion concentration ($[CO_3^{2-}]$) and increases proton concentration, resulting in lower pH (Zeebe & Wolf-Gladrow 2001). Surface ocean pH is already 0.1 unit lower than preindustrial values and is projected to decrease by a further 0.3 - 0.4 units by the end of the century, depending on future CO_2 emissions scenarios (Figure 1.3B) (Caldeira & Wickett 2003, Orr et al. 2005).

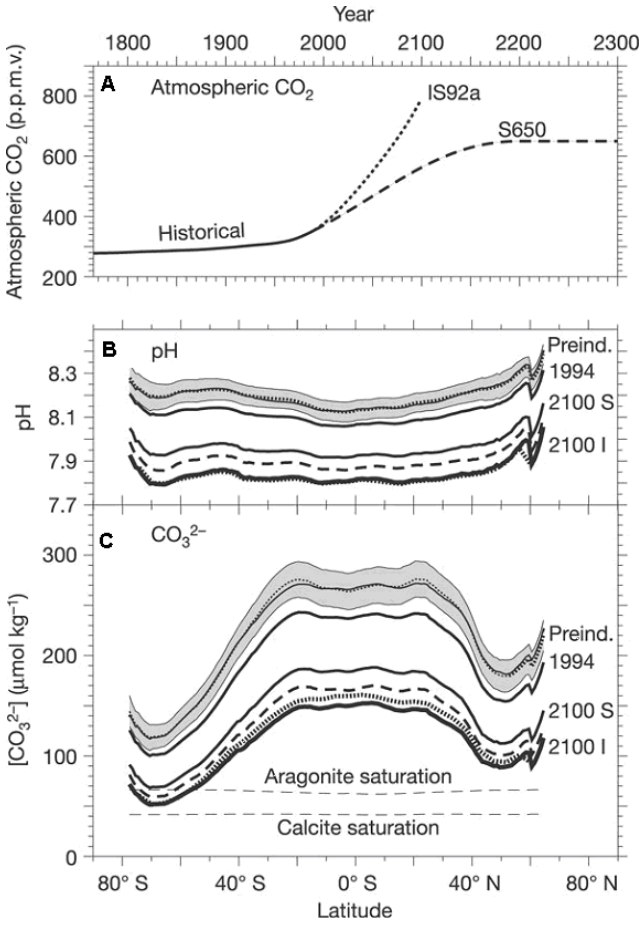

Figure 1.3 A) Atmospheric CO_2 over the preindustrial period and for two future scenarios, and consequent reductions as global zonal averages in B) surface ocean pH and C) surface ocean carbonate ion concentrations. From Orr et al. (2005).

Carbonate ion concentration is predicted to be 50% of preindustrial levels by the year 2100 (Figure 1.3C) (Orr et al. 2005), leading to a halving of calcite saturation state ($\Omega_{calcite}$) which is proportional to $[CO_3^{2-}]$ and $[Ca^{2+}]$ in seawater (Equation 1.6), with potential negative consequences for calcifying organisms (Feely et al. 2004).

$$\Omega_{calcite} = [Ca^{2+}][CO_3^{2-}] / K^*_{sp} \quad (1.6)$$

, where K^*_{sp} is the solubility product of calcium carbonate at the *in-situ* conditions of temperature, salinity and pressure, defined as:

$$K^*_{sp} = [Ca^{2+}]_{sat}[CO_3^{2-}]_{sat} \quad (1.7)$$

Even though Figure 1.3C suggests that the oceans will remain saturated with respect to calcite (and largely to aragonite) even at the highest CO_2 emission scenarios, undersaturation could be reached locally and/or seasonally as has already been observed in parts of the Arctic Ocean (e.g. Chukchi Sea; Bates et al. 2009) and the Baltic Sea (wintertime undersaturation; Tyrrell et al. 2008). Moreover, a reduction in the calcification rates of some organisms such as corals, often occurs well before undersaturation is reached (e.g. Langdon et al. 2000). Polar regions have naturally low $[CO_3^{2-}]$ and $\Omega_{calcite}$ (Figure 1.3C), due to the higher CO_2 solubility at low temperatures. Therefore, the surface waters of these regions are predicted to become under-saturated ($\Omega < 1$) with respect to calcite and aragonite before other regions (Orr et al. 2005). This highlights the need to better understand the processes affecting carbonate chemistry in polar regions and the consequences for calcifying organisms in these areas.

1.3 Coccolithophore ecology and distribution

Coccolithophores are present in a wide range of marine environments. They are found in oceanic and coastal waters and they extend from tropical to subpolar regions (Winter et al. 1994). They are more abundant in subpolar waters, whereas their diversity is highest in the warm oligotrophic subtropical gyres (Winter et al. 1994).

At high latitude regions, such as the North Atlantic, the North Sea, the Barents Sea and the Bering Sea, *Emiliania huxleyi*, the most abundant modern coccolithophore, forms extensive blooms (Tyrrell & Merico 2004). These blooms seem to be favoured by seasonally shallow mixed layers, high irradiances and high temperatures (Merico et al.

2004, Raitsos et al. 2006) and occur at the time of year when carbonate ion concentrations are seasonally high (Merico et al. 2006). Thus, *E. huxleyi* is considered to be closer to an *r*-selected species that is tolerant of a wide range of environmental conditions, has high maximum growth rates and proliferates quickly when conditions are favourable (Brand 1994). *E. huxleyi* also dominates relatively high abundance assemblages in the equatorial Atlantic, as a result of seasonal upwelling (Kinkel et al. 2000).In contrast, subtropical coccolithophores are considered to be *K*-selected, as they live in predictable environments where they have to compete for light and nutrient resources (Brand 1994). Several different morphotypes of *E. huxleyi* are found in high latitudes, each with different calcite contents (Young & Ziveri 2000, Young et al. 2003), that exhibit a poleward decreasing trend (e.g. Cubillos et al. 2007).

In polar regions, only low abundances of a small number of species have been observed (Manton et al. 1977, Thomsen 1981), although *Coccolithus pelagicus* can reach relatively high abundances in some polar regions (e.g. Baumann et al. 2000). There are indications that some of these polar coccolithophores may be mixotrophic or heterotrophic (Garrison & Thomsen 1993, Marchant & Thomsen 1994, Houdan et al. 2006), which could give them an advantage in surviving low light intensities and dark winters in polar waters.

Even though the biogeography of coccolithophores is relatively well known, it is not entirely clear which environmental factors influence their distribution, especially at high latitudes and in polar regions.

1.4 Coccolithophore calcification

Calcification physiology has been studied mainly in *E. huxleyi* due to its wide environmental tolerances which make it easy to culture. During calcification, coccoliths are formed inside the cell, in a specialized coccolith vesicle associated with the Golgi apparatus (Paasche 2002). As a process that requires energy, which in phytoplankton is generated through photosynthesis, calcification is strongly light-dependent and *E. huxleyi* calcification increases with irradiance in cultures (e.g. Zondervan et al. 2002) and decreases with depth in field observations (e.g. Fernandez et al. 1993, Poulton et al. 2007). Calcification decreases with depth more rapidly than does silicification, most likely because it requires more light energy (Poulton et al 2007). However, calcification

in *E. huxleyi* is considerably less light-dependent than photosynthesis and dark calcification has also been observed (see reviews by Paasche 2002, Zondervan 2007).

E. huxleyi normally produces more coccoliths than the 10 – 15 needed to construct a complete coccosphere. The extra coccoliths either form multiple layers or are detached at a rate of 10 – 20 per cell in exponentially growing cultures (Paasche 2002). In cultures, both nitrate (N)- and phosphate (P)-limitation increase calcification, as well as the number of coccoliths produced per cell, although N-limitation results in under-calcification of the individual coccoliths while P-limitation promotes over-calcification (e.g. Paasche & Brubak 1994, Paasche 1998). This agrees with the observation of high numbers of detached coccoliths at the end of coccolithophore blooms when nutrients have been exhausted (Balch et al. 1991). *E. huxleyi*, in comparison with other algae, is a poor competitor for nitrate under N-limitation, whereas it has a high affinity for phosphate, and P-limitation has been shown to increase the organic carbon content of the cells, something not observed under N-limitation (Paasche & Brubak 1994, Paasche 1998, Riegman et al. 2000).

The magnitude of calcification of whole communities (monospecific or not) depends both on cell numbers, and therefore growth rates, and on cell-specific calcification (Poulton et al. 2010). Also, the species composition influences total calcification if it is dominated by heavily calcified species like *C. pelagicus* (Baumann et al. 2000) or if a lot of different species contribute to the community as seen in the subtropical gyres (Poulton et al. 2007). Hence, factors such as light and temperature that control both growth and calcification at the cellular level need to be considered. Even though these are well studied for *E. huxleyi* cultures and from satellite based field observations of bloom conditions, little is known about cell-specific calcification in non-bloom conditions and data is currently available for only a few other coccolithophore species.

A number of studies have measured calcification in different oceanic regions, including the Equatorial Pacific (Balch & Kilpatrick 1996), Arabian Sea (Balch et al. 2000), subtropical gyres (Poulton et al. 2007), Subarctic Pacific (Lipsen et al. 2007), Iceland Basin (Poulton et al. 2010) and Patagonian Shelf (Poulton et al. in prep.). Calcification measurements in high latitude and polar non-bloom assemblages are scarce, especially for the Southern Ocean where satellite data indicate that coccolithophores are widespread (Holligan et al. 2010).

1.5 Ocean acidification (OA) effects on coccolithophores

Most studies of consequences of OA for coccolithophores have involved laboratory and mesocosm experiments. However, very few species have been studied, the most popular being *E. huxleyi*, partly due to its ease of growth.

Reduced calcite production at high CO_2 in monospecific cultures of *E. huxleyi* and *Gephyrocapsa oceanica* was first reported by Riebesell et al. (2000) and Zondervan et al. (2001, 2002). These experiments were carried out under nutrient replete conditions and high irradiances; however, in N-deplete conditions a similar reduction in calcite production is observed (Sciandra et al. 2003). These studies also showed that the calcification (CF) to photosynthesis (PS) ratio decreased under nutrient replete conditions but remained constant under nutrient limitation because of a concurrent reduction in PS. The effect of CO_2 on *E. huxleyi* CF also seems to depend on irradiance, as no sensitivity was observed under low light conditions (Zondervan et al. 2002). More recent laboratory studies (Iglesias-Rodriguez et al. 2008, Shi et al. 2009) have shown an opposite response to these previous experiments, where CF increased at high CO_2, under nutrient replete and high light conditions.

Laboratory experiments, though useful to isolate the impacts of different factors, are not fully realistic. Typically only one species is studied, in isolation from the ecosystem it usually interacts with, and in conditions that are not representative of those that natural coccolithophore assemblages would normally encounter. Moreover, the short timescales of the experiments do not take into account the possibility of evolutionary adaptation to high CO_2 conditions. More realistic approaches have included mesocosm experiments, which generally support the hypothesis of CF decrease with increasing CO_2 (Delille et al. 2005, Engel et al. 2005). However, these studies were also on blooms dominated by *E. huxleyi*. The response of a limited number of coccolithophore species to ocean acidification has shown interspecific and intraspecific variability. *C. pelagicus* did not respond to increased CO_2 whereas *Calcidiscus leptoporus* exhibited an optimum curve with maximum CF at modern surface ocean pCO_2, when a pCO_2 range of 100 – 900 ppm was tested (Langer et al. 2006). The response of four different *E. huxleyi* strains to OA was also different (Langer et al. 2009) suggesting that the use of different strains might be the source of contrasting results in previous studies. However, a recent study argues that there is indeed an overarching trend of decreasing particulate inorganic to

organic carbon ratio (PIC:POC) in *E. huxleyi* in those previous experiments, irrespective of the strain used (Findlay et al. 2011).

The results of experimental studies need to be complemented with field observations, which incorporate the elements of adaptation, realistic environmental conditions, ecosystem interactions and the opportunity to study the full range of species in the areas investigated.

1.6 Motivation and aims of the thesis

The motivation for this thesis was the need for a more realistic approach to studying ocean acidification effects on coccolithophores, which incorporates observational data of these organisms in their natural environment and takes into account more factors that may affect their distribution and calcification.

The present study aimed to take advantage of latitudinal gradients in carbonate chemistry at high latitude and polar regions that are comparable to future ocean acidification (i.e. decrease in $\Omega_{calcite}$ towards the poles, Figure 1.3) and could provide insights into future coccolithophore responses. However, the purpose was not to compare natural variations in coccolithophore distribution and calcification with carbonate chemistry parameters only, but also with other factors such as temperature, irradiance and nutrients. This will provide a balanced and objective view of their relative importance for natural coccolithophore populations and also potentially give insights into the consequences for coccolithophores of concurrent changes in some of these variables in the future ocean.

Two research cruises provided such an opportunity, the first on a transect between the North Sea and Svalbard (Arctic) and a second one in the Drake Passage (Southern Ocean). On the first cruise, carbonate chemistry samples were collected and analysed and one chapter (Chapter 2) is dedicated to interpretation of this data. On the Southern Ocean cruise, carbonate chemistry sample collection and analysis was performed by Dorothee Bakker (University of East Anglia) and so in this thesis these have only been used to calculate pH and calcite saturation states for comparison with the biotic data. On both cruises samples for coccolithophore identification and enumeration were collected and analysed and measurements of calcification and primary production rates, as well as

chlorophyll-*a* were made. Also, data were compiled and analysed for the calculation of mixed layer irradiance used in chapters 3 and 4.

The individual aims of this thesis were:

1) To quantify the effect of biotic and abiotic processes on the carbonate chemistry of the North Sea, Norwegian Sea and Svalbard Arctic region.
2) To investigate the distribution of coccolithophore abundance and diversity, and quantify coccolithophore calcification in two high latitude/ polar regions (North Sea – Svalbard and Drake Passage).
3) To try and determine which environmental variables most strongly influence the distribution of coccolithophores in terms of abundance, diversity and calcification across these regions.

Thesis outline

Chapter 2 describes the carbonate chemistry system sampled between the North Sea and the Arctic Ocean (Svalbard) during summer 2008. The differences in alkalinity and dissolved inorganic carbon between the surface and subsurface waters are attributed to physical and biological processes, using salinity and nutrient data. The effects of freshwater input and primary production on the carbonate chemistry system are discussed. Finally, the results are discussed in the context of Arctic change and more generally global change.

Chapter 3 describes the distribution of coccolithophores between the North Sea and the Arctic Ocean (Svalbard) during summer 2008. Coccolithophore abundance and diversity are compared to environmental gradients, including temperature, salinity, nutrients, irradiance and the carbonate chemistry parameters described in Chapter 2. A multivariate approach is used to attribute variation in the biotic variables to variation in the abiotic variables. Coccolithophore calcification data measured during the cruise are discussed in relation to species composition. Finally the results are discussed in the context of future changes in the oceans. This chapter has been published as:

Charalampopoulou A, Poulton AJ, Tyrrell T, Lucas MI (2011) Irradiance and pH affect coccolithophore community composition on a transect between the North Sea and the Arctic Ocean. Marine Ecology Progress Series 431:25-43

Chapter 4 describes the distribution of coccolithophores and calcification rates in the Drake Passage (Southern Ocean) during late austral summer 2009. Latitudinal trends in *E. huxleyi* coccolith size, coccolith calcite content and coccolith production rates are examined and the values compared to those of northern hemisphere *E. huxleyi* assemblages. Finally, the biotic parameters are compared to a set of environmental variables including temperature, salinity, nutrients, irradiance and carbonate chemistry parameters.

Chapter 5 aims to provide an overarching summary of the previous three chapters, including a comparison of the regions examined in the northern and southern hemisphere. The wider implications of the main findings are discussed, as well as the limitations of the study and future directions.

Chapter 2: Freshwater input and primary production affect carbonate chemistry parameters between the North Sea and the Arctic Ocean

Abstract

Total Alkalinity (TA) and Dissolved Inorganic Carbon (DIC) were measured in summer 2008 in the surface and subsurface waters of the North Sea, the Norwegian Sea and the Svalbard Arctic region. Deficits in TA and DIC between the surface and subsurface waters were attributed to physical and biological processes using deficits in salinity and nutrient concentrations. During summer there are two main processes that shape the carbonate chemistry of these regions: freshwater inputs and biological processes. Firstly, the freshwater sources of the Baltic Sea, sea ice melt and terrestrial runoff accounted for more than half of the change in TA and DIC in the northern North Sea and Svalbard. Additionally, the TA-rich freshwater sources of the Baltic Sea and terrestrial runoff also contributed towards high saturation states in the northern North Sea, the Norwegian Sea and Rijpfjorden. Secondly, the absence of seasonal stratification caused CO_2 supersaturation and lower saturation states in the southern North Sea, whereas elsewhere along the transect, and especially north of Svalbard, primary production promoted CO_2 undersaturation and high pH and calcite saturation states. Even though biological processes seem to play a major role in shaping the saturation state and pH of these regions, the carbonate chemistry of the freshwater sources (Baltic Sea, sea-ice melt, riverine input/ terrestrial runoff) is also important and may accentuate the effects of biological activity.

2.1 Introduction

Anthropogenic activities over the last few centuries have released large quantities of carbon dioxide (CO_2) into the atmosphere (IPCC 2007), primarily through fossil fuel burning. The oceans have absorbed much of this CO_2, and about one quarter of this fossil-fuel effluent now resides in the surface ocean, where it forms carbonic acid (H_2CO_3) and changes the balance of carbonate (CO_3^{2-}) and bicarbonate (HCO_3^-) ions making the ocean more acidic (Caldeira & Wickett 2003, Orr et al. 2005). Surface ocean pH is already 0.1 unit lower than preindustrial values (Caldeira & Wickett 2003) and will, unless emissions are curtailed, become another 0.3 - 0.4 units lower by the end of the century, as predicted by various models (Caldeira & Wickett 2003, 2005, Orr et al. 2005). This will induce a three times higher [CO_2 (aq)] and a decrease in [CO_3^{2-}] by about 50% (Orr et al. 2005), leading to a halving of calcite saturation state ($\Omega_{calcite}$). The implications of such changes for many marine calcifiers (Fabry et al. 2008, Doney et al. 2009), have increased the need to understand the variability and forcing of the carbonate chemistry system, especially in high latitude and polar oceans which will be the first to experience undersaturation with respect to calcite and aragonite (Orr et al. 2005).

The processes affecting the carbonate system can be described by considering the changes in dissolved inorganic carbon (DIC) and total alkalinity (TA) that are associated with them (see Figure 1.2 in General introduction). DIC and TA concentrations are affected by CO_2 release or invasion, photosynthesis or respiration and remineralisation, and calcium carbonate formation or dissolution. The two processes of each pair have the opposite result on the carbonate system. CO_2 release or invasion in the ocean (e.g. through air-sea CO_2 exchange), has an effect on DIC but not on TA because the charge balance does not change. Photosynthesis reduces DIC, as a result of CO_2 consumption, but slightly increases TA because of the simultaneous consumption of nitrate. Respiration and remineralisation, which return CO_2 and nutrients into the water column, have the opposite effect. Calcium carbonate formation decreases both DIC and TA in a ratio 1:2, as for each mole of $CaCO_3$ precipitated one mole of carbon and one mole of double positively charged Ca^{2+} ions are taken up ($Ca^{2+} + 2HCO_3^- \leftrightarrow CaCO_3 + H_2O + CO_2$). Dissolution of $CaCO_3$ has the opposite effect. Other processes affecting the carbonate system include upwelling, entrainment and episodic mixing.

The Arctic Ocean is generally undersampled for carbonate chemistry data. Previous studies have shown that it is an important CO_2 sink, contributing 5-14% to the global sink and source balance (Bates & Mathis 2009 and references within). Future sea-ice loss and increased phytoplankton production (Arrigo et al. 2008) are expected to increase the capacity of the Arctic Ocean to absorb CO_2. Freshwater inputs from sea-ice melt and river runoff have been reported to reduce saturation states in surface waters of the Chukchi Sea, Canada Basin and the Bering Sea (Bates et al. 2009, Mathis et al. 2011), and in some areas of the Canadian Archipelago and the Mackenzie shelf (Chierici & Fransson 2009, Azetsu-Scott et al. 2010). On the other hand, intense phytoplankton primary production elevates saturation state and pH values across much of the Chukchi Sea shelf and Canada Basin (Bates et al. 2009, Chierici & Fransson 2009). However, the increased production and export of organic matter has been found to lead to high remineralisation rates in subsurface waters, leading to calcite and aragonite undersaturation in the Chukchi Sea (Bates et al. 2009). More carbonate chemistry data is needed in the Arctic to try and understand how rapid changes, including rising temperature, sea-ice loss, changes in productivity and freshwater inputs, will affect the seawater chemistry of this region.

There has been extensive research on the carbonate chemistry of the North Sea, a region that acts as a continental shelf carbon pump due to its high biological activity and efficient exchange with the Atlantic Ocean (Thomas et al. 2004, Bozec et al. 2005). Previous studies have been regional, concentrating in the southern North Sea and the Southern Bight (Frankignoulle & Borges 2001, Borges & Frankignoulle 2002, 2003, Gypens et al. 2004, Gypens et al. 2009). Carbon budgets for the whole North Sea and for its regions have been calculated in a number of studies (Thomas et al. 2004, Bozec et al. 2005, Thomas et al. 2005a, Bozec et al. 2006). In the present study the relative effects of processes on the carbonate system were compared between three different regions: the North Sea, the Norwegian Sea and the Svalbard Arctic region.

The aims of this study were: 1) to quantify the effect of biotic and abiotic processes on the carbonate chemistry of the North Sea, Norwegian Sea and Svalbard Arctic region, and 2) to investigate the ability of the method used to fully account for observed variations in the carbonate chemistry in each of these regions.

2.2 Methods

2.2.1 Study area

The study area included four main hydrographic regions (Figure 2.1): a) the English Channel (EC) and the North Sea, subdivided into the well mixed southern part (EC and SNS), the Atlantic influenced central part (CNS) and the stratified northern part (NNS) influenced by the Baltic Sea outflow (Kempe & Pegler 1991); b) the Norwegian Sea (NORW), characterised by the Norwegian Current flowing northward off the Scandinavian coast (Swift 1986); c) the continental shelf and slope south of Svalbard (ARCT), influenced by the Arctic Front (Swift 1986); and d), the partially ice-covered region north of Svalbard (SVAL).

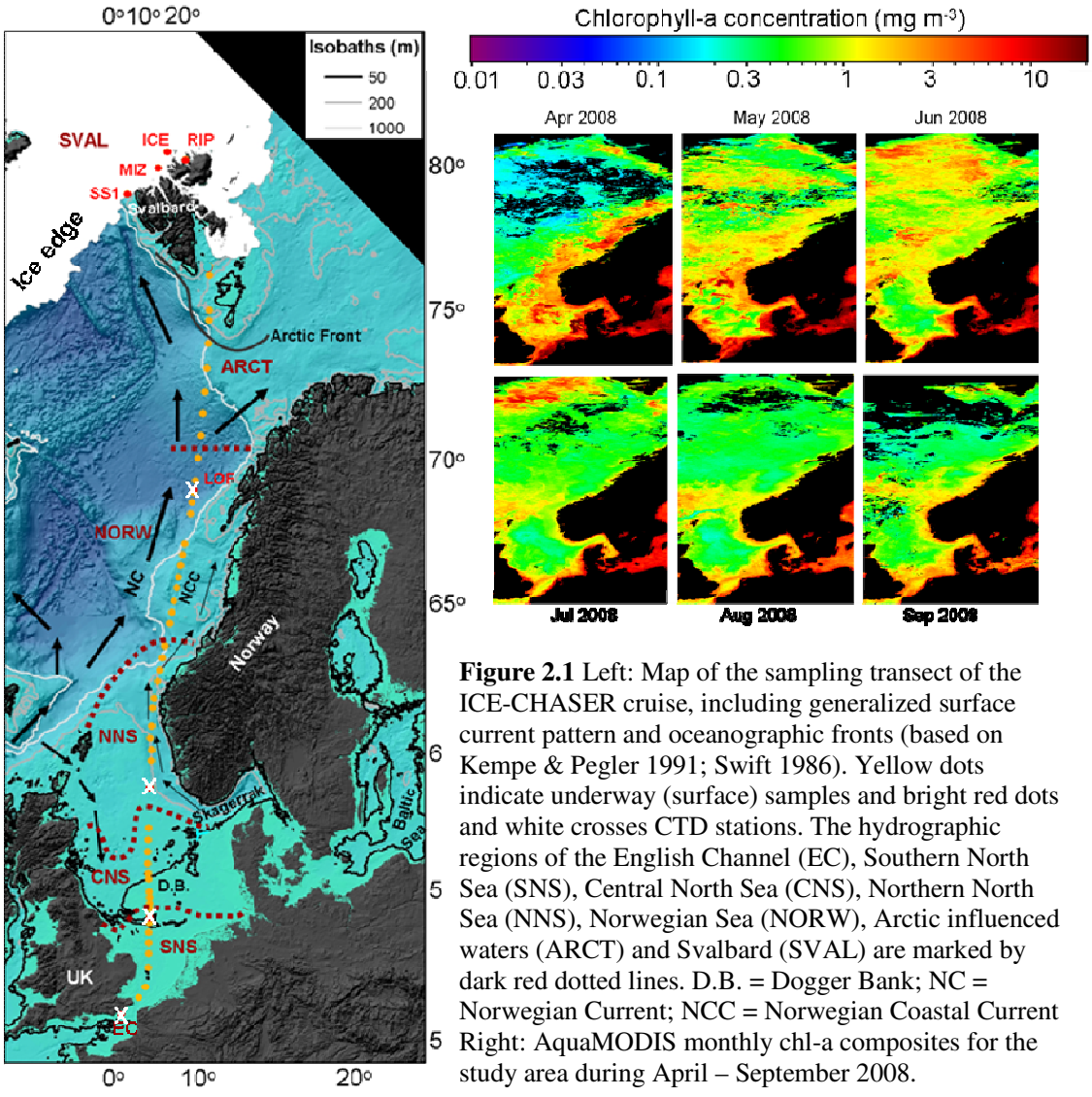

Figure 2.1 Left: Map of the sampling transect of the ICE-CHASER cruise, including generalized surface current pattern and oceanographic fronts (based on Kempe & Pegler 1991; Swift 1986). Yellow dots indicate underway (surface) samples and bright red dots and white crosses CTD stations. The hydrographic regions of the English Channel (EC), Southern North Sea (SNS), Central North Sea (CNS), Northern North Sea (NNS), Norwegian Sea (NORW), Arctic influenced waters (ARCT) and Svalbard (SVAL) are marked by dark red dotted lines. D.B. = Dogger Bank; NC = Norwegian Current; NCC = Norwegian Coastal Current Right: AquaMODIS monthly chl-a composites for the study area during April – September 2008.

2.2.2 Sampling

Sampling was conducted during the ICE-CHASER cruise (23/07/2008 – 21/08/2008) on board the ice-strengthened *RRS James Clark Ross* during a transect from Portland, U.K. to Svalbard in the Arctic (Figure 2.1). Both vertical CTD profiles and the ship's continuous non-toxic underway supply were used for water sampling. Water samples for carbonate chemistry parameters and ancillary measurements were collected from 50 underway locations (~ 5m depth) and from 8 CTD deployments (see Figure 2.1); one in each of the EC (ECcast), SNS (SNScast), NNS (NNScast), NORW (off the Loffoten Islands, LOF), an open water shelf station west of Svalbard (SS1), the Marginal Ice Zone (MIZ), an Ice station (ICE) and an Arctic fjord station at Rijpfjorden (RIP). Samples for primary production (PP) were collected from the CTD deployments and PP was measured as described in Charalampopoulou et al. (2011).

2.2.3 Carbonate chemistry

Samples for the determination of Dissolved Inorganic Carbon (DIC) and Total Alkalinity (TA) were drawn in 250 ml Schott ® SUPRAX borosilicate glass bottles following Dickson et al. (2007) to minimise gas exchange. A headspace of 1% was allowed for water expansion and samples were poisoned with 50 µL saturated mercuric chloride solution (7g per 100 mL). Sample analysis was undertaken at 25ºC using a VINDTA 3C (Marianda, Germany) instrument. DIC was determined coulometrically (coulometer 5011, UIC, USA) and TA was determined using a semi-closed cell titration (Dickson et al. 2007). Repeated measurements on the same batch of seawater ($n \geq 5$) were undertaken every day prior to sample analysis to assess the precision of the method. Relative precision of DIC and TA measurements was 0.05% – 0.08% and 0.03% – 0.10%, respectively. Certified Reference Materials (from A.G. Dickson, Scripps Institute of Oceanography) were analysed as standards to calibrate the instrument at the beginning and end of each day of analysis. A daily correction factor was applied to all measured values based on the analysis of the reference material. Calcite and aragonite saturation states ($\Omega_{calcite}$, $\Omega_{aragonite}$), pH and pCO_2 were calculated from DIC, TA, nutrients, temperature, salinity and pressure data using the CO2SYS.XLS program (Pierrot et al.

2006) and the equilibrium constants of CO_2 from Mehrbach et al. (1973) refitted by Dickson & Millero (1987).

2.2.4 Nutrients, mixed layer depth and ice cover

Phosphate and nitrate concentrations were determined using a Lachat 'QuikChem 8500' flow injection autoanalyser following the manufacturers' recommended methods for orthophosphate and nitrate/nitrite (Lachat method nos. 31-115-01-1-G and 31-107-04-1-A). Samples were run in triplicate and corrected for salinity by analyzing Low Nutrient Sea Water purchased from OSIL (Batch LNS 16) prior to and within each batch of samples. The precision of nutrient measurements was ± 0.03µM for both phosphate and nitrate. Nutrient data used to calculate DIC and TA deficits (see paragraph 2.6) were normalized to salinity 34 using a direct normalization. The salinity correction was less than 0.3 units.

Mixed layer depth (MLD) was determined as the shallowest depth corresponding to a density difference ($\Delta\sigma_t$) with the surface waters of more than $\Delta\sigma_t = 0.125$ sigma units (Monterey & Levitus 1997).

Visual observations of sea ice coverage were made and recorded daily and as the ships' position changed (Leakey 2008). Additional ice cover data for the time period preceding our cruise were obtained from the National Ice Centre of NOAA (http://www.natice.noaa.gov/products/products_on_demand.html). The ice cover extended the furthest south at the end of April/ beginning of May 2008 and still extended south of Svalbard 4 weeks before we visited the area. At the end of July there was open water north of Svalbard (Appendix, Figure A.1), which became partially ice covered by the beginning of August. Station SS1 (03 August 2008) was free from ice, the ICE station (06 August 2008) had 10/10 ice coverage and the MIZ station (10 August 2008) had 7/10 ice coverage. The RIP station (arctic fjord; 16 August 2008) was ice covered until the 15 August when the ice started breaking up; we encountered ice floes at the south part of the fjord (sampling site), although the northern part was covered by thick ice (Figure A.1).

2.2.5 Salinity normalised TA and DIC

Most TA and DIC data subsets (both surface and water column samples) exhibited salinity dependence with a positive intercept at zero salinity. Five different slopes were observed, corresponding to five different regimes (Figure 2.4): 1) EC and the North Sea, 2) NORW, 3) ARCT, 4) SVAL (without RIP), and 5) RIP station.

The TA - salinity relationships for the five regimes were:

EC – North Sea: $TA = 26.60\ S + 1388$ ($R^2 = 0.88$, $p < 0.01$, n = 43)
NORW: $TA = 30.42\ S + 1253$ ($R^2 = 0.89$, $p < 0.01$, n = 19)
ARCT: $TA = 55.97\ S + 360$ ($R^2 = 0.83$, $p < 0.05$, n = 9)
SVAL: $TA = 60.80\ S + 193$ ($R^2 = 0.94$, $p < 0.01$, n = 15)
RIP: $TA = 30.77\ S + 1207$ ($R^2 = 1.00$, $p < 0.01$, n = 5)

The DIC - salinity relationships for the five regimes were:

EC – North Sea: $DIC = 29.70\ S + 1057$ ($R^2 = 0.80$, $p < 0.01$, n = 44)
NORW: $DIC = 42.42\ S + 599$ ($R^2 = 0.65$, $p < 0.01$, n = 19)
ARCT: $DIC = 39.65\ S + 699$ ($R^2 = 0.51$, $p < 0.01$, n = 9)
SVAL: $DIC = 60.59\ S - 32$ ($R^2 = 0.88$, $p < 0.01$, n = 15)
RIP: $DIC = 52.95\ S + 271$ ($R^2 = 0.94$, $p < 0.01$, n = 5)

To identify changes in TA associated with changes in salinity, TA data were normalised to salinity 34, the average salinity of all samples, using equation (2.1) to account for the non-zero end member for each regime (Friis et al. 2003):

$$TA_{34} = \left(\frac{TA - TA_0}{S} \right) \times 34.0 + TA_0 \qquad (2.1)$$

, where TA and S are the *in-situ* total alkalinity and salinity, respectively, and TA_0 is the alkalinity intercept at zero salinity for each regime.
The same procedure was followed for DIC data.

Equation (2.1) was used to normalise both surface and depth profile data. Any dilution effects from the Baltic Sea outflow or ice melt would mainly affect the surface waters down to the mixed layer and not the deeper layers. However, in the case of the NNS, even though there is strong stratification at the surface there is still lateral mixing with the SNS within the bottom layers. Also, the SVAL stations are on the continental shelf, where we would also expect prominent lateral mixing. Hence, it was decided for these reasons and for simplicity and consistency to treat all data in the same way.

2.2.6 TA and DIC deficits

One of the aims of this study was to understand how the differences in TA and DIC between the surface and subsurface waters were caused by various processes. These differences were attributed to salinity changes (dilution), carbon and nutrient uptake via organic matter production, and $CaCO_3$ precipitation or dissolution.

The total TA and DIC deficits were expressed as a sum of the contributing processes as in Jones et al. (2010):

$$\Delta TA_{deficit} = \Delta TA_{salinity} + \Delta TA_{org} + \Delta TA_{residual\ (=CaCO3)} \quad (2.2)$$

$$\Delta DIC_{deficit} = \Delta DIC_{salinity} + \Delta DIC_{org} + \Delta DIC_{CaCO3} + \Delta DIC_{residual} \quad (2.3)$$

Total TA and DIC deficits were determined from the difference between surface and bottom measured values for each vertical profile. Deficits due to salinity changes were determined from the difference between measured and salinity normalized deficits. DIC deficits due to organic matter production were estimated from nitrate and phosphate deficits, using a C:N:P molar uptake ratio of 117:16:1 (Anderson & Sarmiento 1994). TA deficits due to organic matter production were determined from nitrate, phosphate and ammonia deficits assuming a 1 mol increase in TA for every 1 mol of nitrate and phosphate consumed by algae and 1 mol decrease in TA for every mol of ammonia consumed (Zeebe & Wolf-Gladrow 2001). The TA residuals were attributed to $CaCO_3$ production/ dissolution and the DIC deficits due to these latter processes were calculated using a 2:1 molar change in TA:DIC.

2.2.7 Propagation of TA and DIC deficit errors

Errors were propagated following three basic rules (Taylor 1982). When various quantities x, …, w with associated independent and random errors δx, …, δw were used to calculate a quantity q, then the uncertainty in q, δq, was calculated as follows:

Where q was the sum and difference, i.e. $q = x + \ldots + z - (u + \ldots + w)$, then

$$\delta q = \sqrt{(\delta x)^2 + \ldots + (\delta z)^2 + (\delta u)^2 + \ldots + (\delta w)^2} \tag{2.4}$$

Where q was the product and quotient, i.e. $q = \frac{x \times \ldots \times z}{u \times \ldots \times w}$, then

$$\frac{\delta q}{|q|} = \sqrt{\left(\frac{\delta x}{x}\right)^2 + \ldots + \left(\frac{\delta z}{z}\right)^2 + \left(\frac{\delta u}{u}\right)^2 + \ldots + \left(\frac{\delta w}{w}\right)^2} \tag{2.5}$$

And where $q = Bx$, where B was known exactly, then

$$\delta q = |B| \delta x \tag{2.6}$$

These rules were applied to calculate the error in total TA and DIC deficits, and deficits due to organic matter production and $CaCO_3$ production/ dissolution, by using initial errors of less than 2 μmol kg^{-1} in TA and DIC measurements, and less than 0.1 μmol kg^{-1} in nitrate and phosphate measurements.

To estimate the uncertainty in deficits due to salinity changes, the uncertainty in salinity normalized TA and DIC derived from equation (2.1) was first calculated. The error in TA_0 and DIC_0 estimates was accounted for by changing the TA and DIC values by ±2 μmol kg^{-1}, one at a time, in each of the regimes and recording the change in the TA and DIC intercepts. The resulting calculated uncertainty in TA_0 and DIC_0 was between 1 and 9 μmol kg^{-1} except for ARCT (16 μmol kg^{-1}, however deficits in this region were not calculated). The uncertainty in salinity measurements and in the average salinity of all samples (S = 34) was 0.1and 0.01 units, respectively.

2.3 Results and Discussion

2.3.1 Overview of surface properties distribution

The cruise transect covered a great range of bathymetry (<50 – 3000 m) and water masses (Figure 2.1). Temperature decreased with latitude, from >15ºC in SNS to <0ºC in SVAL, but peaked at 17.8ºC in NNS (Figure 2.2A). Salinity was generally >34 with the exception of the Skagerrak-derived water mass in NNS and NORW (min. 30.6), and at SVAL (min. 30.7) (Figure 2.2A). Nitrate concentrations were generally low (<0.2 μM), with the exception of three samples (SNS and ARCT) where higher nitrate values (1.2 – 1.6 μM) were measured (Figure 2.2B). Phosphate was higher (<0.5 μM), compared to phytoplankton requirements. Mixed layer depth (MLD) varied from a well mixed water column in EC, SNS and SS1 to 16 m in NNS and 6 m in RIP (Figure 2.3A).

DIC ranged between 1860 and 2100 μmol kg^{-1} with minimum values in NNS and SVAL. TA ranged between 2090 and 2330 μmol kg^{-1} and followed the same trend as DIC (Figure 2.2C). It would be expected that DIC would increase northwards due to the lower temperature and higher solubility of CO_2 in seawater. An 18ºC decrease in temperature, as in the case of this transect, at constant salinity, TA and pCO_2, would cause a northward increase in DIC of ~130 μmol kg^{-1}, much smaller than the observed range in DIC of 240 μmol kg^{-1}. However, such a south-north trend was not observed and the DIC distribution followed the salinity distribution instead.

pCO_2 decreased with latitude from >400 μatm in SNS to just over 100 μatm in SVAL, opposite to the expected equilibrium between sea surface and atmospheric pCO_2 due to gas exchange. In a scenario where the 240 μmol kg^{-1} reduction in DIC was due to phytoplankton uptake, then at constant temperature and TA, this would cause a decrease in pCO_2 of ~310 μatm, similar to the observed range. pH exhibited an opposite trend to that of pCO_2 and increased with latitude from a minimum of 8.01 in EC and SNS to a maximum of 8.43 in SVAL (Figure 2.2D). $\Omega_{calcite}$ and $\Omega_{aragonite}$ were higher in NNS, NORW and SVAL (up to 4.3 and 2.7, respectively) and lower in SNS, CNS and ARCT (typically ~ 3.5 – 4.0 and 2.2 – 2.5, respectively) (Figure 2.2E).

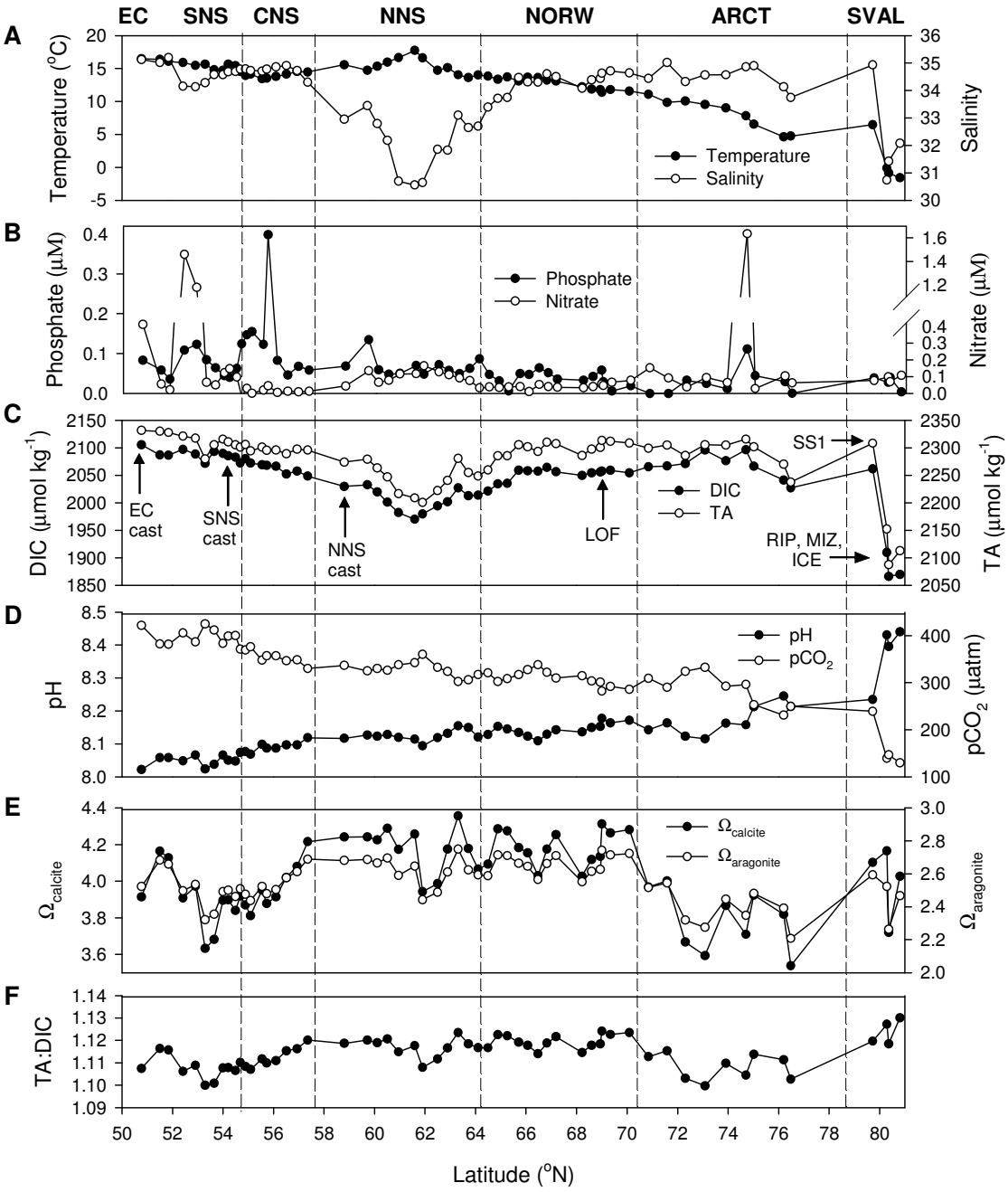

Figure 2.2 Physicochemical parameters along the UK – Svalbard transect. A) Temperature and salinity. B) Phosphate and nitrate. C) Dissolved Inorganic Carbon (DIC) and Total Alkalinity (TA). D) pH and pCO_2. E) Saturation states of calcite ($\Omega_{calcite}$) and aragonite ($\Omega_{aragonite}$). F) TA:DIC ratio. Observed DIC and TA values are presented here. See Figure 2.5 for normalised DIC and TA values. The arrows indicate the position of the CTD stations as described in the text.

Despite the large temperature difference across the transect, it is obvious that temperature was not the main controlling factor over the distribution of carbonate chemistry parameters.

2.3.2 The English Channel and the North Sea

The EC exhibited a well mixed water column as the vertical profiles of temperature and salinity show (Figure 2.3A). The SNS water column was also relatively well mixed. However, there was some stratification at the time of sampling, with the mixed layer extending down to 16 m above the seafloor (MLD = 26 m, bottom depth = 42 m, Figure 2.3A), with slightly cooler and more saline water observed below 26 m. In contrast, the NNS was clearly stratified with a 16 m deep mixed layer of fresher, warmer water overlying more saline, colder water below the mixed layer (Figure 2.3A). The measured DIC and TA values in these regions agree well with previous work (Kempe & Pegler 1991, Bozec et al. 2005, Thomas et al. 2005b). During summer, higher DIC and TA were observed in the EC and the SNS (mean values, DIC = 2087 μmol kg^{-1}, TA = 2312 μmol kg^{-1}) than in the NNS (mean values, DIC = 2005 μmol kg^{-1}, TA = 2240 μmol kg^{-1}), with intermediate values found in the CNS (mean values, DIC = 2068 μmol kg^{-1}, TA = 2297 μmol kg^{-1}) (Figure 2.2C). The differences between the southern and northern North Sea can be attributed to 1) freshwater input from the Baltic Sea, and 2) the shallow depth in the EC and the SNS resulting in absence of stratification in these regions.

2.3.2.1 TA and DIC deficits

In the EC, the difference between surface and subsurface TA ($\Delta TA_{deficit}$) and DIC ($\Delta DIC_{deficit}$) values was virtually zero, as expected because of the lack of stratification. Small deficits were also observed in the SNS ($\Delta TA_{deficit}$ = -8 μmol kg^{-1}, $\Delta DIC_{deficit}$ = -38 μmol kg^{-1}), whereas the greatest surface-subsurface differences in the North Sea were observed in the NNS: $\Delta TA_{deficit}$ was -74 μmol kg^{-1} and $\Delta DIC_{deficit}$ was -116 μmol kg^{-1} (Table 2.1).

Salinity and nutrient vertical distributions in the EC were also homogeneous (Figure 2.3) and hence there was no net effect on the vertical profiles of TA and DIC due to freshwater addition/ evaporation or organic matter production/ remineralisation.

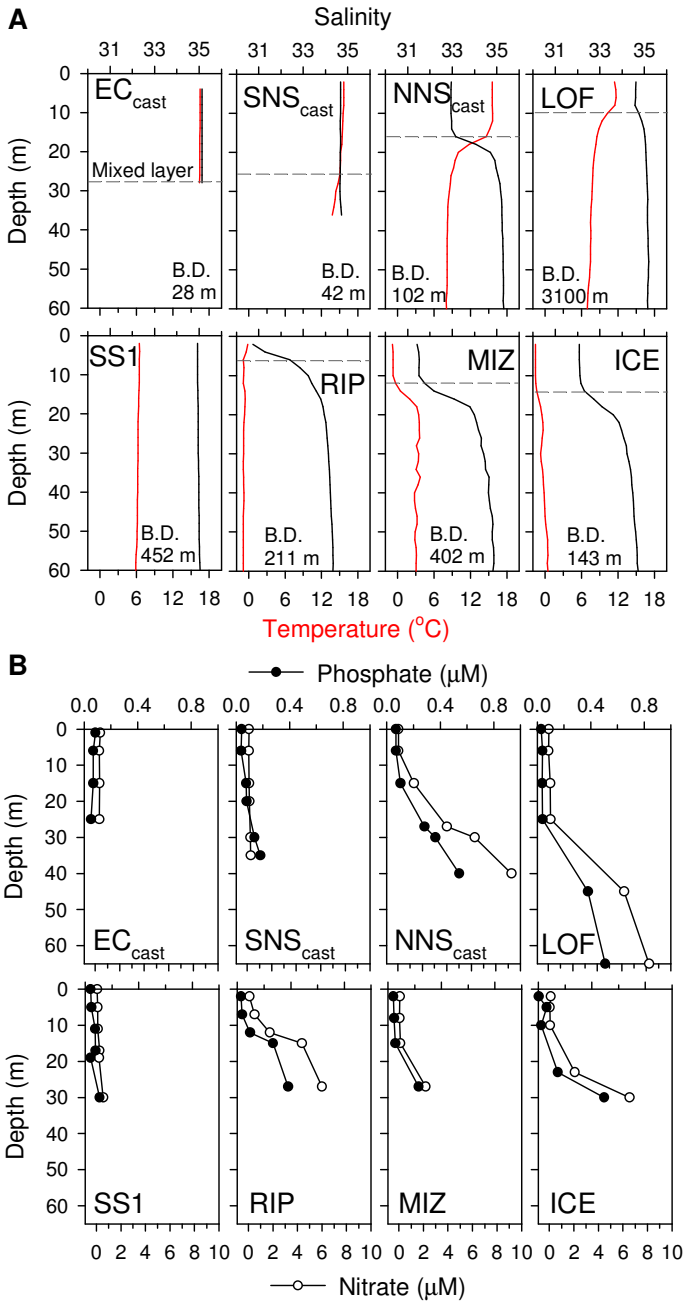

Figure 2.3 Vertical distributions of A) salinity and temperature and B) phosphate and nitrate concentrations, at each of the CTD stations. B.D. = Bottom Depth

Salinity changes in the SNS contributed very little to the observed deficits and organic matter production estimated from the phosphate deficits accounted for around half (-16 μmol kg^{-1}) of the DIC deficit (but no contribution was observed when nitrate was used) (Figure 2.6, Table 2.1). Salinity changes in the NNS accounted for 84% of the TA deficit and half of the DIC deficit (Figure 2.6, Table 2.1). The remaining DIC in the NNS deficit could be explained mostly by organic matter production. When the TA residuals in the NNS were attributed to calcite production (which also contributed a little to the DIC deficit), DIC residuals of up to 27 μmol kg^{-1} remained unexplained (Table 2.2). In the SNS, where the TA residuals were not significant, DIC residuals of up to -35 μmol kg^{-1} remained unexplained (Table 2.1). A process which could not be identified caused a greater difference between surface and subsurface DIC than expected in these regions.

2.3.2.2 Freshwater inputs

The NNS (100 – 400 m bottom depth) was affected by the Baltic Sea outflow at the surface layer which has a distinctive low salinity (30 – 33) signature. Below the mixed layer the water consisted of the Atlantic water inflow (salinity 35) (Figure 2.2A, 2.3A). The surface values of DIC and TA in NNS showed a concomitant decrease with salinity, which resulted from dilution of the North Sea water with Baltic Sea low salinity water. The low surface DIC (1970 - 2030 μmol kg^{-1}) and TA (2190 - 2270 μmol kg^{-1}) values in the NNS agree with other measurements in the Skagerrak (TA: 2000 – 2200 μmol kg^{-1}, Hjalmarsson et al. 2008) and the Baltic Sea outflow (DIC: 1900 – 2000 μmol kg^{-1}, TA: 2120 – 2300 μmol kg^{-1}, Kempe & Pegler, DIC: 1930 – 2030 μmol kg^{-1}, Bozec et al. 2006). TA and DIC versus salinity plots (Figure 2.4A, C) show clearly the dilution of these properties in the NNS. The positive TA intercept of 1388 μmol kg^{-1} at zero salinity (TA_0) is indicative of the relatively high TA of Baltic Sea waters (compared to a simple linear correlation with salinity), due to high TA riverine input to the Baltic from rivers that drain limestone rich basins (Hjalmarsson et al. 2008). The regression equation gives TA values typical of the central Baltic Sea: TA = 1574 μmol kg^{-1} at S = 7.0 is very close to values of ~ 1600 μmol kg^{-1} reported by Hjalmarsson et al. (2008). DIC values estimated from the respective DIC vs. salinity regression equation are lower than those reported previously for the Baltic Sea: DIC = 1253 μmol kg^{-1} at S = 6.6 (compared to 1441 μmol kg^{-1} reported by Tyrrell et al. 2008). This discrepancy is probably the result of

DIC uptake by phytoplankton as the water mass travelled from the Baltic Sea and mixed into the North Sea.

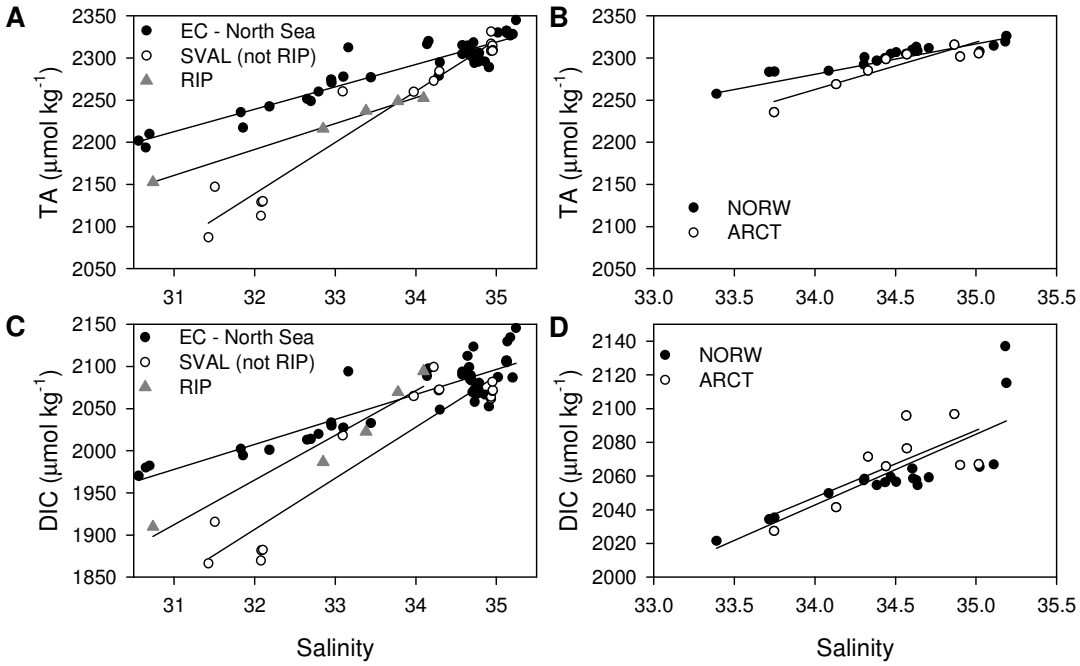

Figure 2.4 Relationships between A, B) TA and salinity C, D) DIC and salinity. All regression models were significant ($p < 0.01$; see text for equations).

Normalisation of surface TA and DIC to salinity 34 removed most of the otherwise unusually low values observed in the NNS (Figure 2.5A). Normalised DIC exhibited a slight peak in the NNS which is due to the underestimation of DIC in the Baltic Sea (see previous paragraph).

2.3.2.3 Bathymetry and biological processes

The shallow bottom depth in the EC and the SNS (<50 m) results in a rather well mixed water column throughout the year which is the reason for the mostly homogeneous DIC (Bozec et al. 2006) and TA vertical distributions also observed in this study (Figure 2.5B). The combination of continuous mixing and a warm water column also results in high pCO_2 values during summer: the CO_2 that was taken up during the spring bloom is released later during the summer and is distributed throughout the water column rather

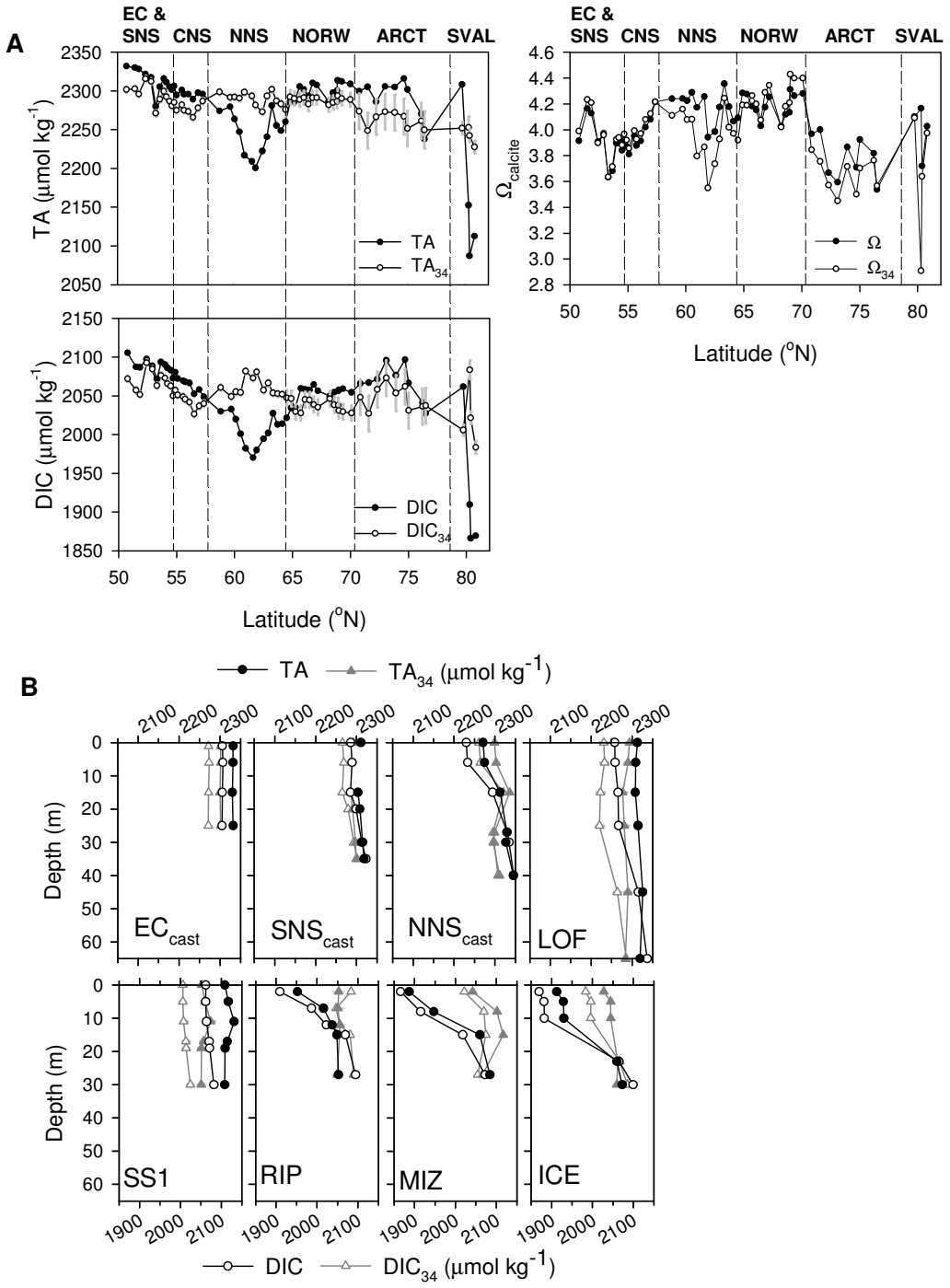

Figure 2.5 Surface (A) and vertical (B) distribution of observed and salinity normalized (S = 34) values of TA and DIC. Also shown (A) is the calculated $\Omega_{calcite}$ for observed and salinity normalized values. The error for the observed TA and DIC values was less than ±2 µmol kg^{-1} and for the normalized values ±1-9 µmol kg^{-1} (grey bars).

than being sequestered below the thermocline, leading to CO_2 supersaturation in the SNS (Thomas et al. 2004). The calculated surface pCO_2 values in the EC and the SNS in this study were 382 - 440 μatm (Figure 2.2D).

Sequestration of respiration products below the mixed layer explains the higher DIC values observed in the subsurface NNS, compared to the SNS. Indeed, in summer both the SNS and the bottom layer of the NNS are likely to be net heterotrophic while the surface layer of the NNS is net autotrophic (Bozec et al. 2005), resulting in the biological activity being the main controlling factor of pCO_2 in the NNS (Thomas et al. 2005b).

2.3.3 The Norwegian Sea

The surface properties of the Norwegian Sea varied relatively little along the route with no major fluctuations, apart from the transitional zone towards the North Sea, where lower salinity was observed (Figure 2.2A). Temperature ranged between 11.4 and 13.8ºC and salinity between 33.4 and 34.7, with warmer and fresher water towards the North Sea. DIC and TA mean values were ~2050 and 2295 μmol kg^{-1}, respectively, and were lower by 20 – 40 μmol kg^{-1} at the southern end due to dilution from Baltic Sea water. Salinity normalized TA was much more constant, only ranging between 2279 and 2293 μmol kg^{-1} (Figure 2.5A). Salinity normalized DIC fluctuated by a maximum of 19 μmol kg^{-1} between stations. However, the errors associated with the normalized TA and DIC values were ~ 10 μmol kg^{-1} (Figure 2.5A).

The surface – subsurface deficit of TA in LOF was rather small (-6 μmol kg^{-1}) compared to the DIC deficit (-79 μmol kg^{-1}). Salinity changes accounted for ~ 30% (-25 μmol kg^{-1}) of the total DIC deficit and around three times (-17 μmol kg^{-1}) the total TA deficit, however the errors associated with the deficits due to salinity were of the same order of magnitude (± 14 μmol kg^{-1}) (Figure 2.6, Table 2.1). Production of organic material accounted for most of the DIC deficit (~70%) and also contributed to the TA deficit. After accounting for these processes, no significant residuals remained for either TA or DIC, suggesting that there are no other processes exerting a major influence on TA or DIC in this location.

Table 2.1 Deficits in TA and DIC between surface and subsurface layers in each station. Deficits were attributed to salinity changes, organic matter production and other processes (residual). DIC deficits were based on either nitrate or phosphate uptake. $\Delta TA_{deficit}$ and $\Delta DIC_{deficit}$ are the total deficit in TA and DIC.

Station	**ΔTA deficit** µmol kg^{-1}	**ΔTA salinity** µmol kg^{-1}	**ΔTA org.** µmol kg^{-1}	**ΔTA residual** µmol kg^{-1}	**ΔDIC deficit** µmol kg^{-1}	**ΔDIC salinity** µmol kg^{-1}	**ΔDIC org. N** µmol kg^{-1}	**ΔDIC org. P** µmol kg^{-1}	**ΔDIC (N) residual** µmol kg^{-1}	**ΔDIC (P) residual** µmol kg^{-1}
EC_{cast}	0 ± 3	0 ± 6	0 ± 1	0 ± 7	1 ± 2	0 ± 6	0 ± 0	3 ± 1	0 ± 6	-3 ± 6
SNS_{cast}	-8 ± 3	-1 ± 6	-1 ± 0	-6 ± 7	-38 ± 2	-2 ± 6	-1 ± 0	-16 ± 2	-35 ± 6	-20 ± 7
NNS_{cast}	-74 ± 3	-62 ± 6	9 ± 2	-21 ± 7	-116 ± 2	-69 ± 6	-63 ± 1	-52 ± 10	17 ± 6	5 ± 12
LOF	-6 ± 3	-17 ± 13	8 ± 1	2 ± 13	-79 ± 2	-25 ± 14	-56 ± 1	-53 ± 5	2 ± 14	-2 ± 15
SS1	0 ± 3	-1 ± 11	0 ± 1	1 ± 11	-20 ± 2	-2 ± 11	-3 ± 1	-8 ± 7	-15 ± 11	-11 ± 13
RIP	-100 ± 3	-103 ± 20	5 ± 1	-1 ± 20	-185 ± 2	-179 ± 17	-42 ± 1	-40 ± 4	37 ± 17	34 ± 18
MIZ	-197 ± 3	-173 ± 12	1 ± 0	-25 ± 12	-206 ± 2	-173 ± 11	-15 ± 0	-21 ± 5	-18 ± 11	-12 ± 12
ICE	-160 ± 3	-129 ± 12	6 ± 1	-37 ± 12	-230 ± 2	-128 ± 11	-46 ± 1	-55 ± 8	-56 ± 11	-47 ± 14

2.3.4 The Arctic front and Svalbard

Two different Arctic environments were visited in this study, one south of Svalbard (ARCT: open water, influenced by the Arctic front) and one north of Svalbard (SVAL: shelf waters, influenced by the retreating ice). Mean DIC was higher in ARCT

(~2067 μmol kg^{-1}) than in NORW (~2050 μmol kg^{-1}), as was expected due to increased solubility of CO_2 in the colder waters (Figure 2.2C). TA, on the other hand, remained the same as in NORW (mean ~2291 kg^{-1}). Both DIC and TA decreased at the northern part of ARCT as a result of the lower surface salinity (Figure 2.2C), but were high at the well mixed SS1. At the strongly stratified ICE, MIZ and RIP stations, however, TA and DIC were much lower than elsewhere (<1910 and <2160 μmol kg^{-1}, respectively) even though temperature was very low as well (<0ºC) (Figure 2.2A, C). pCO_2 was also exceptionally low (130 – 150 μatm, far below equilibrium with the atmosphere (~385 μatm), as has been found also in other Arctic regions (Bates 2006, Fransson et al. 2009), while pH reached maximum values of up to 8.4 (Figure 2.2D).

These differences between localities were most likely a combined result of a) dilution due to ice melt and other freshwater inputs, b) DIC uptake due to biological activity, and c) partial or complete ice cover which restricted air-sea CO_2 exchange.

Table 2.2 DIC deficits attributed to $CaCO_3$ production/dissolution and associated residuals, when all of the TA residuals were attributed to this process. N.S. denotes not significant residual.

Station	**ΔTA residual (= $CaCO_3$)**	**ΔDIC $CaCO_3$**	**ΔDIC (N) residual**	**ΔDIC (P) residual**
	μmol kg^{-1}	μmol kg^{-1}	μmol kg^{-1}	μmol kg^{-1}
EC_{cast}	N.S.	–	–	–
SNS_{cast}	N.S.	–	–	–
NNS_{cast}	-21 ± 7	-10 ± 4	27 ± 7	16 ± 12
LOF	N.S.	–	–	–
SS1	N.S.	–	–	–
RIP	N.S.	–	–	–
MIZ	-25 ± 12	-13 ± 6	-5 ± 13	1 ± 14
ICE	-37 ± 12	-19 ± 6	-38 ± 13	-28 ± 15

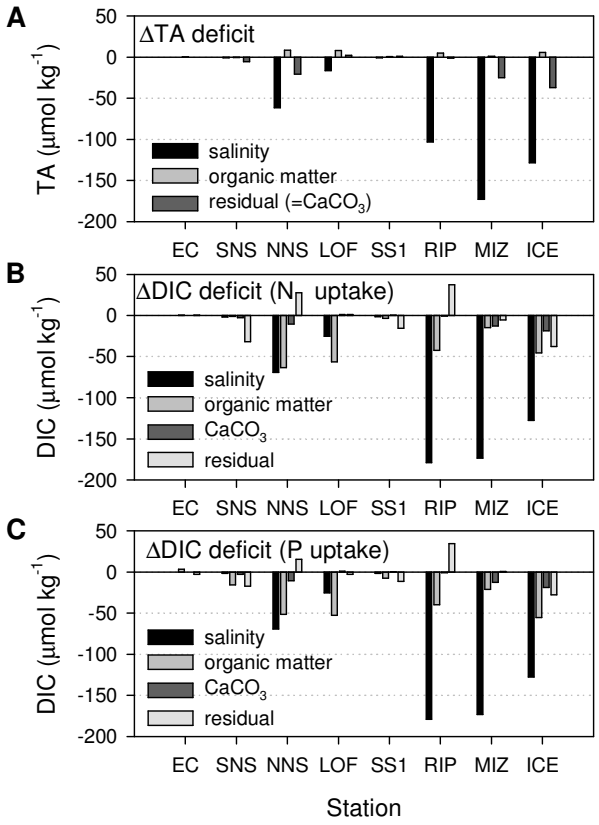

Figure 2.6 Deficits in A) TA and B, C) DIC between surface and subsurface layers at each station. Deficits were attributed to salinity changes, organic matter production, $CaCO_3$ production and other processes (residual). B) shows DIC deficits based on nitrate uptake and C) DIC deficits based on phosphate uptake. See Table 2.1 and 2.2 for errors associated with the deficits.

2.3.4.1 TA and DIC deficits

Water column data were acquired only for SVAL and not ARCT and hence deficits in TA and DIC were only calculated for the former. SS1 was well mixed and both TA and DIC were relatively evenly distributed in the surface layer (Figure 2.5B). $\Delta TA_{deficit}$ was practically zero and the $\Delta DIC_{deficit}$ was only -20 µmol kg^{-1} (Table 2.1). In contrast, the TA and DIC deficits at the stratified RIP, MIZ and ICE stations were the highest of all stations (Table 2.1).

At RIP, the observed total deficits were $\Delta TA_{deficit}$ = -100 µmol kg^{-1} and $\Delta DIC_{deficit}$ = -185 µmol kg^{-1} and salinity changes alone were able to explain the majority of the deficits (>97%, Table 2.1). However, the deficit in nutrients suggested an additional reduction in DIC due to organic matter production of about 42 µmol kg^{-1} in the surface of

RIP, leading to a positive DIC residual of around 37 μmol kg^{-1} (Figure 2.6, Table 2.1). This is considerably larger than the errors (±20 μmol kg^{-1}) associated with the TA and DIC residuals for this station.

At the MIZ station, salinity changes accounted for around 85% of the TA and DIC deficits. The remaining DIC deficit was explained by moderate organic matter production (half of what was estimated at RIP and ICE) (Figure 2.6, Table 2.1). The TA residual of -25 μmol kg^{-1} was attributed to carbonate mineral precipitation (biological or inorganic) which also accounted for most (-12.5 μmol kg^{-1}) of the DIC residual (Table 2.2).

Finally at the ICE station, where the largest DIC deficit was observed (-230 μmol kg^{-1}), salinity differences accounted for 80% of the TA deficit but only 55% of the DIC deficit (Figure 2.6, Table 2.1). The nutrient deficit suggested a decrease by around 50 μmol kg^{-1} in DIC due to organic matter production (Table 2.1). If the TA residual (-37 μmol kg^{-1}) was again attributed to carbonate mineral precipitation then this time it did not also account for most of the DIC residual as well (Table 2.2). A remaining -34 μmol kg^{-1} in the DIC deficit could not be explained by these processes.

2.3.4.2 Freshwater inputs

Temperature and salinity profiles (Figure 2.3A) indicated that the station with both the highest freshwater fraction (lowest salinity) and ice melt (highest temperature compared to the freezing temperature of seawater, -1.88ºC) in the surface layer was RIP (T = -0.11ºC, S = 30.7), followed by MIZ (T = -0.85ºC, S = 31.4) and ICE (T = -1.60ºC, S = 32.1), where the lowest freshwater fraction was observed. Station SS1 had a salinity of 35, so implying no freshwater inputs. Freshwater input originated mainly from sea ice melt but in RIP it is presumed that there was an additional source of land-fast/glacial ice melt and other melt-water runoff.

TA versus salinity plots (Figure 2.4) indicated low TA end members associated with sea ice melt. In ARCT, the freshwater fraction was small (lowest salinity 33.75) and the TA_0 of 360 μmol kg^{-1} suggests mixing of Atlantic waters with TA-poor recent sea ice melt at the northern part of ARCT (Figure 2.4B, D). In SVAL, the calculated end member TA for SS1, MIZ and ICE was low (TA_0 = 193 μmol kg^{-1}) with a near zero DIC_0 (-32 μmol kg^{-1}) indicating that sea ice melt was the freshwater source. The TA_0 for RIP,

however, was high (1207 μmol kg^{-1}) suggesting the input of a high TA freshwater source. The geology of Svalbard indicates some existence of carbonate rocks and calcic plagioclase in the proximity of RIP and under the icefield that drains into the Rijpfjorden (Harland 1997, Dallmann et al. 2002) Therefore, even though freshwater addition typically dilutes chemical properties such as TA and DIC, the scale of reduction depends on the properties of the freshwater source, as was concluded also for the influence of the Baltic Sea outflow (section 2.3.2.2).

TA in Arctic rivers is typically high (>1000 μmol kg^{-1}) (Olsson & Anderson 1997); in Eurasian Arctic rivers (Ob, Yenisey, Lena, Kolyma) TA can be as high as 1500 μmol kg^{-1} (Cooper et al. 2008) and the river runoff to the Mackenzie shelf is estimated to have a TA of 1494 μmol kg^{-1} (Fransson et al. 2009). Thus, it is not surprising to find a similar effect in RIP, where the end member TA is calculated to be 1207 μmol kg^{-1}. In contrast, sea-ice has a lower TA content and consequently sea ice melt would dilute TA to a greater degree than the same amount of river water (or in this case glacial/ melt-water runoff). The TA vs. salinity regression equation for SVAL (excluding RIP) gives TA values typical of sea ice: TA = 497 μmol kg^{-1} at S = 5 is within the range 403 – 573 μmol kg^{-1} reported by Rysgaard et al. (2007) for melted sea-ice in Franklin Bay, N Canada and Young Sound, NE Greenland, and slightly higher than values of 300 – 350 μmol kg^{-1} reported for sea-ice melt in the Chukchi Sea and along the NW Passage (Bates et al. 2009, Fransson et al. 2009). This enrichment in TA of sea-ice, is due to the fact that during wintertime sea-ice growth, DIC is rejected with brine more efficiently than TA (Rysgaard et al. 2007) resulting in a CO_2-rich brine and TA-rich sea-ice compared to the ratio in seawater (Rysgaard et al. 2009).

In sea ice, TA:DIC ratios have been found to be as high as 2:1, which indicates that carbonate minerals precipitate in natural sea-ice (Rysgaard et al. 2009, and references therein). Ikaite is one such mineral that has been found in Antarctic sea-ice (Dieckmann et al. 2008). Precipitation of such minerals might have been able to explain the negative TA residuals of ~ 30 μmol kg^{-1} in MIZ and ICE which suggest removal of TA from the surface waters. However, the precipitation of minerals would have occurred during wintertime ice formation and it is unlikely that the effect of this process on the surface waters would have persisted through to summer. Moreover, the low densities of coccolithophores found in SVAL during this study (up to 10 cells mL^{-1}, Charalampopoulou et al. 2011) and others in this area (up to 95 cells mL^{-1}, Heimdal

1983, Hegseth & Sunfjord 2008), suggest that biogenic calcification would not be able to account for the ~ 30 μmol kg^{-1} of TA residuals. Thus, some other unidentified process was responsible for the removal of surface TA in SVAL.

2.3.4.3 Biological processes

The estimated DIC deficits due to organic matter production were higher at RIP and ICE (~ -45 μmol kg^{-1}), intermediate in MIZ (~ -18 μmol kg^{-1}) and very low at SS1 (~ -5 μmol kg^{-1}). These deficits were the result of ongoing primary production (PP) since spring, when daylight and temperature started to increase. Moreover, two different kinds of algae contributed to DIC uptake: sea ice algae and phytoplankton in the water column. Therefore, it would not be possible to fully explain these deficits by looking at in situ pelagic primary production at the time of sampling, as these only represent instantaneous uptake rates of the pelagic phytoplankton community. Reference to these rates will be made, however, as a comparison with other studies and an indication of bloom/ non-bloom conditions.

In Arctic regions, the ice cover reduces light penetration and, in combination with very cold temperatures, inhibits algal growth in the water column. At the beginning of spring, when days start to become longer, ice algae start to attach on the underside of the ice and form mats. In the Svalbard region this has been observed to happen as early as the end of February or March (Hegseth 1992, 1998). Upon melting and as the ice substrate disappears, ice algae production is terminated and gives way to pelagic production which is favoured by the increased light and nutrient availability resulting from the shallow mixed layer. Pelagic blooms occur after ice break-up, when light can penetrate the water column unobstructed. Such blooms can occur as early as May in NW Spitsbergen, where pelagic PP in open water or in leads in the ice can reach 21 - 43 mmol C m^{-2} d^{-1} (Heimdal 1983). In the northern Barents Sea ice algal PP has been reported to be 0.01 – 4.3 mmol C m^{-2} d^{-1}; with the annual total PP estimated as 5.3 g C m^{-2}, it accounts for 16 – 22 % of total PP (Hegseth 1998). Pelagic PP in the same region during bloom conditions ranges between 16 – 30 mmol C m^{-2} d^{-1}, while in non-bloom conditions it is only 3.6 – 10 mmol C m^{-2} d^{-1} (Hegseth 1998). The pelagic PP rates observed in this study (Charalampopoulou et al. 2011) are intermediate to low and represent a non-bloom community: 5.6 mmol C m^{-2} d^{-1} in SS1, 1.8 mmol C m^{-2} d^{-1} in ICE and ~10 mmol C m^{-2}

d^{-1} in MIZ and RIP. The different values reflect the different stages of the phytoplankton community with respect to ice cover and ice melt. At SS1, an open water station, nutrients were depleted (Figure 2.3B) and the deep mixed layer indicates that the advantage of the shallow halocline resulting from ice melt had already 'been and gone', thus no longer encouraging a higher PP. In contrast, the low PP at ICE was probably the result of 10/10 ice coverage which did not allow light and nutrients to penetrate the water column. The nutrient and DIC deficits between surface and subsurface waters, however, could be attributed to ice algae PP. At MIZ and RIP, however, where the ice had started to break up, higher PP rates were observed.

2.3.5 Controls over saturation states

Calcite and aragonite saturation states are primarily controlled by the carbonate ion concentration and hence the difference (or the ratio) between TA and DIC, ($[CO_3^{2-}] \approx$ TA – DIC), and tend to increase at higher TA to DIC ratios (Bates et al. 2009). Therefore, the differential effects of processes on TA and DIC will have consequences for saturation states. In this study, saturation states co-varied with TA:DIC ratios (Figure 2.2E, F). Variations between 1.095 – 1.130 in TA:DIC caused a maximum change of 0.8 in $\Omega_{calcite}$ (3.5 – 4.3) and 0.5 in $\Omega_{aragonite}$ (2.2 – 2.7) across the sampling transect (Figure 2.2E, F, Figure 2.7).

The lowest Ω values were observed in the SNS and CNS and in ARCT. In contrast, the NNS, NORW and SVAL had higher Ω values. This runs contrary to the global pattern of higher Ω at the equator, declining towards the poles (e.g. Orr et al. 2005), which is behind the understanding that $\Omega < 1$ (undersaturation) will become widespread in polar waters first, as ocean acidification intensifies.

Primary production (drawdown of DIC without associated removal of TA) is known to lead to elevated carbonate ion concentrations and saturation states (Merico et al. 2006). This explains the higher values of Ω in the NNS and NORW regions, and the relatively lower Ω values in the EC and SNS regions where the absence of stratification prevents DIC from being drawn down to low levels by PP. When DIC and TA data are corrected for PP (using nitrate data) at NNScast and LOF stations, the calculated $\Omega_{calcite}$ values are lower than the observed by up to 0.8 units. The NNS was also enriched in TA due to the high alkalinity Baltic Sea input, which contributed towards higher saturation

states. High saturation states (~5) are observed in the central Baltic Sea during summer due to high water temperatures (~20ºC) and high removal of DIC by cyanobacteria, in contrast with the almost undersaturated conditions observed during winter, driven by extremely low temperatures (~0ºC) and low salinities (S ~ 7) (Tyrrell et al. 2008). This contribution of the high TA Baltic Sea water is evident when $\Omega_{calcite}$ is calculated using the normalized (S = 34) TA and DIC values (Figure 2.5A); in the area affected by the outflow (~60 – 63ºN) $\Omega_{calcite}$ is up to 0.3 units lower when calculated at salinity 34 than at *in-situ* salinity (Figure 2.5A).

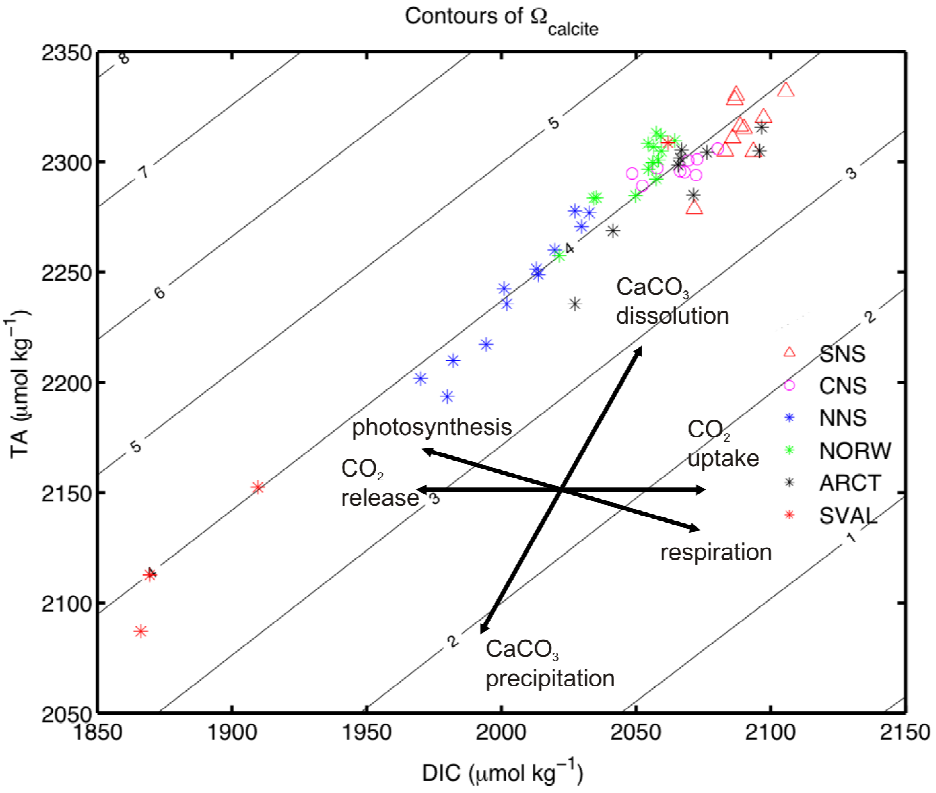

Figure 2.7 Surface calcite saturation state ($\Omega_{calcite}$) as a function of DIC and TA. Samples from different regions are colour coded. The direction and magnitude of change in these parameters due to various processes are indicated by black arrows (adapted from Zeebe & Wolf-Gladrow, 2001).

Mean DIC values were higher in ARCT (~2067 µmol kg^{-1}) than in NORW (~2050 µmol kg^{-1}), while TA remained the same (mean ~2291 µmol kg^{-1}). This led to lower saturation states in ARCT than in NORW. Finally, the intense spring-time PP and limited air-sea CO_2 exchange due to extensive ice cover, resulted in CO_2 undersaturation

in SVAL which in turn led to lower DIC concentrations and higher saturation states. Again, when DIC and TA data are corrected for PP at the SVAL stations, the calculated $\Omega_{calcite}$ values are lower than the observed by up to 0.8 units (Figure 2.5A).The enriched TA values of melt-water in RIP also contributed towards higher saturation states; $\Omega_{calcite}$ using normalised TA and DIC in RIP was lower than the observed values by 1.2 units (Figure 2.5A).

2.3.6 Implications for a changing Arctic

The Arctic is warming up faster than the rest of the world and ice melt becomes more extensive year after year (Stroeve et al. 2007). The results of this study suggest that ice melt will have both a direct impact on carbonate chemistry by diluting TA and DIC in the surface waters, and an indirect impact by altering the seasonal pattern in primary production associated with the ice-edge. Ice algae will contribute even less to total primary production as their habitat disappears. However, pelagic primary production is likely to be facilitated by the absence of ice due to increased light availability (Arrigo et al. 2008), depending on the level of macronutrient supply by vertical and lateral mixing. Earlier sea-ice melt and a longer growing season are likely to result in elevated saturation state and pH for a greater proportion of the year. Finally, the melting of terrestrial ice will increase riverine inputs in the surface Arctic coastal waters; this will decrease surface $[CO_3^{2-}]$ as well as the buffer capacity of these areas (Chierici & Fransson 2009). However, the majority of Eurasian and Canadian Arctic rivers have high TA, and the results of this study suggest that the higher TA:DIC ratio might lead to saturation states higher than expected.

2.4 Conclusions

TA and DIC deficits were measured between surface and subsurface waters in the North Sea, the Norwegian Sea and the Svalbard Arctic region, and deficits in salinity and nutrient concentrations were used to attribute these changes to physical and biological processes. This approach was quite successful, as the observed deficits in TA and DIC were often >100 μmol kg^{-1} but the residuals were always <40 μmol kg^{-1}. Most of the TA deficits (72 – 88%) were accounted for by salinity changes and organic matter

production. Some of the residuals were most likely due to calcium carbonate formation/ dissolution and were attributed to this. More than 65% of the DIC deficits were accounted for by these processes and in most cases the residuals were within the range of the expected errors.

This study showed that during summer there are two main processes that shape the carbonate chemistry of the North Sea, the Norwegian Sea and the Svalbard Arctic region: freshwater inputs and biological processes. Firstly, the freshwater sources of the Baltic Sea, sea ice melt and terrestrial runoff accounted for more than half of the change in TA and DIC in the northern North Sea and Svalbard. Additionally, the TA-rich freshwater sources of the Baltic Sea and terrestrial runoff also contributed towards high saturation states in the northern North Sea, the Norwegian Sea and in Rijpfjorden. Secondly, the absence of seasonal stratification caused CO_2 supersaturation and lower saturation states in the southern North Sea, whereas elsewhere along the transect and especially north of Svalbard primary production promoted CO_2 undersaturation and high pH and saturation states.

In conclusion, freshwater inputs and biological processes are driving the carbonate chemistry changes in the surface waters of the North Sea, the Norwegian Sea and the Svalbard Arctic region. Even though biological processes seem to play a major role in shaping the saturation state and pH of these regions, the carbonate chemistry of the freshwater sources (Baltic Sea, sea-ice melt, riverine input/ terrestrial runoff) is also important and may accentuate the effects of biological activity.

Chapter 3: Irradiance and pH affect coccolithophore community composition on a transect between the North Sea and the Arctic Ocean

Abstract

Little is known about the distribution of coccolithophores in Arctic regions, or the reasons why they are absent from certain locations but thrive in others. Factors thought to affect coccolithophore distribution include nutrients, salinity, temperature and light, as well as carbonate chemistry parameters. Here are presented data collected in summer 2008 along a transect between the North Sea and Svalbard (Arctic). Coccolithophore abundance and diversity were measured and compared to a set of environmental variables that included macronutrients, salinity, temperature, irradiance, pH and $\Omega_{calcite}$. Eighteen coccolithophore species were found in the Southern North Sea where coccolithophores were previously thought to be absent. In the ice-covered region north of Svalbard, coccolithophores were scarce and dominated by the family Papposphaeraceae. A multivariate approach showed that changes in pH and mixed layer irradiance explained most of the variation in coccolithophore distribution and community composition (Spearman's $r_S = 0.62$). Differences between the Svalbard population and those from other regions were mostly explained by pH ($r_S = 0.45$), whereas mixed layer irradiance explained most of the variation between the North Sea, Norwegian Sea and Arctic water assemblages ($r_S = 0.40$). Estimates of cell specific calcification rates showed that species composition can considerably affect community calcification. Consequently, future ocean acidification (changes in pH) and stratification due to global warming (changes in mixed layer irradiance) may influence future pelagic calcification by inducing changes in the species composition of coccolithophore communities.

3.1 Introduction

Coccolithophores are a diverse group of calcifying marine phytoplankton that might be either positively or negatively affected by climate change and ocean acidification (Doney et al. 2009). Their response to such changes is of great importance as they play a major role in the ocean carbon cycle by contributing to both the biological and carbonate pumps. They can contribute up to 20% of total primary production in selected oceanic regions (Poulton et al. 2007, 2010) and produce high numbers of coccoliths, thus dominating (50-80%) pelagic biogenic calcification (Milliman 1993, Broecker & Clark 2009). During calcification CO_2 is produced and as a result pCO_2 is often elevated in bloom areas (Holligan et al. 1993a, Merico et al. 2006). Moreover, coccolithophores may facilitate the transfer of organic carbon from the surface to the deep ocean as a result of the "ballast effect" imparted by their coccoliths (Klaas & Archer 2002). Hence, a change in coccolithophore calcite production, due to changes in either coccolithophore abundance or cellular calcification, could in turn affect the oceanic carbon cycle (Zondervan 2007) and ultimately feed back to climate change.

Predicted future changes in the ocean include sea surface warming (Barnett et al. 2005), shallowing of the mixed layer (Levitus et al. 2000), changing nutrient concentrations and light conditions (Bopp et al. 2001, Sarmiento et al. 2004), as well as ocean acidification (Orr et al. 2005). Extensive experimental and field research on *Emiliania huxleyi*, the most common modern coccolithophore, indicates that calcification in this species depends strongly on irradiance and is stimulated by nutrient stress, even though cells grow well under high nutrient concentrations and low irradiance too (see review by Zondervan 2007). However, elevated pCO_2 levels have varying effects on the calcifying ability of different *E. huxleyi* strains (Riebesell et al. 2000, Iglesias-Rodriguez et al. 2008, Langer et al. 2009) and of different coccolithophore species (Langer et al. 2006). Moreover, effects of simultaneous changes in multiple environmental variables are diverse. For example, light saturation for *E. huxleyi* growth depends on temperature (Paasche 2002, Zondervan 2007), while the sensitivity of *E. huxleyi* calcification and organic C fixation to elevated pCO_2 depend on their replete or depleted nutrient status (Sciandra et al. 2003, Delille et al. 2005, Engel et al. 2005) as well as available light (Zondervan et al. 2002, Feng et al. 2008). Hence, more research on synergistic effects of environmental variables over a wider range of coccolithophore species is essential.

Coccolithophores are widespread in the oceans; they are found in oceanic and coastal waters and they extend from the tropical to subarctic and subantarctic regions (Winter et al. 1994). They are most prominent in high latitude waters where *Emiliania huxleyi*, the most euryhaline and eurythermal species, forms blooms in regions such as the North Atlantic, the North Sea, the Barents Sea and the Bering Sea (Tyrrell & Merico 2004) when conditions are favourable; seasonally shallow mixed layer depths, high irradiances and high temperatures (Merico et al. 2004, Raitsos et al. 2006). Blooms also occur at the time of year when carbonate ion concentrations are seasonally high (Merico et al. 2006). Coccolithophore diversity, on the other hand, is highest in the warm, oligotrophic subtropical gyres (Winter et al. 1994).

Although their biogeography is relatively well mapped, it remains unclear why coccolithophores are absent from some regions whilst thriving in others. They are thought to be scarce in the Arctic, perhaps due to the low temperatures (<0°C) relative to optimal (2 - 15°C) bloom temperatures (Holligan et al. 1993b, Merico et al. 2004, Raitsos et al. 2006), although the exact cause is unknown, since very few studies have examined coccolithophores in polar waters. Early taxonomic work in Homer (South Alaska), Godhavn (West Greenland) and Resolute Bay (Northwest Passage) (Manton et al. 1976a, 1976b, 1977) indicated the presence of some coccolithophore species of *Papposphaera*, *Pappomonas*, *Turrisphaera* and *Wigwamma* in waters of <0^{o}C. The lack of quantitative data on Arctic coccolithophore assemblages and their calcification rates is a significant gap in current knowledge as the Arctic Ocean is particularly vulnerable to environmental changes: it has been warming two times faster than the rest of the world's oceans and models predict that it will be one of the first regions to experience widespread calcite undersaturation of surface waters (Orr et al. 2005, Steinacher et al. 2009).

Coccolithophores are also absent from sediments in the southern North Sea (SNS) and eastern English Channel, whereas they are found in high numbers in sediments of the northern North Sea (NNS) (Houghton 1991) and western English Channel. The high coccolithophore numbers found in the NNS sediments can be explained by the *Emiliania huxleyi* blooms observed there regularly both from satellites and from *in situ* sampling (Holligan et al. 1993b, Van der Wal et al. 1995, Buitenhuis et al. 1996, Marañón & González 1997, Burkill et al. 2002). However, such blooms are not observed in the SNS and water column data for this region are scarce. Blooms in the NNS coincide with enhanced thermal stratification and low summer nutrient concentrations, whereas the

possibly coccolithophore-barren SNS remains well mixed and, for this reason, has unusually high pCO_2 throughout the summer (Thomas et al. 2004), representing conditions potentially unfavourable for coccolithophores.

The main aim of this study was to collect coccolithophore diversity, abundance and calcification data along a transect of strong environmental gradients. This provided the opportunity to investigate whole community responses of natural coccolithophore populations to a wide range of environmental conditions. A sampling transect from the North Sea to Svalbard presented such strong environmental gradients and variability, as well as the opportunity to examine coccolithophore distribution in the SNS and in the high Arctic. A second goal was to use a multivariate approach to investigate which environmental variables, including temperature, salinity, irradiance, macronutrients and carbonate chemistry, most strongly influence coccolithophore distribution along this transect. Finally, *in situ* calcification was measured and used to estimate cellular calcification rates and to relate these to the assemblage composition.

3.2 Methods

3.2.1 Study area

The study area included four main hydrographic regions (Figure 3.1): a) the North Sea, subdivided into the well mixed southern part (SNS), the Atlantic influenced central part (CNS) and the stratified northern part (NNS) influenced by the Baltic Sea outflow (Kempe & Pegler 1991); b) the Norwegian Sea (NORW), characterised by the Norwegian Current flowing northward off the Scandinavian coast (Swift 1986); c) the continental shelf and slope south of Svalbard (ARCT), influenced by the Arctic Front (Swift 1986); and d), the partially ice-covered region north of Svalbard (SVAL).

3.2.2 Sampling

Sampling was conducted during the ICE-CHASER cruise (23/07/2008 – 21/08/2008) on board *RRS James Clark Ross* during a transect from Portland, U.K. to Svalbard in the Arctic (Figure 3.1). Both CTD - rosette deployments and the ship's continuous non-toxic underway supply were used for water sampling. Water samples for coccolithophore community abundance and diversity, carbonate chemistry parameters

and ancillary measurements were collected from 47 underway locations (~ 5m depth) and from 7 CTD deployments (see Figure 3.1); one in each of SNS (SNScast), NNS (NNScast), NORW (off the Loffoten Islands, LOF), an open water shelf station west of Svalbard (SS1), the Marginal Ice Zone (MIZ), an Ice station (ICE) and an Arctic fjord station at Rijpfjorden (RIP). Samples for primary production and calcification rates were collected from all CTD deployments except from SNScast.

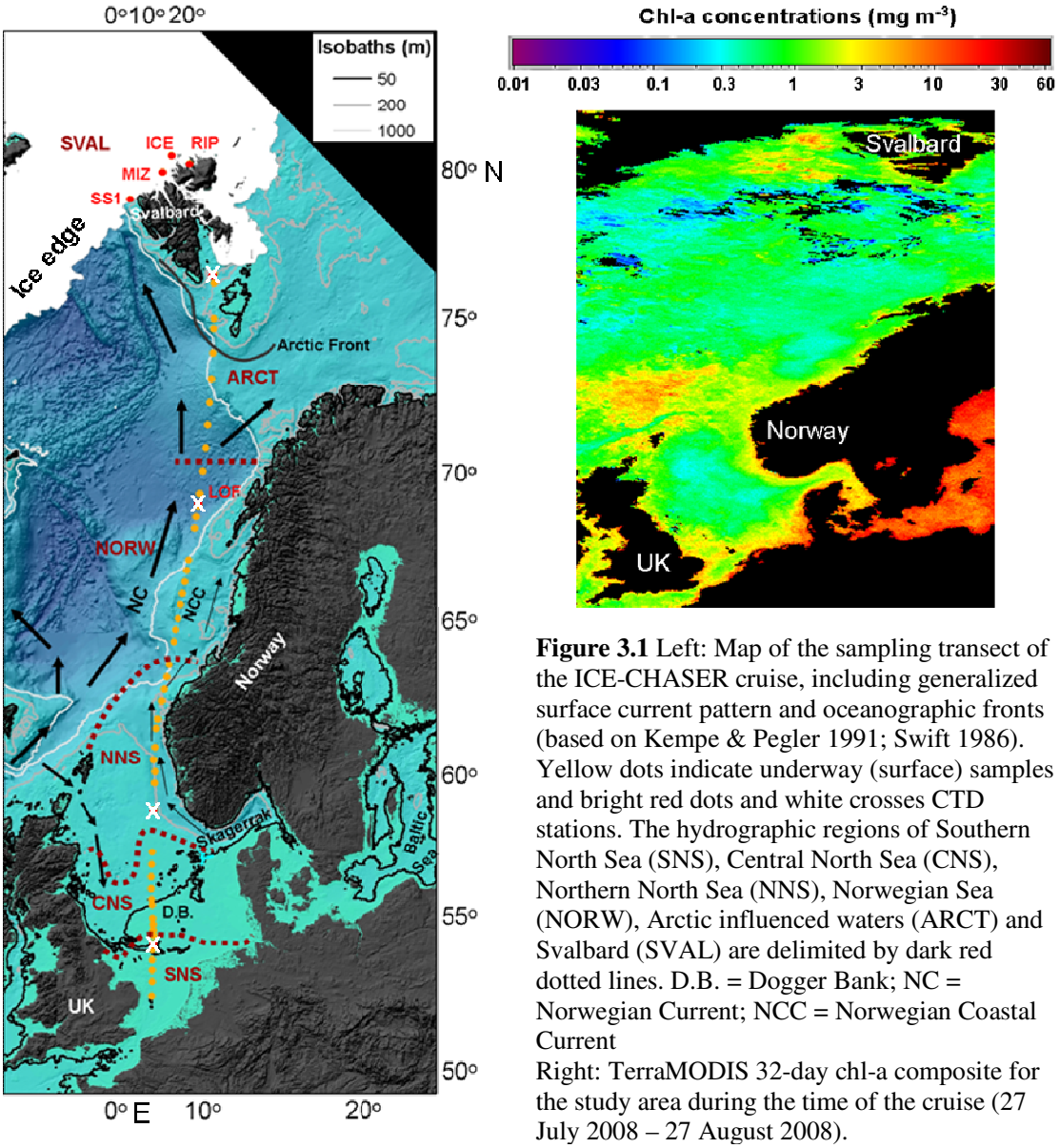

Figure 3.1 Left: Map of the sampling transect of the ICE-CHASER cruise, including generalized surface current pattern and oceanographic fronts (based on Kempe & Pegler 1991; Swift 1986). Yellow dots indicate underway (surface) samples and bright red dots and white crosses CTD stations. The hydrographic regions of Southern North Sea (SNS), Central North Sea (CNS), Northern North Sea (NNS), Norwegian Sea (NORW), Arctic influenced waters (ARCT) and Svalbard (SVAL) are delimited by dark red dotted lines. D.B. = Dogger Bank; NC = Norwegian Current; NCC = Norwegian Coastal Current
Right: TerraMODIS 32-day chl-a composite for the study area during the time of the cruise (27 July 2008 – 27 August 2008).

3.2.3 Coccolithophore community

Water samples (1 L) from either the underway supply or from each of 4 - 6 CTD depths were gently filtered onto Millipore Isopore membrane filters (25 mm diameter, 1.2 μm pore size), with a 25 mm diameter circle of 10 μm nylon mesh acting as a backing filter to achieve even distribution of cells. The membrane filters were rinsed with trace ammonia solution (pH 9-10) to remove salts, oven dried overnight at 30ºC and stored in the dark in sealed petri dishes. A radially cut portion of each filter was mounted on an aluminium stub and gold-coated. For each filter 225 fields of view (FOV; images), equivalent to ~ 1 mm^2, were taken at ×5000 magnification along a predefined meander-shaped transect, using a Scanning Electron Microscope (Leo 1450VP, Carl Zeiss, Germany) combined with the software SmartSEM. For each sample both coccospheres and coccoliths were enumerated until 300 of each were counted. The SmartSEM software allowed to set the scanning for zero overlap between FOVs. Duplicate counting of specimens that were on the edge between FOVs was avoided, by only counting the top and right edges of each FOV but not the bottom and left edges. The number of FOVs counted was used to calculate the area of the filter covered (the size of one FOV was 4.054×10^{-3} mm^2). Both coccospheres and coccoliths were identified to species level following Young et al. (2003), and the abundance of these for each species was calculated as:

$$\text{Coccospheres or coccoliths } mL^{-1} = C \times (F/A) / V \quad (3.1)$$

where C is the total number of coccospheres or coccoliths counted, A is the area investigated (mm^2), F is the total filter area (mm^2) and V is the volume filtered (mL).

Diversity in each sample was determined by three indices: species richness (the total number of species, *S*), Shannon-Wiener diversity index (*H'*) and Pielou's evenness (*J'*). *H'* accounts for both species richness and differing numbers of individuals, whereas *J'* expresses solely how evenly individuals are distributed among the species:

$$H' = -\sum_i p_i \log(p_i) \quad (3.2)$$

$$J' = H' / H'_{max} \quad (3.3)$$

where p_i is the proportion of the total count arising from the *i*th species.

3.2.4 Macronutrients

Phosphate and nitrate concentrations were determined using a Lachat 'QuikChem 8500' flow injection autoanalyser following the manufacturers recommended methods for orthophosphate and nitrate/nitrite (Lachat method nos. 31-115-01-1-G and 31-107-04-1-A). Samples were run in triplicate and salt corrected by analyzing Low Nutrient Sea Water purchased from OSIL (Batch LNS 16) prior to and within each batch of samples. The precision of nutrient measurements was ± 0.03μM for both phosphate and nitrate.

3.2.5 Chlorophyll-*a*

Water samples (200 - 500 mL) for chl-*a* analysis were filtered onto Whatman GFF (~0.7 μm pore size) filters and extracted in 7 mL 90% acetone for 24 h in the dark at 4°C. Chl-*a* fluorescence was measured on a Turner Designs AU-10 fluorometer equipped with Welschmeyer (1994) filters and calibrated using a pure chl-*a* standard (Sigma).

3.2.6 Mixed layer irradiance

In order to calculate average daily irradiance over the mixed layer, the mixed layer depth (MLD) was first determined as the shallowest depth corresponding to a density difference with the surface waters of more than $\Delta\sigma_t = 0.125$ sigma units (Monterey & Levitus 1997). The vertical attenuation coefficient (k_d) for downward irradiance and the subsurface instantaneous irradiance (E_0) at each of the 7 CTD deployments (and one additional deployment in ARCT, south of Svalbard; Figure 3.1) were calculated from PAR data from a CTD-mounted sensor using the relationship describing the exponential diminution of downward irradiance (E_z) with depth (z):

$$E_z = E_0 \times \exp(-k_d \times z) \quad (3.4)$$

The fraction of daily PAR (mol PAR m^{-2} d^{-1}) measured above the sea surface that reached below the sea surface was calculated using a ratio of instantaneous $E_0/E_{\text{above surface}}$

for each CTD station. Daily irradiance was then calculated at every 1 m down to the MLD:

$$E_{z,\ daily} = E_0/E_{above\ surface} \times \text{daily } PAR_{above\ surface} \times \exp(-k_d \times z) \quad (3.5)$$

The average irradiance over the mixed layer, E_{MLD} (mol PAR m^{-2} d^{-1}), was calculated as the sum of $E_{z,\ daily}$ at every 1 m down to the MLD, divided by the MLD.

A highly significant relationship was found between k_d and surface chl-*a* ($y = 0.1841x + 0.0685$, $R^2 = 0.9492$, $p = 0.005$, $n = 5$) which was used to calculate k_d values for the 47 underway locations from chl-*a* data only. These were used together with MLD and $E_0/E_{above\ surface}$ values extrapolated from the CTD stations and daily PAR to calculate E_{MLD} at each of the underway locations.

Comparison of daily PAR data from the ship's sensor with 32-day composite MODIS PAR data during the study period showed good agreement between the two and confirmed that daily PAR values were typical of the time of the year and were not biased by weather conditions at the time of measurement.

3.2.7 Carbonate chemistry

Samples for the determination of Dissolved Inorganic Carbon (DIC) and Total Alkalinity (TA) were drawn in 250 ml Schott ® SUPRAX borosilicate glass bottles following Dickson et al. (2007) to minimise gas exchange. A headspace of 1% was allowed for water expansion and samples were poisoned with 50 µL saturated mercuric chloride solution (7g per 100 mL). Sample analysis was undertaken at 25ºC using the VINDTA 3C (Marianda, Germany). DIC was determined coulometrically (coulometer 5011, UIC, USA) and TA was determined using a semi-closed cell titration (Dickson et al. 2007). Repeated measurements on the same batch of seawater ($n \geq 5$) were undertaken every day prior to sample analysis to assess the precision of the method. Certified Reference Materials (from A.G. Dickson, Scripps Institute of Oceanography) were analysed as standards to calibrate the instrument at the beginning and end of each day of analysis. Calcite saturation state ($\Omega_{calcite}$), pH and pCO_2 were calculated from DIC, TA, nutrients, temperature, salinity and pressure data using the CO2SYS.XLS program (Pierrot et al. 2006).

3.2.8 Multivariate data analysis

Multivariate statistics were used to assess spatial changes in coccolithophore community composition (biotic data) and environmental variables (abiotic data) following the methods described by Clarke (1993), using PRIMER-E (v. 6.0) (Clarke & Gorley 2006).

Analysis of biotic data was carried out on square-root-transformed species abundances, using Bray-Curtis similarity to determine changes in the abundance of dominant species as well as the less abundant species. Analysis of abiotic data was carried out on power transformed (to reduce skewness and stabilize the variance) and standardised (to bring all variables to comparable scales) values of E_{MLD}, salinity, temperature, pH, $\Omega_{calcite}$, nitrate and phosphate, using Euclidean distance to determine spatial changes in these variables.

Biotic and abiotic data were used independently to cluster samples into groups which were mutually similar, by means of both hierarchical agglomerative clustering (CLUSTER) and non-metric multi-dimensional scaling (MDS). Agreement between the two representations and a MDS stress value <0.1 was obtained for both biotic and abiotic data, which strengthened belief in the adequacy of both. Further confirmation of significant differences between clusters was assessed by performing an analysis of similarities (ANOSIM) on the *a priori* specified clusters.

The species typical of each group ('characteristic species') and the species responsible for the differences between groups ('discriminating species') were identified using the similarity percentages (SIMPER) routine. Characteristic species were defined as those cumulatively contributing about 90% to the Bray-Curtis similarity within each group and discriminating species were defined as those cumulatively contributing more than 50% to Bray-Curtis dissimilarity between groups. The SIMPER routine was also used to identify the environmental factors responsible for differences between environmental clusters, as those cumulatively contributing approximately 50% to the Euclidean distance between groups.

Spearman's rank correlation was used to search for relationships between the biotic and abiotic patterns and to identify which environmental variables(s) explained most of the variation in coccolithophore distribution (BEST routine).

3.2.9 Primary production and calcification

Water samples for rate measurements were collected before dawn or at the time of minimum light intensity at the Arctic stations, from 4 – 6 light depths (including 1%, 4.5%, 7%, 14%, 33% and 55% for SNScast, NNScast and LOF stations and 0.1 – 2% , 6 – 9%, 20%, 50% or 80% of incident PAR for SS1, ICE, MIZ and RIP stations) from the upper 65 m of the water column. Daily rates of primary production (PP) and calcification (CF) were determined following the 'micro-diffusion' technique of Paasche & Brubak (1994), as modified by Balch et al. (2000). Water samples (150 mL, 3 replicates, 1 formalin-killed blank) were collected from each light depth, spiked with 100 μCi of ^{14}C-labelled sodium bicarbonate (Perkin Elmer, U.K.) and incubated in on-deck incubators for 24 hrs. Light depths were replicated using a mixture of misty blue and neutral density filters, and samples were kept at ambient sea surface temperature by providing a continuous flow of water from the underway supply through the incubators.

Incubations were terminated by filtration through 25mm 0.2 μm polycarbonate Isopore filters, which were then acidified with 1 mL of 1% phosphoric acid to separate the inorganic fraction (labile, CF) from the organic fraction (non-labile, PP). The inorganic fraction was captured as ^{14}C-CO_2 on a β-phenylethylamine soaked filter and placed in a separate vial. Liquid scintillation cocktail was added to both vials and activity was measured on a TriCarb liquid scintillation counter. Counts were converted to uptake rates using standard methods. The average relative standard deviation (calculated as SD × 100/mean) of triplicate measurements was 18% (2 - 44%) for PP and 30% (2 – 99%) for CF. The formalin blanks represented a significant proportion of the CF signal (mean 61%), because of the low rates measured at all stations except LOF (see Results). Similarly high blank contributions have been reported in other studies, especially at the base of the euphotic zone where CF rates are low (Poulton et al. 2007, 2010). The blanks represented only 5% of the PP signal.

3.3 Results

3.3.1 Physicochemical setting

The cruise transect covered a range of bathymetry (<50 – 3000 m) and water masses (Figure 3.1) and hence strong environmental gradients. Temperature decreased

with latitude, from >15°C in the SNS to <0°C in SVAL, but peaked at 17.8°C in NNS (Figure 3.2A). Salinity was generally >34 with the exception of the Skagerrak water mass in the NNS and NORW (min. 30.6), which was influenced by the low salinity Baltic Sea outflow, and SVAL (min. 30.7), which was influenced by ice melt (Figure 3.2A). Both phosphate and nitrate concentrations were generally low (<0.5 and <0.2 μM, respectively), with the exception of three samples where high nitrate values (1.2 – 1.6 μM) were measured (Figure 3.2B). pH increased with latitude from a minimum of 8.01 in the SNS to a maximum of 8.43 in SVAL, whereas $\Omega_{calcite}$ was higher in the NNS and NORW (up to 4.3) and lower in the SNS, CNS, ARCT and SVAL (typically ~ 3.5 – 4.0) (Figure 3.2, Table 3.1).

The euphotic depth (Z_{eu}, 11 – 52 m) was typically deeper than the MLD (6 – 56 m), apart from within the SNS region and at station SS1 (Figure 3.2C). Daily PAR above the sea surface ($PAR_{above\ surface}$) decreased with latitude and was maximal at the SNS and NORW (Figure 3.2D). E_{MLD} was lowest in the SNS (mean 2.5 mol PAR m^{-2} d^{-1}), which was characterised by a well-mixed water column, where MLD was deeper than Z_{eu} (Figure 3.2C, D). High values of E_{MLD} (mean 6.9 – 7.9 mol PAR m^{-2} d^{-1}) were observed in the well stratified CNS and NNS, but the maximum E_{MLD} (17.8 mol PAR m^{-2} d^{-1}) was observed in NORW, which was characterised by a very shallow MLD (~10 m) (Figure 3.2C, D). Low E_{MLD} values were also found in ARCT and SVAL (mean 4.2 – 4.7 mol PAR m^{-2} d^{-1}) which were characterised by a shallow MLD but low $PAR_{above\ surface}$ (Figure 3.2C, D).

Satellite-derived sea-surface chl-*a* concentrations in the study area during the sampling period were generally <1 mg m^{-3} with slightly higher values in the SNS (up to 2 mg m^{-3}) and on the border between the NNS and NORW (Figure 3.1). *In situ* measurements of surface chl-*a* confirmed this range of values (Figure 3.2C). Integrated chl-*a* over the euphotic zone ranged from 15.7 to 56.3 mg m^{-2}, while integrated primary production (PP data not shown) ranged from 1.8 to 28.6 mmol C m^{-2} d^{-1}. The lowest integrated PP values (1.8 – 5.6 mmol C m^{-2} d^{-1}) were measured at the ICE and SS1 stations, even though these had the highest integrated chl-*a* values (45.1 – 56.3 mg m^{-2}). The highest PP values were measured at the LOF station, where chl-*a* values were moderate (23.4 mg m^{-2}). Moderate values of PP were measured at the NNScast, MIZ and RIP stations (8.1 – 11.2 mmol C m^{-2} d^{-1}), where the lowest integrated chl-*a* values were observed (15.7 – 18.7 mg m^{-2}).

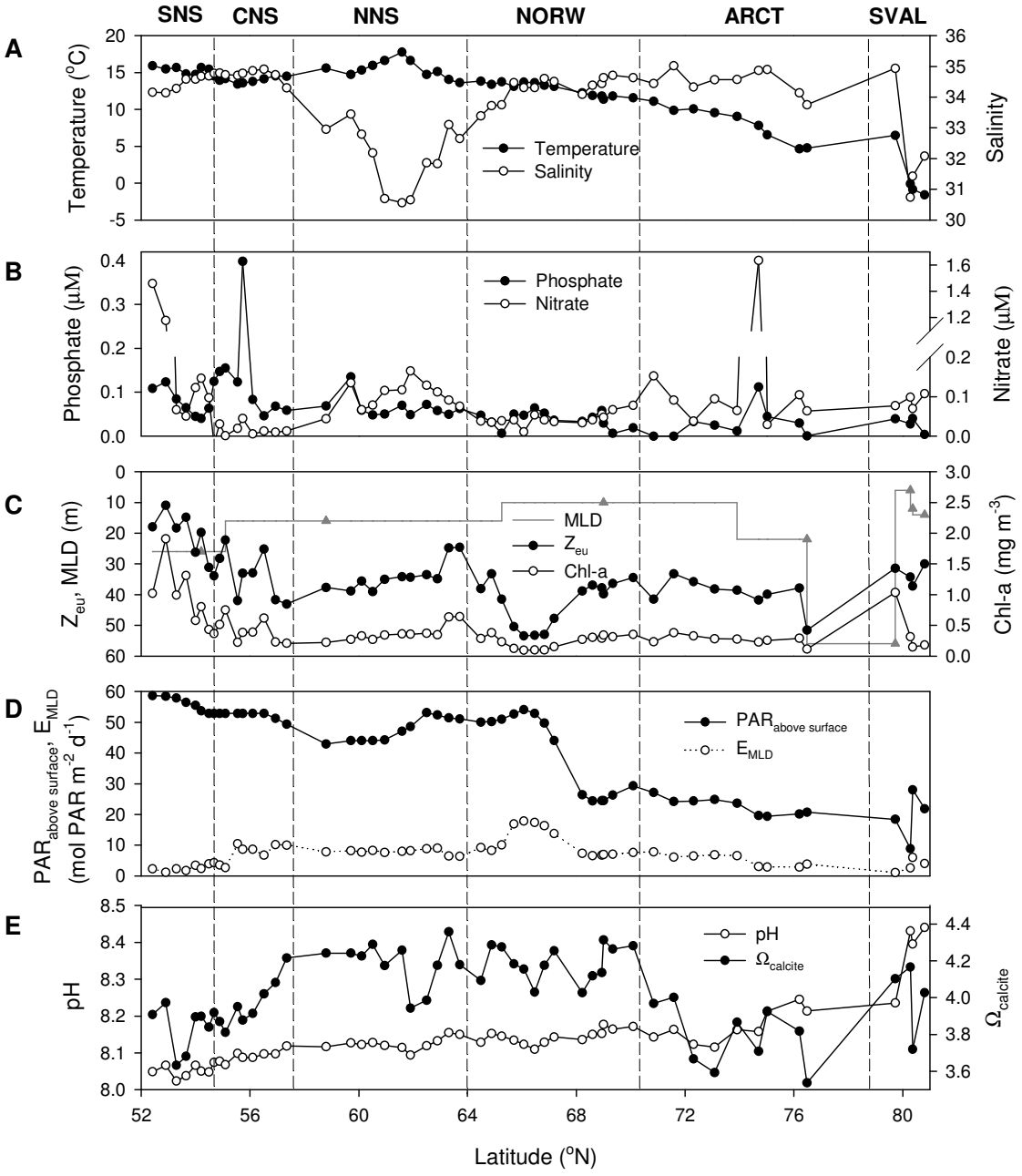

Figure 3.2 Physicochemical variables along the UK – Svalbard transect. A) Surface salinity and temperature. B) Surface phosphate and nitrate. C) Euphotic zone depth (Z_{eu}), mixed layer depth (MLD, triangles indicate CTD stations from which MLD was extrapolated) and surface chl-*a*. D) Above surface photosynthetically active radiation ($PAR_{above\ surface}$) and mixed layer irradiance (E_{MLD}). E) Surface pH and calcite saturation state ($\Omega_{calcite}$).

Table 3.1 Physicochemical characteristics of hydrographic regions. Average values are in bold and ranges in brackets. $\Omega_{calcite}$: calcite saturation state, E_{MLD}: mixed layer irradiance, PAR: Photosynthetically active radiation. Station SS1 has been included in the ARCT region, as it falls within the same range of temperature and salinity.

Region	Latitude (°N)	Influences	Depth (m)	Temperature (°C)	Salinity	pH	$\Omega_{calcite}$	Phosphate (µM)	Nitrate (µM)	E_{MLD} (mol PAR m^{-2} d^{-1})
Southern North Sea (SNS)	52.4 – 54.5	British rivers	<50	**15.4** (15.4 - 16.0)	**34.4** (34.1 – 34.7)	**8.04** (8.01 – 8.06)	**3.82** (3.61 - 3.95)	**0.08** (0.04 – 0.12)	**0.45** (0.05 – 1.46)	**2.5** (1.2 – 3.9)
Central North Sea (CNS)	54.7 – 57.4	Atlantic	<75	**14.0** (13.6 – 14.6)	**34.7** (34.3 – 34.9)	**8.07** (8.06 – 8.11)	**3.91** (3.80 – 4.20)	**0.14** (0.05 – 0.40)	**0.01** (0.00 – 0.04)	**6.9** (2.7 – 10.1)
Northern North Sea (NNS)	58.8 – 64.1	Baltic Sea, Norwegian Coastal Current	100 - 400	**15.3** (13.6 – 17.8)	**32.1** (30.6 – 33.4)	**8.11** (8.07 – 8.14)	**4.10** (3.83 – 4.30)	**0.07** (0.05- 0.13)	**0.10** (0.03 – 0.17)	**7.9** (6.3 – 9.0)
Norwegian Sea (NORW)	64.5 – 70.1	Norwegian Current	400 - 3000	**12.7** (11.4 – 13.8)	**34.3** (33.4 – 34.7)	**8.13** (8.10 – 8.17)	**4.17** (4.01 – 4.30)	**0.04** (0.01 – 0.06)	**0.04** (0.01 – 0.08)	**10.8** (6.6 – 17.8)
Arctic waters (ARCT)	70.8 – 76.5 (incl. SS1: 79.7)	Arctic Front	<200 - 2000	**8.0** (4.6 – 11.1)	**34.6** (33.7 – 35.0)	**8.17** (8.11 – 8.23)	**3.81** (3.51 – 4.10)	**0.03** (0.00 – 0.11)	**0.23** (0.03 – 1.63)	**4.7** (1.1 – 7.8)
North Svalbard (SVAL)	80.3 – 80.8	Ice edge	<200	**-0.9** (-1.6 – 0-.1)	**31.4** (30.7 – 32.1)	**8.40** (8.38 – 8.43)	**3.88** (3.63 – 4.06)	**0.02** (0.00 – 0.04)	**0.09** (0.07 – 0.11)	**4.2** (2.6 – 6.0)

3.3.2 Coccolithophore community composition

Coccolithophore abundance in surface waters was generally low (typically <200 cells mL^{-1}), but with higher values found in the CNS (max. ~950 cells mL^{-1}) and some areas of the SNS and NNS. Very low abundance values were observed in SVAL and throughout most of NORW (1 – 35 cells mL^{-1}) (Figure 3.3A). A total of 40 coccolithophore species were identified in the surface samples: 25 species were present in the NNS, only 5 in SVAL and 16 – 21 species were present in the other regions (Table 3.2). *Emiliania huxleyi* (Plate 1A) was generally the most abundant coccolithophore in most regions, contributing 32 – 100% towards total abundance (Figure 3.3A).

The highest values (1.5 – 2.1) of the Shannon – Wiener diversity index (*H'*) were observed in the CNS, NNS and NORW (Figure 3.3B) where *E. huxleyi* relative abundance was low (32 – 55%). Pielou's evenness (*J'*) was also high in these samples, suggesting a highly diverse community with little dominance by one or a few species. Along the rest of the transect, where relative abundances of *E. huxleyi* were high, both *H'* and *J'* were low, suggesting a less diverse community dominated by *E. huxleyi*. One exception was SVAL, where diversity (*H'*) was low but evenness (*J'*) was extremely high (Figure 3.3B). The coccolithophore community in this case was species-poor, with the individuals evenly distributed among *E. huxleyi* (Figure 3.3A), two species of the family Pappospheraceae (Figure 3.3C) - *Pappomonas* sp. Type 3 (after Young et al. 2003; Plate 1B) and *Papposphaera arctica* (Plate 1C) - and *Coccolithus pelagicus* (included in 'other' in Figure 3.3C). A highly significant relationship was found between diversity (*H'*, *y*) and *E. huxleyi* relative abundance (*x*) ($y = 4 \times 10^{-6}\, x^3 - 0.001\, x^2 + 0.068\, x + 0.454$, $R^2 = 0.923$, $P < 0.0001$). The polynomial trend demonstrates that diversity (*H*') was low both when *E. huxleyi* was dominant (100% relative abundance), but also when *E. huxleyi* was virtually absent (<0.1% relative abundance, Pappospheraceae dominance).

The cumulative relative abundance of the most numerous and commonly occurring species other than *E. huxleyi* is shown in Figure 3.3C. *Acanthoica quattrospina* (Plate 1D) was present in all regions apart from SVAL; *Calciopappus caudatus* (Plate 1E) made important contributions in the CNS, northern NORW and in ARCT. *Syracosphaera corolla* was characteristic of the SNS and CNS. However, the NNS was very diverse, with significant contributions from *A. quattrospina*, *C. caudatus*,

Corisphaera gracilis, *Palusphaera vandelii* and 5 different *Syracosphaera* spp. (Figure 3.3C).

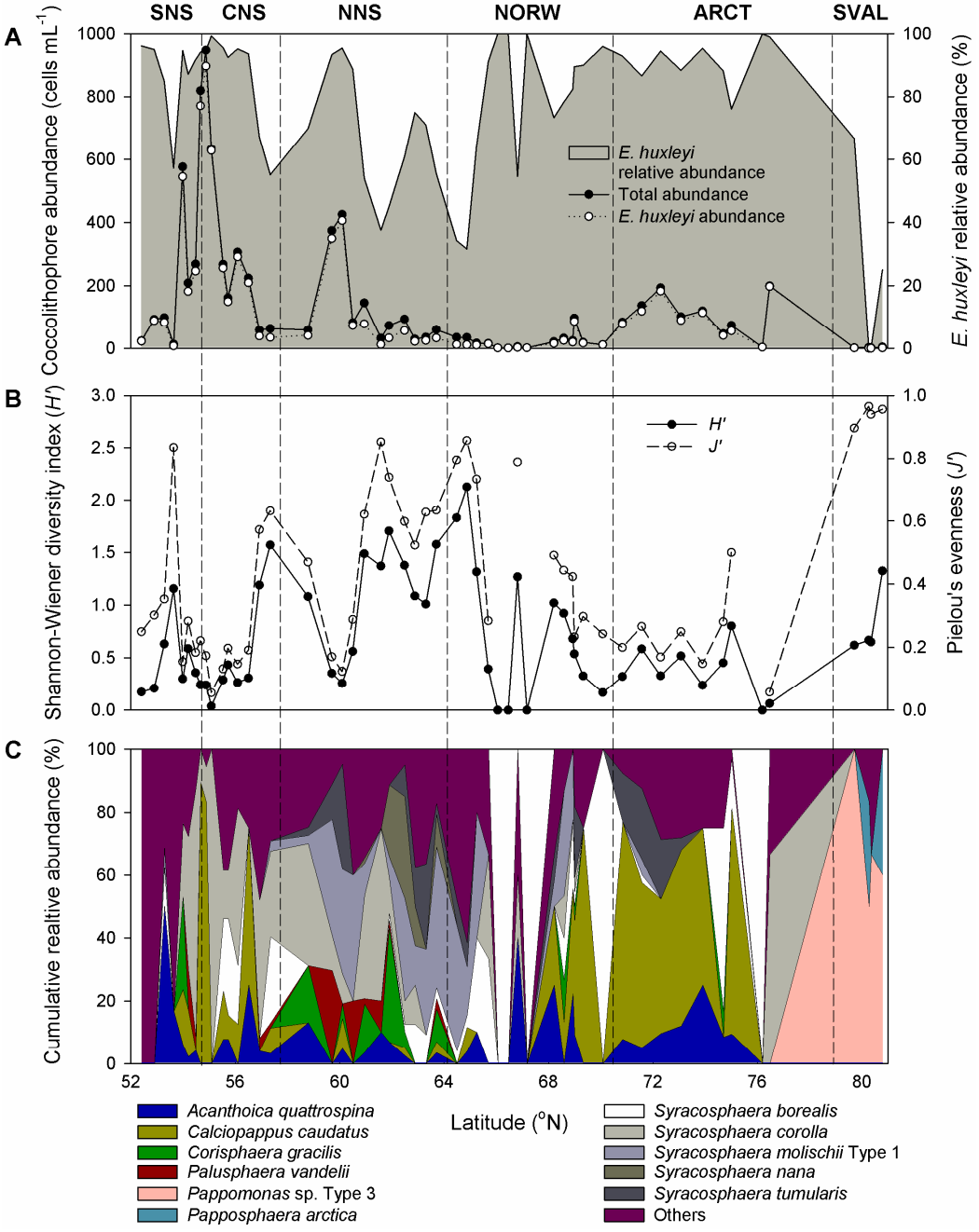

Figure 3.3 Diversity of the coccolithophore population along the UK – Svalbard transect. A) Total coccolithophore abundance, *Emiliania huxleyi* absolute abundance and *E. huxleyi* relative abundance. B) Shannon – Wiener diversity index and Pielou's evenness. C) Cumulative relative abundance of coccolithophores other than *E. huxleyi*. White blank triangles correspond to stations where the population consisted of 100% *E. huxleyi*.

Table 3.2 Species list and occurrence (+) of coccolithophores in surface (<5 m) samples. HOL: holococcolithophore stage.

Region	SNS	CNS	NNS	NORW	ARCT	SVAL
Total number of species	18	16	25	21	20	5
Emiliania huxleyi	+	+	+	+	+	+
Acanthoica quattrospina	+	+	+	+	+	
Acanthoica quattrospina HOL				+		
Algirosphaera robusta	+		+	+	+	
Alisphaera extenta	+	+		+	+	
Alisphaera gaudii					+	
Braarudosphaera bigelowii	+	+	+			
Calcidiscus leptoporous			+	+		
Calciopappus caudatus	+	+	+	+	+	
Calciosolenia murrayi			+			
Calyptrosphaera sphaeroidea			+	+		
Coccolithus pelagicus	+				+	+
Coccolithus pelagicus HOL	+	+	+	+	+	
Corisphaera gracilis	+		+	+		
Florisphaera profunda					+	
Gephyrocapsa oceanica					+	
Helicosphaera carterii HOL *perforata*			+			
Helladosphaera cornifera	+	+	+			
Homozygosphaera vercelii		+	+			
Ophiaster formosus			+	+		
Ophiaster hydroideus			+			
Ophiaster sp.		+	+	+		
Palusphaera vandelii	+	+	+			
Pappomonas sp. *Type 3* [a]					+	+
Papposphaera arctica [b]						+
Rhabdosphaera xiphos	+		+	+	+	
Saturnulus helianthiformis				+		
Sphaerocalyptra sp. HOL					+	
Syracosphaera bannockii				+		
Syracosphaera bannockii HOL	+	+		+	+	
Syracosphaera borealis	+	+	+	+	+	
Syracosphaera corolla	+	+	+	+	+	
Syracosphaera exigua	+					
Syracosphaera marginaporata			+	+		
Syracosphaera molischii type 1	+	+	+	+	+	
Syracosphaera nana			+			
Syracosphaera ossa		+	+		+	
Syracosphaera tumularis			+	+	+	
Syracosphaera sp.	+	+			+	
Wigwamma sp.						+

[a] *Pappomonas* sp. Type 2 was also found in samples deeper than 5 m
[b] *Papposphaera borealis* was also found in samples deeper than 5 m

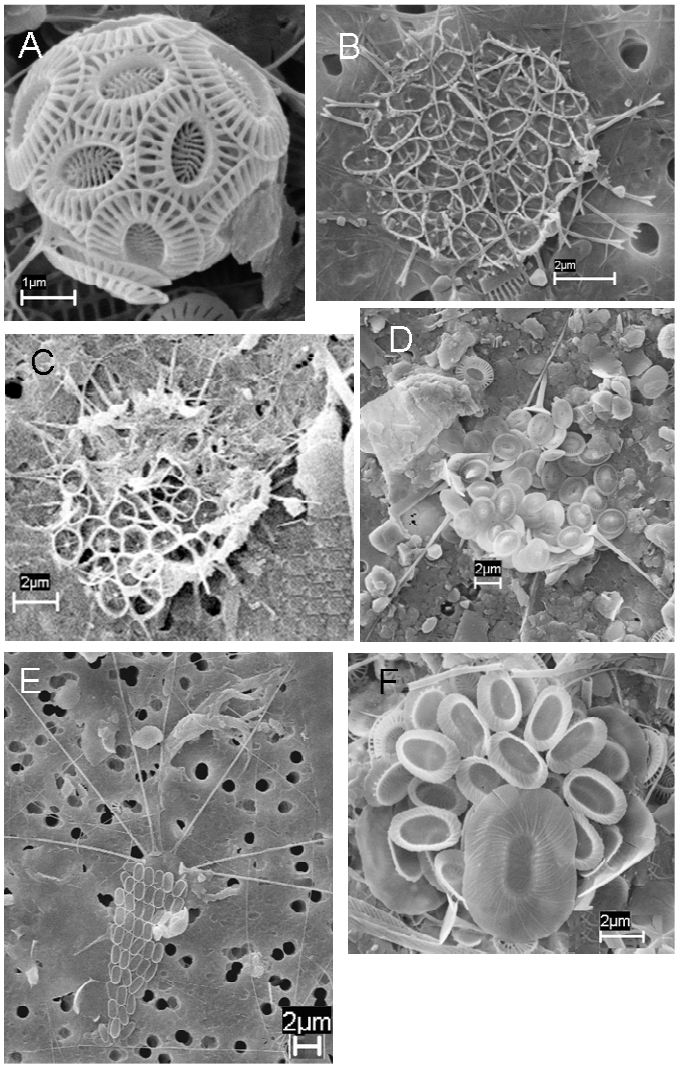

Plate 3.1 SEM images of some characteristic coccolithophore species. A) *Emiliania huxleyi* B) *Pappomonas* sp. Type 3 C) *Papposphaera arctica* D) *Acanthoica quattrospina* E) *Calciopappus caudatus* F) *Syracosphaera corolla*

3.3.3 Multivariate analysis of environmental and coccolithophore community data

3.3.3.1 Environmental data

CLUSTER and MDS analyses of all surface (0 - 5 m) samples based on temperature, salinity, pH, $\Omega_{calcite}$, nitrate, phosphate and E_{MLD} values, revealed six significantly different clusters or groups ($p < 0.05$) at the 2.8 similarity level (Euclidean distance; similarity increases with decreasing distance) (Figure 3.4A). An ANOSIM test

further confirmed that the groups are significantly different from each other ($p < 0.002$). These six groups correspond to the hydrographic regions described in Figure 3.2 and Table 3.1. At the 3.75 similarity level, three groups were formed: SNS samples clustered with ARCT ones, CNS, NNS and NORW clustered together, and SVAL remained a distinct group (Figure 3.4A). The stress value of the 2-dimensional representation was 0.18 which indicates that the 2-dimensional plot (Figure 3.4A) is a good representation of the high dimensional pattern (Clarke 1993).

SIMPER analysis showed that differences between environmental clusters were driven mainly by pH, $\Omega_{calcite}$ and E_{MLD} at the 3.75 similarity level and by these and additional factors (temperature, salinity, nitrate and phosphate) at the 2.8 similarity level (Table 3.3). The high pH at SVAL explained at least 30% of the differences between SVAL and the rest of the groups, whereas high E_{MLD} at NORW consistently explained differences between NORW and the other groups (Table 3.3). Low salinity at the NNS accounted for >27% of differences between NNS and the other groups (Table 3.3).

Table 3.3 SIMPER results of variables responsible for 50% of differences between environmental groups at the 2.8 and 3.75 similarity levels. Contribution of each variable to Euclidean distance between groups is given in brackets. $\Omega_{calcite}$: calcite saturation state, E_{MLD}: mixed layer irradiance.

Similarity level 2.8	SNS	CNS	NNS	NORW	ARCT
CNS	Nitrate (54%)				
NNS	Salinity (34%)	Salinity (39%)			
	$\Omega_{calcite}$ (25%)	Nitrate (27%)			
NORW	E_{MLD} (35%)	Phosphate (36%)	Salinity (37%)		
	$\Omega_{calcite}$ (23%)	E_{MLD} (25%)	E_{MLD} (18%)		
ARCT	Temperature (32%)	Phosphate (36%)	Temperature (27%)	$\Omega_{calcite}$ (31%)	
	Phosphate (22%)	Nitrate (23%)	Salinity (24%)	E_{MLD} (28%)	
SVAL	pH (45%)	pH (34%)	pH (38%)	pH (30%)	pH (36%)
	Temperature (26%)	Temperature (17%)	Temperature (34%)	E_{MLD} (16%)	Salinity (29%)
Similarity level 3.75	SNS-ARCT	CNS-NNS-NORW			
CNS-NNS-NORW	$\Omega_{calcite}$ (20%) E_{MLD} (19%)				
SVAL	pH (41%) Salinity (20%)	pH (34%) Temperature (21%)			

3.3.3.2 Coccolithophore community data

CLUSTER and MDS analysis of all surface (0 – 5 m) samples based on coccolithophore species composition and abundance rather than environmental data, also revealed six significantly different clusters or groups ($p < 0.05$) (Figure 3.4B). An ANOSIM test further confirmed the groups are significantly different from each other ($p < 0.05$). Overlaying the environmental clusters, as identified by the independent MDS analysis (see Figure 3.4A), onto the species clusters, showed a clear match between the two patterns. Species cluster 1 was associated with the southern NORW, species cluster 2 with the CNS, species cluster 3 with ARCT, species cluster 4 with the NNS, species cluster 5 with SVAL, and species cluster 6 with northern NORW (Figure 3.4B, Table 3.4). The biotic and abiotic characteristics of each of these groups are given in Table 3.4.

The characteristic species for each cluster, as identified by the SIMPER routine, agreed with those described in Figure 3.3C. *Emiliania huxleyi* was present in all regions apart from SVAL; *Syracosphaera borealis* and *Syracosphaera molischii* were typical of species cluster 1; *Syracosphaera corolla* of species cluster 2; *Calciopappus caudatus* and *Acanthoica quattrospina* of species cluster 3; *S. corolla*, *A. quattrospina*, *S. molischii*, *Corisphaera gracilis*, *Palusphaera vandelii* and *Syracosphaera nana* of species cluster 4; *Pappomonas* sp. Type 3 and *Papposphaera arctica* of species cluster 5; and *E. huxleyi* was the only characteristic species of cluster 6 (Table 3.4). The same species were also good discriminators between groups, as demonstrated by the SIMPER routine.

3.3.3.3 Matching biotic to abiotic data

Multivariate analysis (Spearman's Rank correlation, r_s) of the coccolithophore assemblage and environmental patterns showed that most of the variation in coccolithophore distribution could be explained by variation in pH and E_{MLD} ($r_s = 0.62$), and the single environmental variable explaining most of the variation in the biotic pattern was pH ($r_s = 0.45$) at the 0.1% significance level (Table 3.5). As SVAL was very different in terms of coccolithophore composition and environmental variables from all other regions, Spearman's Rank correlation analysis was repeated on all samples except SVAL to identify which variables could explain coccolithophore variation within the more closely related SNS, CNS, NNS, NORW and ARCT regions. Again, variation in

pH and E_{MLD} explained most of the variation in coccolithophore distribution (r_s = 0.45) at the 0.1% significance level (Table 3.5). The single environmental variable, however, explaining most of the variation in the biotic pattern in these regions was E_{MLD} (r_s = 0.40 at the 0.1% significance level) (Table 3.5). This is the first time that a recognised multivariate statistical approach has been used on observational data to relate coccolithophore distribution to all of the environmental variables influencing coccolithophore growth.

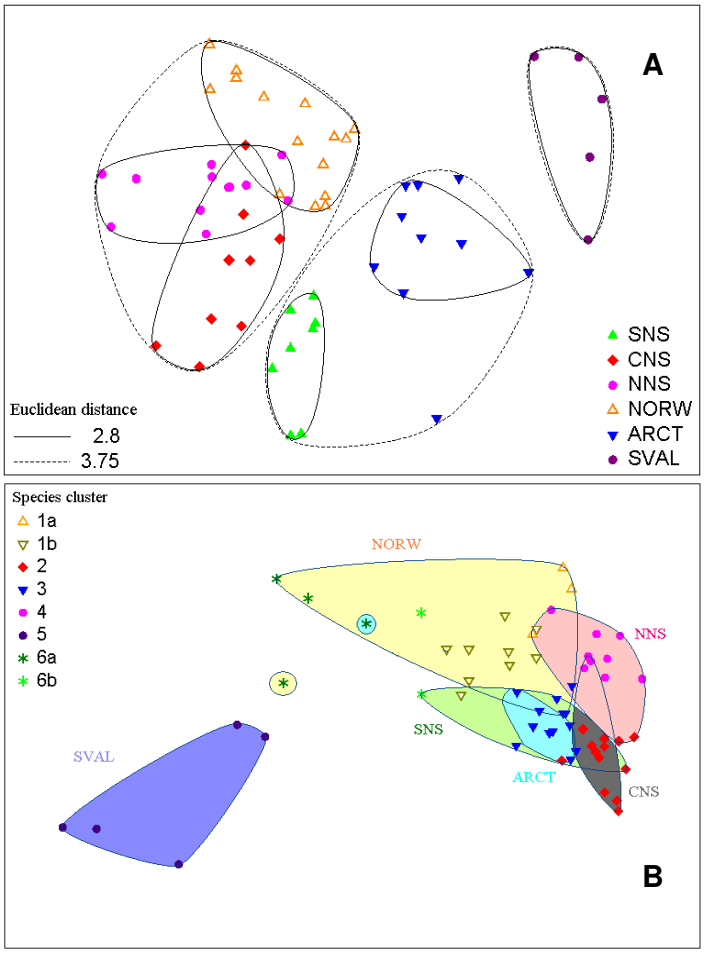

Figure 3.4 Non-metric multidimensional scaling (MDS) ordination of A) environmental variables based on Euclidean distance; and B) coccolithophore abundance and species composition (symbols) based on Bray-Curtis similarity. A) demonstrates spatial environmental changes; solid and dashed lines represent the superimposed sample clusters at the similarity levels of 2.8 and 3.75 Euclidean distance, respectively. B) demonstrates spatial community changes; superimposed shaded areas represent the hydrographic regions associated with the species groups as identified by independent MDS analysis, shown in (A).

Table 3.4 Summary of coccolithophore assemblage and physicochemical properties of each group identified by MDS analysis. Average values are in bold and ranges in brackets. The regions associated with each cluster are given. $\Omega_{calcite}$: calcite saturation state, E_{MLD}: mixed layer irradiance.

Cluster	Total abundance (cells mL^{-1})	*Emiliania huxleyi* relative abundance (%)	Characteristic species [a]	No. of species	Temperature (°C)	Salinity	pH	$\Omega_{calcite}$	Phosphate (µM)	Nitrate (µM)	MLD irradiance (mol PAR m^{-2} d^{-1})
1 NORW (south)	**25** (12 – 35)	**74** (32 – 96)	*E. huxleyi* *S. borealis* *S. molischii*	**6** (2 – 12)	**13.2** (11.6 – 15.9)	**33.9** (31.8 – 34.7)	**8.14** (8.05 – 8.17)	**4.17** (3.91 – 4.36)	**0.04** (0.01 – 0.06)	**0.06** (0.03 – 0.11)	**8.6** (6.4 – 16.9)
2 SNS, CNS	**415** (161 – 948)	**94** (87 – 99)	*E. huxleyi* *S. corolla*	**6** (2 – 9)	**13.8** (4.8 – 15.7)	**34.4** (32.8 – 34.9)	**8.09** (8.04 – 8.21)	**3.91** (3.54 – 4.24)	**0.11** (0 – 0.40)	**0.07** (0 – 0.15)	**5.4** (2.4 – 10.5)
3 ARCT	**111** (46 – 224)	**89** (76 -95)	*E. huxleyi* *C. caudatus* *A. quattrospina*	**6** (2 – 10)	**11.4** (6.5 – 16.0)	**34.4** (32.2 – 35.0)	**8.13** (8.02 – 8.11)	**3.94** (3.59 – 4.30)	**0.03** (0 – 0.08)	**0.06** (0.01 – 0.15)	**6.2** (2.3 – 8.3)
4 NNS	**71** (33 – 145)	**57** (38 – 70)	*E. huxleyi* *S. corolla* *A. quattrospina* *S. molischii* *C. gracilis* *P. vandelii* *S. nana*	**10** (5 – 13)	**15.5** (13.6 – 17.8)	**32.4** (30.6 – 34.7)	**8.11** (8.09 – 8.15)	**4.13** (3.94 – 4.26)	**0.06** (0.05 – 0.07)	**0.08** (0.01 – 0.17)	**8.3** (6.3 – 10.1)
5 SVAL	**2.5** (1.4 – 3.7)	**9** (0 – 25)	*Pappomonas* sp. *P. arctica*	**3** (1 – 4)	**-1.0** (-1.6 - -0.1)	**31.8** (30.7 – 32.9)	**8.40** (8.36 – 8.43)	**3.89** (3.63 – 4.06)	**0.03** (0 – 0.06)	**0.16** (0.04 – 0.51)	**3.8** (2.6 – 6.0)
6 NORW (north)	**3.7** (0.5 – 13)	**83** (55 – 100)	*E. huxleyi*	**2** (1 -5)	**11.4** (4.6 – 14.8)	**34.5** (34.1 – 34.9)	**8.15** (8.04 – 8.25)	**4.05** (3.68 – 4.25)	**0.05** (0.03 – 0.06)	**0.06** (0.01 – 0.11)	**10.1** (1.1 – 17.8)

Table 3.5 Spearman's Rank correlation (BEST routine) of coccolithophore assemblage distribution and environmental variables using data from all regions and excluding SVAL (Svalbard). Correlations of $r_S > 0.3$ are significant ($p < 0.001$). $\Omega_{calcite}$: calcite saturation state, E_{MLD}: mixed layer irradiance.

All regions		Excluding SVAL	
Environmental variable	Spearman's Rank correlation	Environmental variable	Spearman's Rank correlation
pH, E_{MLD}	0.622	pH, E_{MLD}	0.447
pH	0.454	E_{MLD}	0.399
Temperature	0.311	pH	0.149
E_{MLD}	0.292	Salinity	0.085
Salinity	0.258	$\Omega_{calcite}$	0.082
$\Omega_{calcite}$	0.058	Temperature	0.041
Phosphate	0.008	Nitrate	-0.009
Nitrate	-0.072	Phosphate	-0.075

3.3.4 Calcification: Total and cell-normalised

Discrete total calcification (CF) values ranged from <1 to ~300 µmol C m^{-3} d^{-1} (Figure 3.5). At the NNScast and LOF stations, CF was high at the surface but also exhibited a deep maximum, well below the mixed layer. CF was uniform with depth at stations SS1 and MIZ, whereas a deep CF maximum below the mixed layer was observed at stations ICE and RIP (Figure 3.5). Highest CF values were observed at the LOF station (100 – 300 µmol C m^{-3} d^{-1}), whereas low CF was measured at all other stations (<1 – 16 µmol C m^{-3} d^{-1}), except for a deep maximum (~50 µmol C m^{-3} d^{-1}) at 20 m at the ICE station.

Cell-CF was generally <1 pmol C $cell^{-1}$ d^{-1}. Exceptions included surface and deep maxima at the LOF station and SS1 and MIZ surface values, where higher cell-CF was estimated (1.4 – 2.9 pmol C $cell^{-1}$ d^{-1}), whereas the maximum cell-CF was found at 20 m at the ICE station (5.9 pmol C $cell^{-1}$ d^{-1}) (Figure 3.5). Cell-CF was generally minimal at the base of the euphotic zone, except at the LOF station where a deep maximum was observed just below the base of the euphotic zone (Figure 3.5).

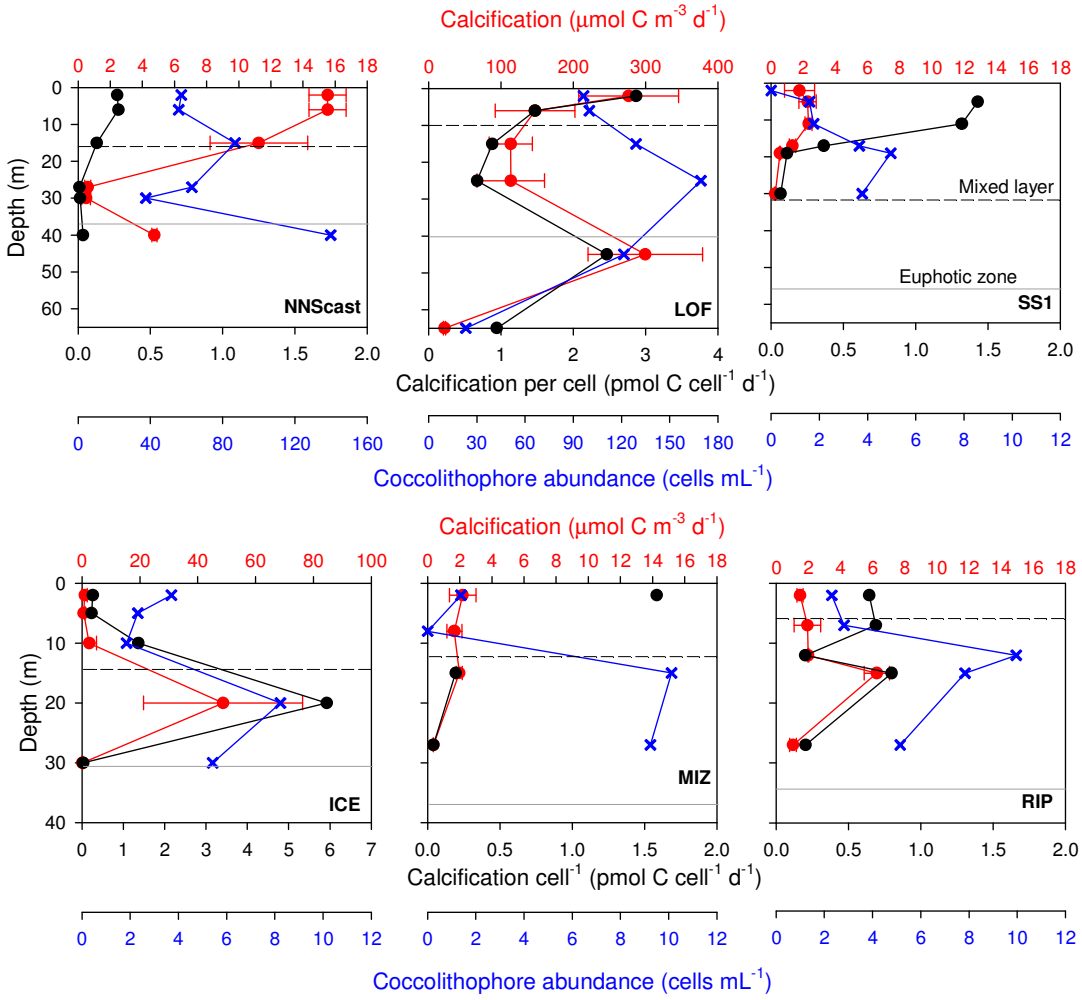

Figure 3.5 Total calcification rates (red), calcification rates per cell (black) and coccolithophores abundance (blue) at NNScast, LOF, SS1, ICE, MIZ and RIP stations. For station locations see Figure 3.1.

3.4 Discussion

3.4.1 Regional coccolithophore distribution

3.4.1.1 North Sea

In this study, surface waters were directly sampled to test the picture of diversity suggested by the sediments, i.e. that coccolithophores are more diverse in the NNS but are virtually absent south of ~ 54ºN (Braarud et al. 1953, Houghton 1991). Thirty coccolithophore species were found in the North Sea (as opposed to 13 recorded by Braarud et al. 1953), and most were observed both in the SNS and the NNS, although

decreasing diversity towards the south was also noted. *Emiliania huxleyi* was generally dominant, in agreement with studies by Braarud et al. (1953) and Houghton (1991). However, *E. huxleyi* numerically contributed as little as 30 – 60% of total counts in some of these samples.

A few of the characteristic species have not been recorded before in the North Sea. *Calciopappus caudatus* has only been reported in the low salinity Skagerrak water mass (Schei 1975), whereas in this study it was present in both the SNS and CNS. Most of the *Syracosphaera* species, as well as *Corisphaera gracilis* and *Palusphaera vandelii,* have not been reported in the North Sea before, either in water samples or in sediments. The disagreement with previous studies most likely results from more effective methods of preservation and species identification used in this study compared to those used in the past. Tidal activity might explain the absence of coccolithophores from sediments. Strong tidal currents characteristic of the North Sea may prevent accumulation and/or preservation of coccoliths on the seafloor, through advective removal and mechanical breakdown.

3.4.1.2 Norwegian Sea

Coccolithophores have been relatively well studied in the Norwegian Sea (Samtleben & Schröder 1992, Samtleben et al. 1995). Up to 20 species have been previously recorded (Samtleben & Schröder 1992, Samtleben et al. 1995) with *Acanthoica quattrospina*, *Syracosphaera borealis*, *Syracosphaera corolla*, *Syracosphaera molischii*, *Syracosphaera nana*, and *Corisphaera gracilis* all being characteristic of the region and occurring at temperatures >9 – 10ºC. A similar species composition was found in this study, with 21 species recorded in total. In addition, *Calciopappus caudatus*, which is known to tolerate cooler temperatures and to have a distribution similar to polar species such as *Coccolithus pelagicus* (Samtleben & Schröder 1992), was observed in the northern part of the Norwegian Sea. The low abundances (<100 cells mL^{-1}) found in early August agree with other studies of the same area at similar times of the year (e.g. max. 70 cells mL^{-1} in the Norwegian Current east of Jan Mayen; Samtleben & Shröder 1992).

3.4.1.3 Arctic Ocean

Two different Arctic assemblages (Figure 3.4B) were observed in this study. One assemblage, south of Svalbard (ARCT) in an area of mixed Arctic surface waters of Atlantic origin (4 – 10°C) was dominated by *Emiliania huxleyi*, with contributions from *Acanthoica quattrospina*, *Calciopappus caudatus*, *Syracosphaera borealis* and *Syracosphaera tumularis*. The other assemblage, north of Svalbard (SVAL) and influenced by retreating ice (<0°C), was characterised by *Pappomonas* spp. and *Papposphaera* spp.

Emiliania huxleyi and *Calciopappus caudatus* are thought to be characteristic of Atlantic-Arctic mixed waters (Samtleben & Schröder 1992, Samtleben et al. 1995), and cell densities observed in this study (average: 111 cells mL^{-1}) agree with previous studies south of Svalbard (Samtleben et al. 1995, Baumann et al. 1997, Baumann et al. 2000). However, the only other studies that have recorded coccolithophores in high Arctic regions such as the area north of Svalbard (SVAL) are early taxonomic studies in which most of these species were first described (Manton et al. 1977, Thomsen 1981 and references therein). The genera *Pappomonas*, *Wigwamma*, *Turrisphaera*, *Papposphaera*, *Balaniger*, *Calciarcus*, *Trigonaspis* and *Quaternariella* were reported in Godhavn (West Greenland) in1972 and 1977. *Wigwamma* and *Turrisphaera* were also found in Resolute Bay (Northwest Passage) in 1973, and the genera *Pappomonas*, *Papposphaera*, *Calciarcus*, *Wigwamma* and *Turrisphaera* were all present in Homer (South Alaska) in 1975. The findings in this study of *Pappomonas* spp. and *Papposphaera* spp. north of Svalbard are consistent with these previous studies. Also, individuals of *Wigwamma* spp. were found in surface and subsurface (>15 m) samples of the ICE, MIZ and RIP stations. None of *Calciarcus*, *Turrisphaera* and *Trigonaspis* were found, however, these are thought to be holococcolith-bearing phases of the genera *Wigwamma*, *Papposphaera* and *Pappomonas*, respectively (Thomsen et al. 1991).

Coccolithus pelagicus was occasionally found at low cell densities (up to 4 cells mL^{-1}) in SVAL samples, in contrast to the relatively high densities of this species (up to 100 cells mL^{-1}) usually encountered in the Greenland Sea (Baumann et al. 2000). Hence, it appears that the Svalbard assemblage was more similar to other polar assemblages from continental shelf locations (Godhavn, Resolute Bay, Homer) rather than the oceanic assemblage usually found in the Greenland Sea. *Emiliania huxleyi* cells were also

occasionally found at very low densities (<2 cells mL^{-1}) at the SS1 and ICE stations, whereas Manton et al. (1977) and Thomsen (1981) found this species to be completely absent from Godhavn, Resolute Bay and Homer during the 1972 – 1977 period. *Emiliania huxleyi*, however, was found in moderate densities (8 – 69 cells mL^{-1}) north of Svalbard in September – October 1979 (Heimdal 1983) and more recently in August 2003 (19 – 95 cell mL^{-1}; Hegseth & Sundfjord 2008). It is most likely that *E. huxleyi* cells from the northern North Atlantic are occasionally transported along the west coast of Svalbard by the West Spitsbergen Current and into high Arctic areas, as has been found for other Atlantic phytoplankton species (Hegseth & Sundfjord 2008). Similarly, *E. huxleyi* blooms in the Barents Sea also follow the Atlantic water distribution (Smyth et al. 2004). On the other hand, the absence of *E. huxleyi* from the Northwest Passage and the West Greenland shelf could be attributed to the fact that these areas are influenced by Arctic water masses (i.e. the West Greenland Current) rather than currents of Atlantic origin; or it could simply mean that previous sampling was inadequate and further sampling in these regions is required.

3.4.2 Environmental variables influencing coccolithophore community composition and distribution

This is the first multivariate approach in which carbonate chemistry parameters (pH, $\Omega_{calcite}$) have been used together with other environmental variables (light, nutrients, temperature and salinity) to determine which factors influence coccolithophore species distribution. Previous studies have included in their approach nutrient and light availability in addition to temperature and salinity (seasonal variability: Cortés et al. 2001, Haidar & Thierstein 2001, spatial variability: Boeckel & Baumann 2008), or have related carbonate chemistry parameters with coccolith mass (Beaufort et al. 2008), but all of these variables have not been considered simultaneously before.

Spearman's rank correlation showed that pH and mixed layer irradiance (E_{MLD}) are the combination best able to explain variation in coccolithophore distribution in the North Sea, Norwegian Sea and the Arctic ($r_s = 0.62$). The high pH values and low temperatures at SVAL are most likely responsible for this cluster separating from the rest in terms of hydrography, species composition (Papposphaeraceae dominance) and abundance (very low, 3 cells mL^{-1}). Boeckel & Baumann (2008) found that temperature

explained much of the variation in coccolithophore distribution across the subtropical frontal zone in the South Atlantic. However, the results of this study show that pH could explain more of the coccolithophore variation between the SNS and SVAL ($r_s = 0.45$) than did temperature ($r_s = 0.31$). In both studies, the colder frontal zone and Arctic waters could be considered as more productive and hence associated with higher pH values due to uptake of DIC, creating a pH gradient that matches the temperature gradient. Indeed, in this study, pH and temperature were strongly negatively correlated ($R^2 = 0.83$). However, apart from primary production and respiration, pH is also affected by physical mixing and air-sea CO_2 exchange (Chierici & Fransson 2009) and the results of this study suggest that pH controls coccolithophore distribution to a greater degree than temperature. As mentioned earlier, in laboratory studies, different coccolithophore species and even strains exhibit different responses to changes in pCO_2 and or pH (e.g. Langer et al. 2006, Langer et al. 2009) and recent studies have begun to consider metabolic pH balance as an important component of cellular physiology in terms of the calcification process and its interaction with the environment (Mackinder et al. 2010, Rickaby et al. 2010). Rickaby et al. (2010) recently hypothesized that cell size within the coccolithophores influences cellular pH balance and carbon acquisition. However, a considerable amount of further research is required in testing this hypothesis and the role of other environmental parameters on coccolithophore physiology and growth.

Interestingly, pH was more important when there were larger differences between locations (~0.4 unit difference between the SNS and SVAL). E_{MLD} became more important when the pH range was smaller (~0.2 unit difference between the SNS and ARCT), as the Spearman's Rank correlation showed when SVAL was excluded from the analysis. In this case, high average E_{MLD} (~8.7 mol PAR m^{-2} d^{-1}) was associated with high diversity in the NNS and southern NORW (low *Emiliania huxleyi* relative abundance and significant contributions of *Syracosphaera* spp., *Palusphaera vandelii* and *Corisphaera gracilis*) and explained much of the variation in coccolithophore distribution ($r_s = 0.40$). However, maximum E_{MLD} in NORW (~17.8 mol PAR m^{-2} d^{-1}) was associated with *E. huxleyi* contributing 100%, albeit to a low abundance (<3 cells mL^{-1}). This might be a result of *E. huxleyi* showing no photoinhibition in contrast to other phytoplankton species (Zondervan 2007 and references therein). Boeckel & Baumann (2008) found that, other than temperature, sampling depth (upper or lower photic zone) and nutricline depth best explained variation in species composition in the

subtropical frontal zone in the South Atlantic. In the present study, nutrients did not seem to be important as both phosphate and nitrate concentrations were generally low across the transect and the photic zone was relatively shallow (<50 m) compared to subtropical waters (100 – 150 m). Sampling depth relates to how much light is available to coccolithophores and this controls the vertical distribution of coccolithophore species at the HOT station (Cortés et al. 2001). However, Boeckel & Baumann (2008) did not include light availability in their multivariate approach and their results implied that "*other unidentified and more important variables accounted for species variation, light availability being a potential control*". In the approach of the present study, both light availability and mixed layer depth are accounted for in the E_{MLD} calculation, which explains the relatively high Spearman's r_s value (0.40) for this variable. A possible explanation as to why irradiance levels would have a different effect on different coccolithophore species is the fact that there is extraordinary diversity in the pigment composition of different species, even different strains (Van Lenning et al. 2004). These variations include different pigment contents with an efficient light energy transfer function or with photoprotective function, and have an evolutionary origin which may result from adaptations to low or high irradiance.

Multivariate data analysis also showed salinity to be less important than pH and E_{MLD} in explaining species variation. However, examination of individual samples shows that high diversity in the NNS was also associated with low salinity in this region. Similarly, $\Omega_{calcite}$ did not appear to influence coccolithophore distribution, as Spearman's r_s deviated little from 0. However, MDS analysis showed that the SNS, CNS and ARCT coccolithophore assemblages were very similar to each other (high average coccolithophore abundance, high *Emiliania huxleyi* relative abundance, low diversity and contribution of *Calciopappus caudatus*, *Acanthoica quattrospina* and *Syracosphaera corolla*) and that the two regions had very similar $\Omega_{calcite}$ values (average ~3.8), which were the lowest of the transect. The lack of correlation between coccolithophore distribution and $\Omega_{calcite}$ might be due to the relatively small range encountered (3.5 – 4.5) compared to the much larger pH range (8.0 – 8.4).

Finally, it is important to mention that growth and mortality, with the latter including grazing, competition and viral infection, also control coccolithophore abundance and distribution. These biotic controls may or may not be related to

environmental variation, and could potentially explain the remaining variation in coccolithophore distribution.

3.4.3 Species composition and calcification rates

Coccolithophore species composition in the surface ocean ultimately affects calcite fluxes to the sediments, as the coccoliths of each species contain different amounts of calcium carbonate (Beaufort & Heussner 1999, Young & Ziveri 2000). This is also mirrored in the total CF rates measured, as 'heavier' species tend to calcify at higher rates than 'lighter' species. *Emiliania huxleyi* cellular CF rates are <1 pmol C cell^{-1} d^{-1} (Poulton et al. 2010), whereas *Calcidiscus leptoporus* and *Coccolithus pelagicus* can calcify at rates as high as 8 and 18 pmol C cell^{-1} d^{-1}, respectively (Langer et al. 2006). Hence, cell-CF, growth rate and each species' contribution to total abundance determine how high the community CF is.

Species of the weakly calcified Arctic genera (Plate 3.1) *Pappomonas*, *Papposphaera* and *Wigwamma* dominated the Arctic stations ICE, MIZ and RIP. Cell-CF rates were generally <1 pmol C cell^{-1} d^{-1} (0.03 – 0.8 pmol C cell^{-1} d^{-1}) at these stations. Assemblage composition for these rates varied from 100% Arctic species (RIP station) to 50% Arctic species and 6 – 25% *Emiliania huxleyi*, 30 – 50% *Coccolithus pelagicus* HOL (holococcolith-bearing), and 15% *Algirosphaera robusta* (MIZ and ICE stations). Coccolith calcite content information does not exist for these species (except for *E. huxleyi*), so for the weakly calcified Arctic genera (coccolith length ~ 1 μm) a value equivalent to that estimated for a small *Syracosphaera* coccolith was used (coccolith length ~1.5 μm, calcite content ~0.001 pmol C; Young & Ziveri 2000) and it was calculated that in the 100% Arctic species assemblages, cell-CF rates were equivalent to a coccolith production rate of 200 – 800 coccoliths cell^{-1} d^{-1}. These rates appear physiologically unrealistic: *E. huxleyi* can produce up to 30 coccoliths cell^{-1} d^{-1} (Poulton et al. 2010), indicating that either the calcite content of these weakly calcified coccoliths is higher, or that we have overestimated total CF rates, or underestimated coccolithophore abundance.

These coccolith production rates can, however, be reduced to more realistic values of 9 – 35 coccoliths cell^{-1} d^{-1} if we use a calcite content equivalent to that of *Emiliania huxleyi* (coccolith length ~3.5 μm, calcite content ~0.023 pmol C, Young &

Ziveri 2000). At the MIZ and ICE stations, the few exceptionally high cell-CF rates calculated (1.4 – 5.9 pmol C cell^{-1} d^{-1}) can potentially be justified by the 13 – 33% contribution of the 'heavier' *Coccolithus pelagicus* and *Algirosphaera robusta* to total abundance (*C. pelagicus* coccolith calcite content = 1.4 pmol C, Young & Ziveri 2000).

At the NNScast, LOF and SS1 stations, *Emiliania huxleyi* usually dominated (70 – 90%) the total species abundance in the upper photic zone, but co-occurred in the lower part of the photic zone with *Calciopappus caudatus*, *Algirosphaera robusta*, *Coccolithus pelagicus*, *Acanthoica quattrospina* and *Syracosphaera* spp. Cell–CF rates were generally <1 pmol C cell^{-1} d^{-1} and so within the *Emiliania huxleyi* calcification range, but with a few exceptions. High rates (1.3 – 2.9 pmol C cell^{-1} d^{-1}) were measured at 5 – 10 m at the SS1 and LOF stations, and also at 45 m at the LOF station. Since the relative abundance of *E. huxleyi* ranged between 33 – 90% at these depths and species diversity was high, it was difficult to attribute these high rates to a certain species. However, again using the *E. huxleyi* coccolith calcite content (0.023 pmol C), a coccolith production rate of 56 – 126 coccoliths cell^{-1} d^{-1} was estimated for these depths. These are somewhat higher than previous measurements (7 – 29 coccoliths cell^{-1} d^{-1}, Poulton et al. 2010), but the high ratio of detached coccoliths to cells observed at these stations (40 at LOF, ≤250 at SS1) might justify the high rates.

These rough estimates of cell-CF rates highlight the need for more calcite content and CF data across a wider range of coccolithophore species. It is obvious that highly diverse coccolithophore communities have very different community CF rates depending on their species composition. The contribution of *Coccolithus pelagicus* to the ICE assemblage increased integrated community CF by an order of magnitude in comparison to the SS1, MIZ and RIP assemblages (0.51 compared to 0.04 – 0.08 mmol C m^{-2} d^{-1}). If pH and E_{MLD} affect species composition and distribution, as the data of the present study suggest, then they must also indirectly influence community CF rates.

3.5 Conclusions and wider implications

In this study, multivariate analysis of coccolithophore community composition and environmental data indicates that pH and mixed layer irradiance are best able to account for species composition and distribution between the North Sea and Svalbard. These results also show that low temperature and high pH are associated with a very

distinct assemblage north of Svalbard during summer while high irradiance and low salinity are associated with highly diverse assemblages in the northern North Sea.

Overall, the results imply that in a changing ocean there may well be significant community shifts within coccolithophore assemblages. Sea surface warming, retreating sea ice and changes in oceanic currents are already influencing polar ecosystems. Increased temperatures and reduced seasonal ice cover are likely to result in increased primary production (Arrigo et al. 2008), raising pH values in the Arctic surface waters throughout summer (although, the main trend will be towards lower pH values; Orr et al. 2005). These changes might already be assisting Atlantic species like *Emiliania huxleyi*, which has been blooming with increasing frequency in the Barents Sea for the last few years (Smyth et al. 2004), to advance into colder Arctic waters. Whether these Atlantic species will outcompete weakly calcified Arctic species in the future remains to be determined. Moreover, changing light conditions due to shallower mixed layers (stratification) could also lead to changes in coccolithophore community structure and calcification rates in some regions, hence affecting the overall efficiency of the carbonate pump. It is also important to consider the effects of climate change and ocean acidification not only on single coccolithophore species, but on whole communities. Changes in future pelagic calcite production may result from physiological changes acting on single species and/or from shifts in the species composition of coccolithophore assemblages induced by ocean acidification and stratification.

Chapter 4: Coccolithophore distribution and calcification in the Drake Passage (Southern Ocean)

Abstract

Coccolithophores, and especially the species *Emiliania huxleyi*, are widespread in the Southern Ocean during the summer months, however, little is known about their calcification in this region, or how they relate to environmental variables. This study presents data on coccolithophore distribution and calcification collected in February 2009 in the Drake Passage. Morphotype B/C of *E. huxleyi* was the dominant coccolithophore. *E. huxleyi* coccolith length (total range 1.8 – 4.4 μm) and estimates of coccolith calcite (overall average 0.01 pmol C coccolith^{-1}) were low relative to other field studies. Both cell specific (0.01 – 0.16 pmol C cell^{-1} d^{-1}) and total calcification (0.3 – 18.6 μmol C m^{-3} d^{-1}) of *E. huxleyi* were much lower than in subarctic regions, where morphotypes A and B are dominant, but coccolith production rates were similar (2 – 18 coccoliths cell^{-1} d^{-1}). Temperature and irradiance were best able to explain variation in coccolithophore species distribution and abundance (r_S = 0.4). Calcification parameters and *E. huxleyi* abundance were positively correlated with the strong latitudinal gradient in temperature and also with irradiance. It was not possible to determine the individual influences of nutrients and $\Omega_{calcite}$ on the calcification parameters as these were closely coupled with temperature. These results suggest that future sea surface warming and possible increased irradiance may result in a poleward advance of *E. huxleyi* and consequently in higher coccolithophore calcification across the Southern Ocean.

4.1 Introduction

Coccolithophores have received a lot of scientific interest in the last couple of decades, mainly due to their role in the ocean carbon cycle, as they contribute to both the biological and carbonate pumps. *Emiliania huxleyi*, the most widespread coccolithophore, has been extensively studied in cultures. Although there are currently several distinct morphotypes of this species recognised in the literature (Young et al. 2003), the most common in culture are morphotypes A and B (Paasche 2002). Morphotype A forms blooms in the North Atlantic and the Norwegian coastal waters, whereas morphotype B is primarily found in the North Sea (Van Bleijswijk et al. 1991, Paasche et al. 1996). The ecophysiology of these two morphotypes is thus relatively well studied and seasonally shallow mixed layers, high temperature and high irradiance conditions are associated with their blooms (Merico et al. 2004, Raitsos et al. 2006).

Morphotype B/C is the dominant morphotype of *E. huxleyi* in the colder waters of the Southern Ocean. A number of observations show that this coccolithophore is widespread in all sectors of the Southern Ocean except close to the Antarctic continent (e.g. Findlay & Giraudeau 2000, Cubillos et al. 2007, Gravalosa et al. 2008, Mohan et al. 2008). In contrast with the well studied morphotypes A and B, most of the current knowledge on morphotype B/C regards the different morphological characteristics of its coccoliths, which are lightly calcified. A recent study, however, has shown that this Southern Ocean morphotype is morphologically, physiologically and genetically distinct (Cook et al. 2011). There is currently no information on the growth and calcification of this morphotype, either from cultures or from field studies. Moreover, direct calcification measurements on Southern Ocean coccolithophore assemblages have never been made.

Laboratory and field studies on *E. huxleyi* show that calcification in this species depends strongly on irradiance and is also stimulated by nutrient stress (Zondervan 2007, and references within), which give clues for its response to changing nutrient and light conditions in the future ocean. However, the response of this species to ocean acidification seems to depend greatly on the strain (Langer et al. 2009) studied. Moreover, the sensitivity of *E. huxleyi* to elevated pCO_2 also depends on the light (Zondervan et al. 2002, Feng et al. 2008) and nutrient conditions (Sciandra et al. 2003, Delille et al. 2005, Engel et al. 2005). Future changes in the ocean are expected to happen simultaneously, due to sea surface warming (Barnett et al. 2005), shallowing of the

mixed layer (Levitus et al. 2000) and ocean acidification (Orr et al. 2005). Thus, it is important to validate the findings of laboratory studies with field studies, in order to understand how natural coccolithophore populations might respond to simultaneous changes in environmental variables.

The Southern Ocean has naturally low calcite saturation states ($\Omega_{calcite}$), due to the low temperatures of polar waters, and is likely to be one of the first regions to experience widespread undersaturation of the surface waters (Orr et al. 2005). There are indications that the distribution of *E. huxleyi* has recently extended polewards and the degree of coccolith calcification follows the north-south gradient of decreasing temperature and $\Omega_{calcite}$ (Cubillos et al. 2007). In this context, the lack of information on coccolithophore calcification in the Southern Ocean is a significant gap in our understanding of the effects of future changes on the marine carbon cycle.

The main aim of this study was to investigate the distribution of coccolithophores and directly measure community (total) calcification rates across Drake Passage in the Southern Ocean. A second aim was to investigate whether a north-south trend in the degree of *E. huxleyi* coccolith calcification was also observed in the Drake Passage, and also to examine whether a similar trend was observed in community and cell specific calcification. Finally, a third aim was to investigate the relationships between coccolithophore distribution, calcification parameters and a variety of environmental variables (temperature, salinity, nutrient, light and carbonate chemistry parameters) and determine which of these most likely control coccolithophore distribution in the Drake Passage.

4.2 Methods

4.2.1 Study area

The Drake Passage is characterised by the eastward flow of the Antarctic Circumpolar Current (ACC), driven by strong westerly winds. The current's boundaries are defined by oceanic fronts, where rapid changes in temperature and salinity occur over a short distance. The northern boundary of the ACC is the Subtropical Front (STF), which separates the warm sub-tropical waters from the cold subantarctic waters (Orsi et al. 1995). South of the STF, the three fronts associated with the ACC are, from north to south: the Subantarctic Front (SAF), the Polar Front (PF) and the Southern ACC Front

(SACCF). These three fronts define three zones in the ACC. The area between the STF and the SAF is referred to as the Subantarctic Zone (SAZ), between the SAF and the PF is the Polar Frontal Zone (PFZ) and between the PF and the SACCF is the Antarctic Zone (AZ) (Orsi et al. 1995). A fourth zone, located between the southern boundary of the ACC (SB) and the Antarctic continent, is referred to as the Continental Zone (Whitworth 1980).

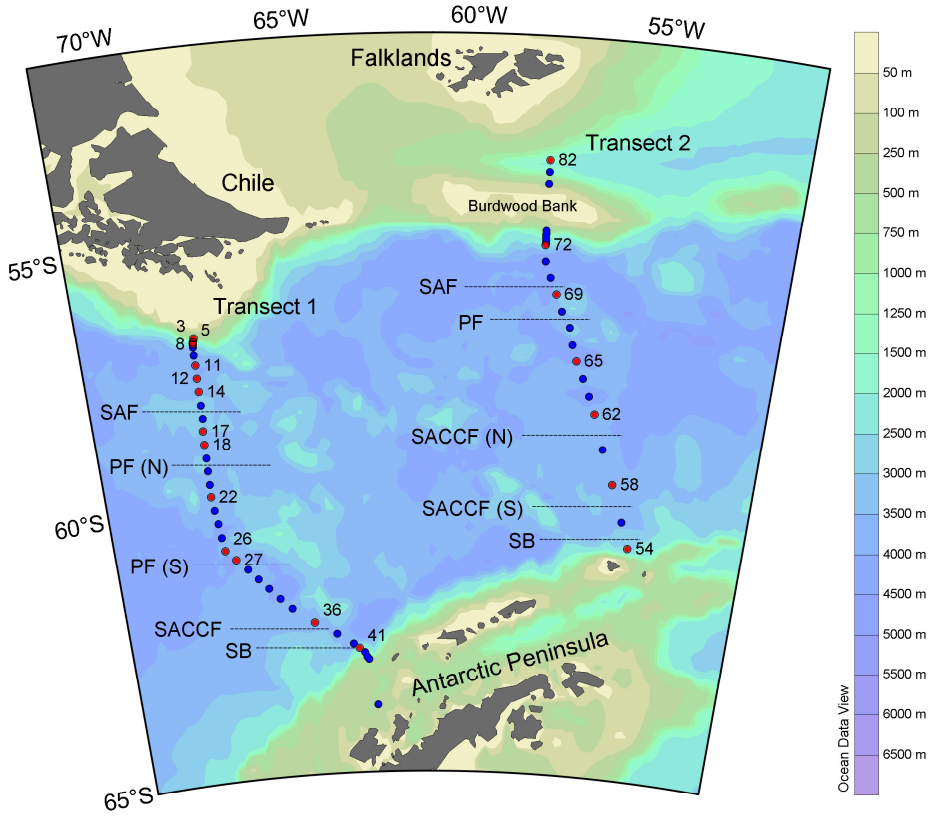

Figure 4.1 JC31 cruise track, showing Transect 1 (Chile to Antarctica) and Transect 2 (Antarctica to Falklands). Blue and red circles indicate sampling stations. Red circles are numbered and indicate stations where calcification rates were measured. The locations of the following fronts are shown on each transect: Subantarctic Front (SAF), Polar Front (PF), Southern Antarctic Circumpolar Current Front (SACCF) and Southern Boundary of the ACC (SB). Where two possible locations or two branches of a front were observed, these are denoted with a northern (N) or southern (S) suffix.

The positions of these fronts during the two transects of the cruise are shown in Figure 4.1. Dynamic height (Sun & Watts 2001), as well as the more traditional criteria of Orsi

et al.(1995), were used to determine the positions of the fronts (pers. comm. Sally Close and Gavin Evans, NOCS). The results of the two methods were in close agreement, however the Orsi et al. (1995) criteria indicated the presence of two branches of the PF during Transect 1 (west), and the dynamic height method indicated two possible locations of the SACCF during Transect 2 (east). The multiple positions of these fronts are indicated on the map with a north (N) or south (S) suffix.

4.2.2 Sampling

Sampling was conducted during cruise JC031 (03/02/2009 – 03/03/2009) on board the *RRS James Cook*, from Punta Arenas, Chile, to the Antarctic Peninsula (Transect 1) and back to the Falklands (Transect 2) (Figure 4.1). A stainless steel CTD rosette was deployed at every sampling station and samples were collected from the upper 100 m of the water column. Water samples for nutrients, chlorophyll-*a* (chl-*a*), and ancillary parameters were collected at a total of 61 stations. Samples for coccolithophore community abundance and diversity were collected at 53 stations, carbonate chemistry parameters at 5 m depth were measured at 51 stations, and samples for calcification and primary production rates were collected at 20 stations (red circles in Figure 4.1).

4.2.3 Coccolithophore community

Water samples (1 L) from up to 5 CTD depths over the upper 100 m were gently filtered onto Millipore Isopore membrane filters (25 mm diameter, 1.2 μm pore size), with a 25 mm diameter circle of 10 μm nylon mesh acting as a backing filter to achieve even distribution of cells. The membrane filters were rinsed with trace ammonia solution (pH 9 - 10) to remove salts, oven dried overnight at 30ºC and stored in the dark in sealed Petri dishes. A radially cut portion of each filter was mounted on an aluminium stub and gold-coated. For each filter 225 fields of view (FOV = images), equivalent to ~1 mm^2, were taken at ×5000 magnification along a predefined meander-shaped transect, using a Scanning Electron Microscope (Leo 1450VP, Carl Zeiss, Germany) combined with the software SmartSEM. For each sample both coccospheres and coccoliths were enumerated until 300 of each were reached or until all FOV had been counted. The SmartSEM software allowed to set scanning for zero overlap between FOVs. In order to avoid

double-counting specimens that were on the edge between FOVs, only the top and right edges of each FOV were counted but not the bottom and left edges. The number of FOVs counted was used to calculate the area of the filter covered (the size of one FOV was 4.054×10^{-3} mm^2). Both coccospheres and coccoliths were identified to species level following Young et al. (2003), and the abundance of these for each species was calculated as:

$$\text{Coccospheres or coccoliths } mL^{-1} = C \times (F/A) / V \quad (4.1)$$

where C is the total number of coccospheres or coccoliths counted, A is the area investigated (mm^2), F is the total filter area (mm^2) and V is the volume filtered (mL).

The uncertainty (standard error, S.E.) in coccolithophore abundance was calculated as the square root of the counted number of cells ($\sqrt{C}$) divided by the equivalent volume of sample investigated ($A\times V/ F$) (Taylor 1982). Ninety five per cent (95%) confidence limits of coccolithophore abundance were obtained by multiplying the standard error by the appropriate z-score where more than 30 cells were counted, and so the uncertainty was $\pm1.96 \times$ S.E. cells mL^{-1}. When less than 30 cells were counted the appropriate t-values were used instead of z-scores (Fowler et al. 1998).

4.2.4 *Emiliania huxleyi* coccolith morphology and calcite content

Detached coccoliths were predominantly (>99%) of the species *Emiliania huxleyi*. The distal shield lengths (DSL) of 50 *E. huxleyi* detached coccoliths were measured in each of the 20 stations where calcification was also measured, using the image processing software ImageJ (Abramoff et al. 2004). At the same time, each coccolith was classified as morphotype A, B or B/C following Young et al. (2003). Only type B/C was found in our samples (distal shield elements delicate, central area open or thin plate). Coccolith calcite content (pmol C or $CaCO_3$) was calculated from the volume of each coccolith and the density (2.7 pg μm^{-3}) and molecular weight (100 g mol^{-1}) of calcite. Coccolith volume was a function of DSL and a shape dependent constant, k_s (0.015 for type B/C, Young, unpublished) (Young & Ziveri 2000):

$$\text{Coccolith calcite (pmol C)} = k_s \times DSL^3 \times \text{calcite density/molecular weight} \quad (4.2)$$

4.2.5 Calcification and primary production

Water samples for rate measurements were collected before dawn (or early in the morning in a few cases), from 3 – 5 light depths within the upper 100 m of the water column (including 0.1 – 1.5%, 7%, 14%, 33% and 55% of incident Photosynthetically Active Radiation, PAR) or only from the surface (55%). Daily rates of primary production (PP) and calcification (CF) were determined following the 'micro-diffusion' technique of Paasche & Brubak (1994), as modified by Balch et al. (2000). Water samples (each 150 mL, 3 replicates plus 1 formalin-killed blank) were collected from each light depth, spiked with 100 μCi of ^{14}C-labelled sodium bicarbonate (Perkin Elmer, U.K.) and incubated in on-deck incubators for 24 hrs. Light depths were replicated using a mixture of misty blue and neutral density filters, and samples were kept at ambient sea surface temperature by providing a continuous flow of water from the underway supply through the incubators.

Incubations were terminated by filtration through 25mm 0.2 μm polycarbonate Isopore filters, which were then acidified with 1 mL of 1% phosphoric acid to separate the inorganic fraction (labile, CF) from the organic fraction (non-labile, PP). The inorganic fraction was captured as ^{14}C-CO_2 on a β-phenylethylamine soaked filter and placed in a separate vial. Liquid scintillation cocktail was added to both vials and activity was measured on a TriCarb liquid scintillation counter. Counts were converted to uptake rates using standard methods. The average relative standard deviation (calculated as SD × 100/mean) of triplicate measurements was 6% (1 – 19%) for PP and 36% (2 – 86%) for CF, with the higher deviations observed at the base of the euphotic zone were rates of PP and CF were close to zero. The formalin blanks represented a significant proportion of the CF signal (mean 35%, range 5 – 87%) at the upper 50 m. Blank contribution was even higher below 75 m and close to Antarctica, where the CF rates were very low. Similar high blank contributions have been reported in other studies (Poulton et al. 2007, Poulton et al. 2010). The blanks represented only ~1% of the PP signal.

4.2.6 Cell specific calcification and coccolith production

Cell specific calcification (cell-CF) was calculated from total CF and coccolithophore abundance. The associated error was derived from propagation of the

individual errors of total CF (± 0 – 3.5 μmol C m^{-3} d^{-1}) and coccolithophore abundance (± 0 – 53 cells mL^{-1}) following Taylor (1982). Daily coccolith production per cell at each station was calculated from cell-CF and coccolith calcite estimated for each station. The uncertainty in coccolith production rates at each station, due to associated errors in measurement of CF and coccolithophore abundance, was smaller than the range of coccolith production rates observed due to the variation in coccolith size. Hence, differences in coccolith production between stations could be attributed to changes in coccolith size, rather than to errors associated with the method by which these were estimated.

4.2.7 Chlorophyll-*a*

Water samples (200 – 250 mL) for chl-*a* analysis were filtered onto Whatman GFF (~0.7 μm pore size) filters and extracted in 8 mL 90% acetone for 24 h in the dark, at 4°C. Chl-*a* fluorescence was measured on a Turner Designs AU-10 fluorometer equipped with Welschmeyer (1994) filters and calibrated using a pure chl-*a* standard (Sigma).

4.2.8 Macronutrients

Phosphate, nitrate and silicic acid micro-molar concentrations were determined using a Scalar San Plus Autoanalyser following the methods described by Kirkwood (1996). The error associated with phosphate, nitrate and silicic acid was ±0.01, ±0.16 and ±0.05 μmol L^{-1}, respectively.

4.2.9 Carbonate chemistry

Dissolved Inorganic Carbon (DIC) and Total Alkalinity (TA) sampling and analysis were performed by Dorothee Bakker (University of East Anglia) and detailed methods are described by Bakker et al. (2009). In brief, water samples were drawn into 500 mL Schott ® SUPRAX borosilicate glass bottles following Dickson et al. (2007) to minimise gas exchange. Samples were analysed within 6 hours of collection, however if

such rapid analysis was not possible the samples were poisoned with 100 µL of a saturated solution of mercuric chloride (7g per 100 mL).

Three different instruments were used for DIC and TA analysis. The first was used for DIC only and has an extractor unit built after the design by Robinson and Williams (1992), operating at 4ºC. The second was a VINDTA 3C combined DIC/TA instrument (Marianda, Germany) operating at 25°C. The third was another VINDTA 3C, which was used for determining TA after DIC analysis on the stand-alone DIC extractor. Water samples were analysed for DIC by the coulometric method after Johnson et al. (1987). The TA measurements were made by potentiometric titration with the two VINDTA 3C instruments. Two replicate analyses were made on each sample bottle, and replicate samples were also drawn from the CTD rosette. Certified Reference Materials (CRMs) (from A.G. Dickson, Scripps Institute of Oceanography) were used for instrument calibration and at least two CRMs were run per station. The precision and accuracy for both TA and DIC was less than 3 µmol kg^{-1}. Calcite saturation state ($\Omega_{calcite}$), pH and pCO_2 were calculated from DIC, TA, nutrients, temperature, salinity and pressure data using the CO2SYS.XLS program (Pierrot et al. 2006).

4.2.10 Mixed layer irradiance

In order to calculate average daily irradiance over the mixed layer, the mixed layer depth (MLD) was determined as the shallowest depth corresponding to a density difference ($\Delta\sigma_t$) with surface waters of more than $\Delta\sigma_t = 0.03$ sigma units, as is recommended for the Southern Ocean (Dong et al. 2008).

The vertical attenuation coefficient (k_d) for PAR for downward irradiance at each station was calculated from the monthly averaged (February 2009) light attenuation coefficient at 490 nm wavelength (k_{490}) measured by the MODIS ocean colour satellite (http://oceancolor.gsfc.nasa.gov/) following Rochford et al. (2001):

$$k_d = 0.0085 + 1.6243 \times k_{490} \quad (4.3)$$

The relationship describing the exponential diminution of downward irradiance (E_z) with depth (z) is:

$$E_z = E_0 \times \exp(-k_d \times z) \quad (4.4)$$

where E_0 is the instantaneous subsurface irradiance.

E_0 was calculated from minute averaged PAR above the sea surface ($PAR_{above\ surface}$) data, obtained from the ship-mounted sensors, assuming E_0 was 55% of $PAR_{above\ surface}$. Daily $PAR_{above\ surface}$ was calculated as the sum of the minute averaged data over 24 hours and daily irradiance was then calculated at every 1 m down to the MLD:

$$E_{z,\ daily} = 0.55 \times \text{daily } PAR_{above\ surface} \times \exp(-k_d \times z) \qquad (4.5)$$

The average irradiance over the mixed layer, E_{MLD} (mol PAR m^{-2} d^{-1}), was calculated as the sum of $E_{z,\ daily}$ at every 1 m down to the MLD, divided by the MLD. The euphotic depth at each station (Z_{eu}), defined as the depth at which E_z falls to 1% of the subsurface value, was equal to an optical depth of 4.6 and hence $Z_{eu} = 4.6/k_d$ (Kirk 1983).

Comparison of daily PAR data from the ship's sensor with a 32 d composite of MODIS PAR data during the study period, showed good agreement between the two and confirmed that daily PAR values were typical of the time of the year and were not biased by weather conditions at the time of measurement.

4.2.11 Multivariate data analysis

Multivariate statistics were used to assess spatial changes in coccolithophore community composition and abundance in the context of environmental variables following the methods described by Clarke (1993), using PRIMER-E (v. 6.0) (Clarke & Gorley 2006).

Analysis of biotic data was carried out on square-root-transformed ($\sqrt{x}$) species abundances, using Bray-Curtis similarity to determine changes in the abundance of both dominant and less abundant species. Analysis of abiotic data was carried out on power transformed (to reduce skewness and stabilize the variance) and standardised (to bring all variables to comparable scales) values of temperature, salinity, phosphate, nitrate, pH, $\Omega_{calcite}$, E_{MLD}, and $PAR_{above\ surface}$, using Euclidean distance to determine spatial changes in these variables.

Principal Component Analysis (PCA) was carried out on environmental data to reduce the 8-fold variability to a low-dimensional representation of spatial changes in these variables. The abundances of the major species were then superimposed on the PCA plot to illustrate their environmental preferences.

The BEST routine was used to search for relationships between the biotic and abiotic patterns and to identify which environmental variables(s) explained most of the variation in coccolithophore distribution. This routine selects a subset of abiotic variables that maximizes Spearman's rank correlation between biotic and abiotic similarity matrices. Spearman's rank correlations were also used to identify relationships between calcification parameters (coccolith calcite content, coccolith production rate, total and cell-specific calcification) and environmental variables. Spearman's rank correlations were selected over Pearson's product moment correlations because the data distribution was not normal and the pairs of observations were <30.

4.3 Results

4.3.1 Physicochemical setting

Most physicochemical variables exhibited a strong north-south trend, with temperature and salinity decreasing towards Antarctica (Figure 4.2A). Temperature was highest to the south of Chile and the Falkland Islands (8 – 9ºC) and lowest off the Antarctic Peninsula (~ 2ºC). Salinity only varied by 0.4, with the highest values (~34.1) associated with SAF on Transect 1, and the lowest values (~ 33.7 – 33.8) observed in the Antarctic Zone just north of the SACCF on both transects. Macronutrient concentrations increased towards Antarctica (Figure 4.2B), with nitrate values between 16.5 and 27.0 μmol L^{-1}, phosphate values between 1.2 and 1.8 μmol L^{-1}, and silicate between 1.4 and 50.9 μmol L^{-1}. Silicate concentrations changed rapidly at frontal positions. The N:P ratio ranged from 14:1 to 16:1, and hence neither macronutrient was considered to be limiting. The Si:N ratio was 2:1 close to Antarctica but fell to 1:13 north of the PF, suggesting silicate limitation across most of this region. pH fluctuated by 0.08 units and did not exhibit a clear latitudinal trend (Figure 4.2C). The highest pH value (8.12) was observed at station 24, between the two branches of the PF on Transect 1, and the lowest value (8.04) was observed at station 63, just north of the SACCF (N) on Transect 2. Calcite saturation state ($\Omega_{calcite}$) ranged between 2.5 and 3.3 and exhibited an overall decrease towards Antarctica (Figure 4.2C).

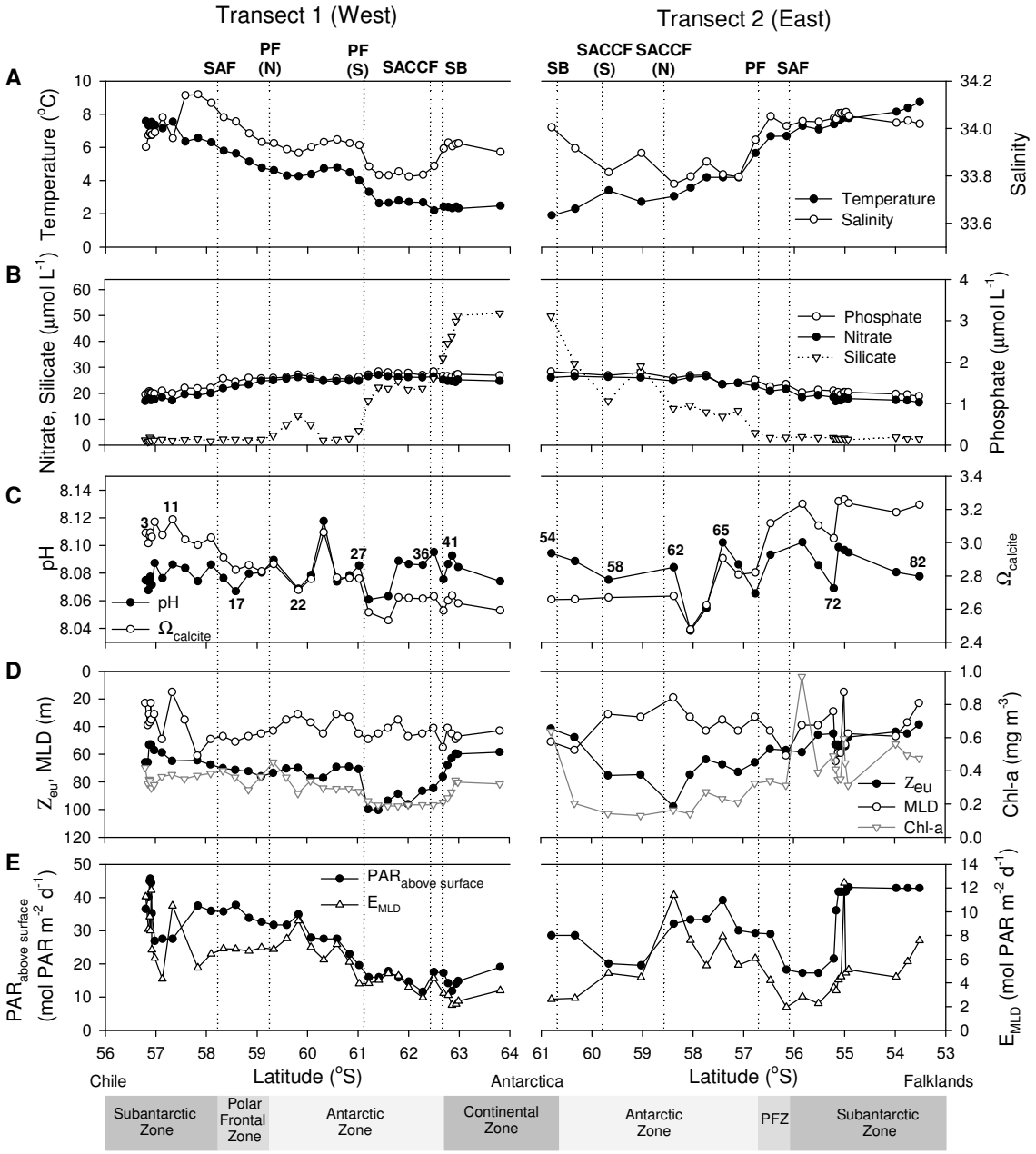

Figure 4.2 Surface distribution of physicochemical variables along Transect 1 (left) and Transect 2 (right). A) Temperature and salinity. B) Nitrate, silicate and phosphate concentrations. C) pH and calcite saturation state ($\Omega_{calcite}$). D) Euphotic zone depth (Z_{eu}), mixed layer depth (MLD) and chl-a. E) Above surface irradiance ($PAR_{above\ surface}$) and mixed layer irradiance (E_{MLD}).

The calculated euphotic zone depths (Z_{eu}, 39 – 100 m) were generally deeper than the MLD (15 – 65 m) across both transects (Figure 4.2D) indicating that phytoplankton

was not mixed down to depths where there was no light. Z_{eu} was deepest in the Antarctic Zone, just north of the SACCF on both transects, and shallowest close to the continental shelves of Chile, Antarctica and the Falkland Islands. MLD did not exhibit a clear trend and was shallowest off the Chile and Falkland shelves and at a number of stations in the Subantarctic and Antarctic Zones. Daily PAR above the sea surface ($PAR_{above\ surface}$) ranged from 12 to 46 mol PAR m^{-2} d^{-1} (Figure 4.2E). The highest $PAR_{above\ surface}$ was observed close to the Chile and Falkland shelves and decreased sharply towards the SAF. High values were also observed at some stations south of the PF and SAF. Low $PAR_{above\ surface}$ was observed close to Antarctica, especially on Transect 1. Average mixed layer irradiance (E_{MLD}) ranged between 2 and 12 mol PAR m^{-2} d^{-1} and generally followed the $PAR_{above\ surface}$ distribution, with the exception of a few stations where MLD was exceptionally shallow resulting in high E_{MLD} (Figure 4.2E).

Finally, chl-*a* values along both transects are shown in Figure 4.2D. Average chl-*a* was 0.26 mg m^{-3} and was higher in the Subantarctic and Continental Zones, with the maximum (0.97 mg m^{-3}) associated with the SAF on Transect 2.

4.3.2 Coccolithophore species

Fifteen coccolithophore species were identified in the samples (Table 4.1). The highest number of species was found in the Subantarctic Zone, with 8 species observed south of Chile (Transect 1) and 14 species observed south of the Falklands (Transect 2). The lowest number of species was observed in the Continental Zone, closest to Antarctica, where only 2 – 3 species were found. Between 4 and 6 species were observed in the Polar Frontal Zone and the Antarctic Zone.

Emiliania huxleyi was found in all regions (Table 4.1) and on average comprised ~93% (50 – 100%) of total coccolithophore abundance in the surface samples (Figure 4.3). Maximum abundance was associated with the SAF on both transects. Along Transect 1, *E. huxleyi* reached a maximum of ~ 580 cells mL^{-1} in the Polar Frontal Zone and 289 cells mL^{-1} between the two branches of the PF (Figure 4.3). Along Transect 2, *E. huxleyi* abundance was generally less than 200 cells mL^{-1}, but peaked at 260 cells mL^{-1} at the SAF. In the Continental Zone near to Antarctica, it was only found in deeper samples (>25 m) at relatively low abundances (<13 cells mL^{-1}).

Table 4.1 Species list and occurrence of coccolithophores in water samples.

	Transect 1				Transect 2			
Species	Subantarctic Zone (8 spp.)	Polar Frontal Zone (5 spp.)	Antarctic Zone (5 spp.)	Continental Zone (3spp.)	Subantarctic Zone (14 spp.)	Polar Frontal Zone (4 spp.)	Antarctic Zone (6 spp.)	Continental Zone (2 spp.)
Emiliania huxleyi	+	+	+	**	+	+	+	**
Acanthoica quattrospina	+				+	+	+	
Calciopappus caudatus	+				+	+		
Calcidiscus leptoporus	+		*		+			
Gephyrocapsa ericsonii					+			
Gephyrocapsa muellerae		*			+			
Gephyrocapsa ornata					*			
Ophiaster hydroideus	+	*			+			
Pappomonas sp.	+	+	+	+	+	+	+	
Papposphaera sp.	+		**		+		*	
Rhabdosphaera xiphos					*			
Syracosphaera dilatata					+			
Syracosphaera halldalii					*			
Syracosphaera molischii							*	
Wigwamma antarctica	+	+	+	+	+	+	+	+

+ presence

* only 1 cell found

** found in deep (>25 m) samples only

Gephyrocapsa muellerae was characteristic of the Subantarctic Zone south of the Falkland Islands, where it reached up to 34 cells mL^{-1} (Figure 4.3) and contributed 10 – 36% towards total coccolithophore abundance at some stations. This species was not consistently observed in any of the other regions. The distribution of other coccolithophore species that were consistently found in the samples in low abundances (<6 cells mL^{-1}) is shown in Figure 4.3. *Pappomonas* sp. and *Wigwamma antarctica* were found in all regions and were the only species found in the surface waters of the Continental Zone. *Acanthoica quattrospina* and *Calciopappus caudatus* were found in the Subantarctic Zone of both transects and the Polar Frontal Zone of Transect 2. Finally, *Calcidiscus leptoporus* was also observed in the Subantarctic Zone of both transects, and additionally in the Antarctic Zone of Transect 1.

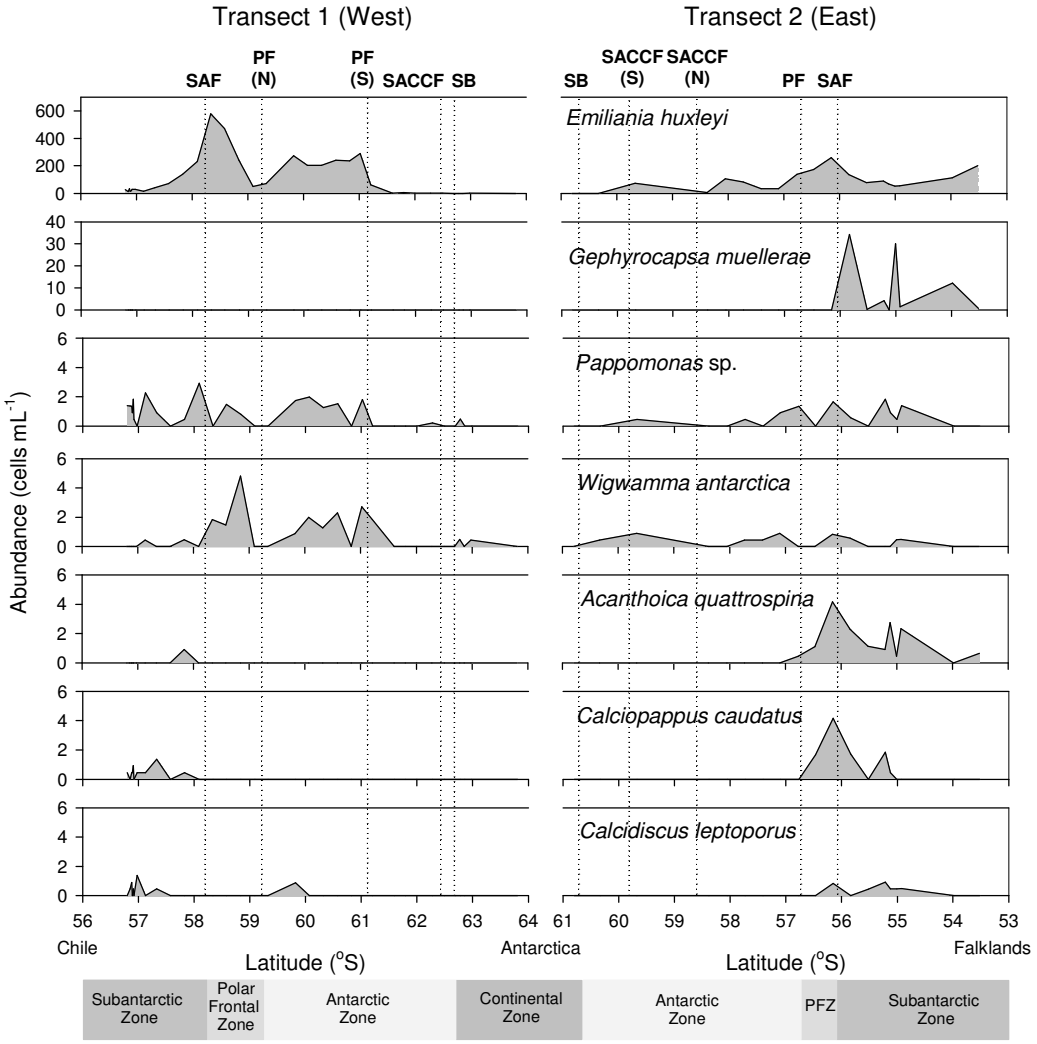

Figure 4.3 Abundance of major coccolithophore species at the surface along Transect 1 (left) and Transect 2 (right). Note the different scales of the abundance axis.

4.3.3 Coccolithophore total abundance and calcification

The surface distribution of total coccolithophore abundance was similar to that of *E. huxleyi*. Along Transect 1, total coccolithophore abundance reached a maximum of ~ 583 cells mL^{-1} at the SAF and 293 cells mL^{-1} between the two branches of the PF (Figure 4.4A). Along Transect 2, coccolithophore abundance was generally less than 200 cells mL^{-1}, but peaked at 268 cells mL^{-1} at the SAF. Almost all detached coccoliths (~99%) came from *E. huxleyi* rather than other species and the average coccolith:cell ratio was 24:1. The coccolith concentration was maximal (11,900 coccoliths mL^{-1}) between the SAF and southern branch of the PF, PF (S), on Transect 1, and the coccolith:cell ratio was as high as 44:1. The maximum coccolith concentration on Transect 2 was associated with the SAF (8,500 coccoliths mL^{-1}), and the coccolith:cell ratio was 33:1. At the majority of the stations coccolithophore abundance was maximal at the surface. However, at stations 18, 36, 62, 72 and 82 the maximum coccolithophore abundance was observed at 50 m depth (grey squares in Figure 4.4A). The difference between surface and 50 m values at these stations was less than 60 cells mL^{-1}.

Total or community calcification (CF) at the surface ranged between 0.3 and 18.6 μmol C m^{-3} d^{-1} (Figure 4.4B). Relatively high CF was measured on either side of the SAF on Transect 1 (14.8 – 18.6 μmol C m^{-3} d^{-1}). Unfortunately, CF measurements were not made at the station of maximum coccolithophore abundance. On Transect 2, maximum CF was measured at the SAF and just south of the Falkland Islands (~10 μmol C m^{-3} d^{-1}). Minimum CF was measured close to the Antarctic Peninsula in the Continental Zone (<1 μmol C m^{-3} d^{-1}). As with coccolithophore abundance, CF was generally maximal at the surface apart from stations 18, 36, 62, 72 and 82 where the maximum was observed at 50 m (grey squares in Figure 4.4B). The difference between surface and 50 m values in stations 18, 36, 62, and 82 was less than 1 μmol C m^{-3} d^{-1} and was significant only at station 72 (ANOVA, pairwise Holm-Sidak tests, $p < 0.001$), where the difference was 9 μmol C m^{-3} d^{-1}. The vertical CF distribution at six representative stations is shown in Figure 4.5.

Cell-specific calcification (cell-CF) at the surface ranged between 0.01 and 0.16 pmol C $cell^{-1}$ d^{-1} (Figure 4.4C). The highest values of cell-CF (0.13 – 0.16 pmol C $cell^{-1}$ d^{-1}) were observed in the Subantarctic Zone of Transect 1, although significantly lower values (0.04 – 0.06 pmol C $cell^{-1}$ d^{-1}) (ANOVA, pairwise Holm-Sidak tests, $p < 0.001$)

were also observed in this region. Cell-CF was <0.03 pmol C cell^{-1} d^{-1} south of the SAF on Transect 1. On Transect 2, maximum cell-CF (0.10 pmol C cell^{-1} d^{-1}) was observed just north of the SACCF (N). North of station 62, average cell-CF was ~0.05 pmol C cell^{-1} d^{-1} and south of it ~0.02 pmol C cell^{-1} d^{-1}. Cell-CF was zero at stations 36 and 54, due to the virtual absence (<1 cell mL^{-1}) of coccolithophores. The differences between the surface and 50 m in coccolithophore abundance and CF resulted in different cell-CF at 50 m (grey open squares in Figure 4.4C) at stations 18, 36, 62, 72 and 82. However, none of these were significantly different from the surface cell-CF values (ANOVA, $p < 0.001$).

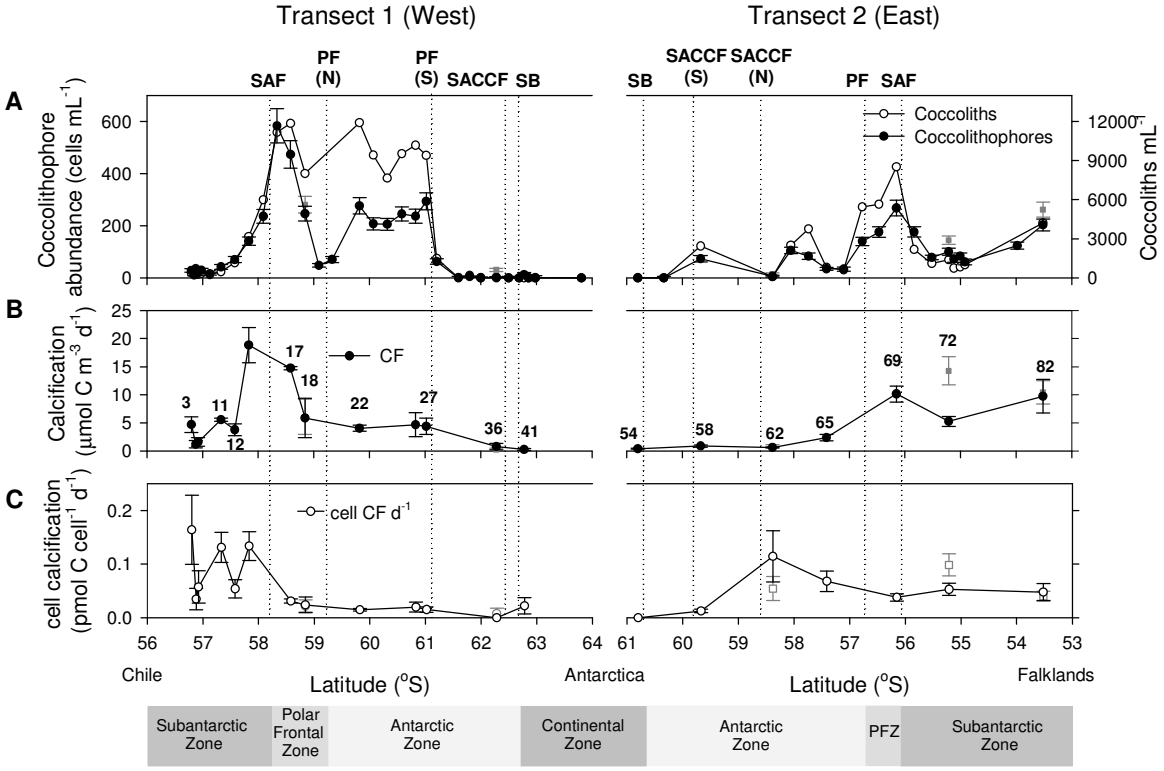

Figure 4.4 Surface distribution of coccolithophore variables along Transect 1 (left) and Transect 2 (right). A) Total coccolithophore and detached coccolith abundance. B) Community calcification rates. C) Cell-specific calcification rates. Grey filled and open squares show coccolithophore abundance, calcification and cell-specific calcification at 50 m depth, where the maximum was observed.

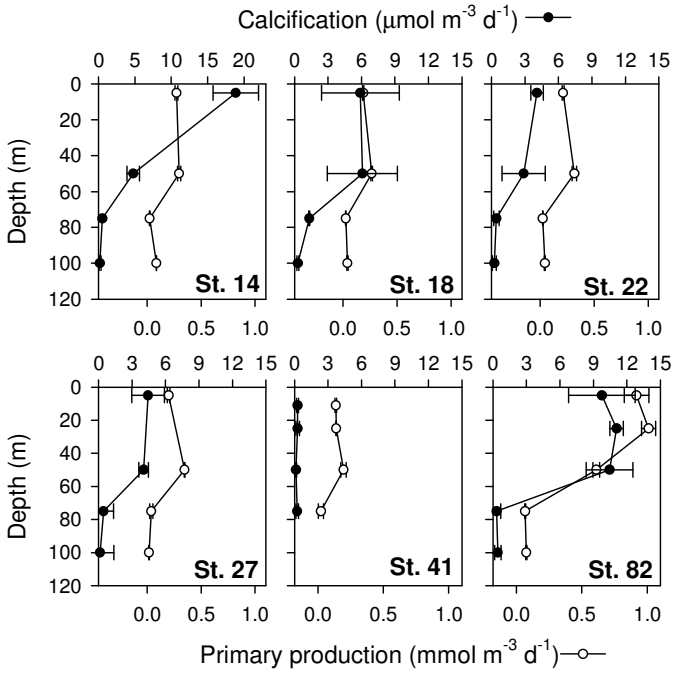

Figure 4.5 Vertical profiles of calcification (filled circles) and primary production (open circles) in six representative stations.

4.3.4 *E. huxleyi* coccolith size, calcite content and production rates

The distribution of coccolith size (distal shield length, DSL) at each station is shown in Figure 4.6A in the form of box-whisker plots. The overall mean of the DSL was 2.8 µm, while the median (solid line) for each station ranged between 2.5 and 3.3 µm and the full range was from 1.8 to 4.4 µm. DSL medians were lowest in the Polar Frontal Zone on Transect 1 and in the Antarctic Zone on Transect 2. A Kruskal – Wallis test on DSL medians showed significant difference between stations ($p < 0.001$). Maximum DSL medians were measured at the stations located south of the Chile shelf (ST. 3, 5, 8 and 11) and were significantly larger (pairwise Tukey tests, $p < 0.05$) than at the rest of the stations. The minimum DSL median was measured at station 62 (2.5 µm).

The distribution of coccolith calcite content at each station, estimated from the DSL, the shape dependent constant (k_s) for B/C coccoliths and calcite density, is shown in Figure 4.6B. The overall mean of coccolith calcite was 0.010 pmol and the median for each station ranged between 0.007 and 0.015 pmol, while the full range of coccolith calcite was from 0.003 to 0.035 pmol.

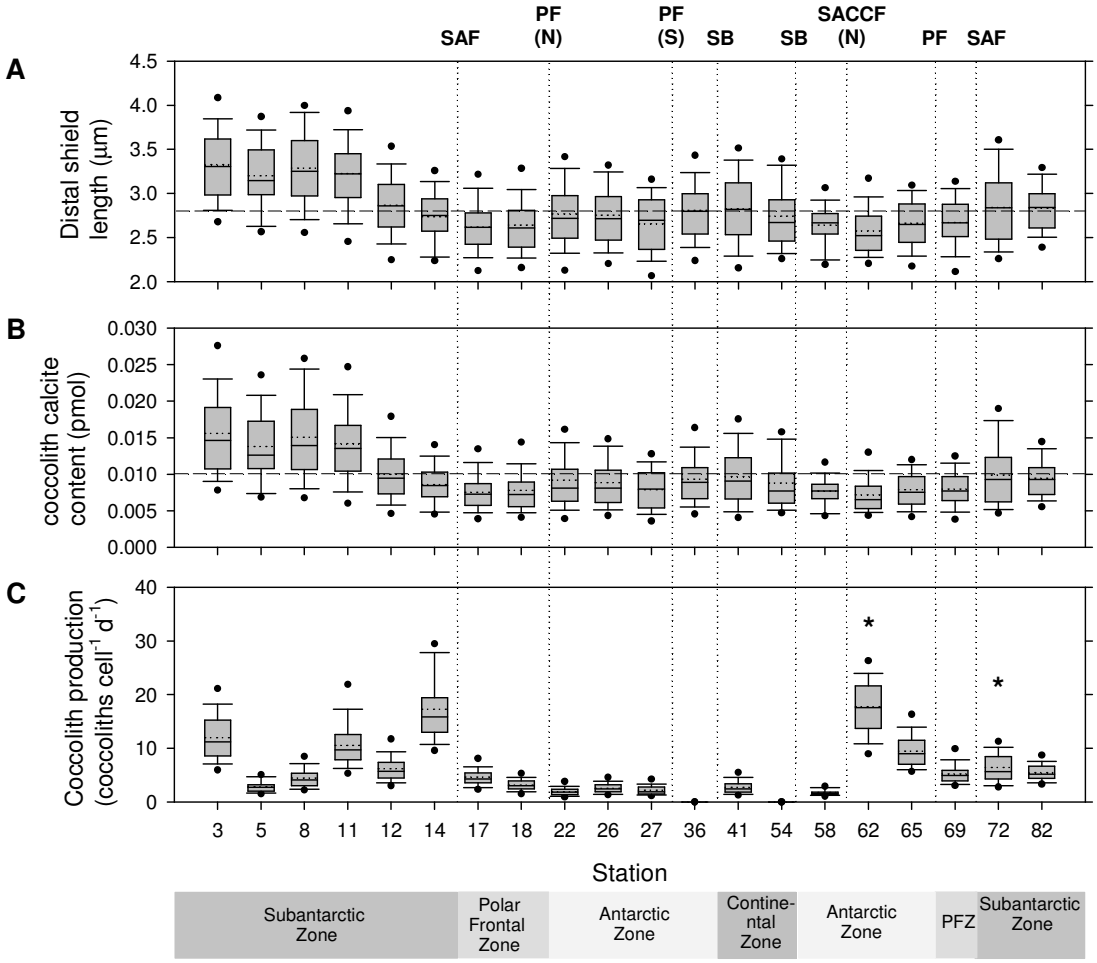

Figure 4.6 Box-whisker plots showing, for *Emiliania huxleyi* only, the size distribution of A) Coccolith distal shield length, B) Coccolith calcite content and C) Surface coccolith production rates per cell, in each of twenty stations. Each box describes the distribution of these variables based on 50 coccolith measurements. The boundary of each box closest to zero indicates the 25th percentile, the solid line within each box marks the median and the dotted line the mean, and the boundary of each box farthest from zero indicates the 75th percentile. Whiskers (error bars) above and below each box indicate the 90th and 10th percentiles and dots indicate the 95th and 5th percentiles. The overall average of coccolith length and calcite content is shown by the horizontal dashed lines. Asterisks indicate the stations where maximum coccolithophore abundance and CF was measured at 50 m depth.

Coccolith production rates per cell, estimated from cell-CF and coccolith calcite content, are shown in Figure 4.6C. The overall mean was 6 coccoliths cell^{-1} d^{-1}, while the median ranged between 2 and 18 coccoliths cell^{-1} d^{-1} at different stations. Coccolith production rates were not calculated for stations 36 and 54 where cell-CF was zero. A

Kruskal – Wallis test ($p < 0.001$) and pairwise Tukey tests ($p < 0.05$) showed statistically significant differences between stations (Table 4.2). Coccolith production rates were significantly lower south of 59 ºS (<2 coccoliths cell^{-1} d^{-1} in Continental and Antarctic Zones, St. 22 – 58) compared to the Polar Frontal Zone, the Subantarctic Zone and the northern part of the Antarctic Zone on Transect 2 (rates of 3 – 18 coccoliths cell^{-1} d^{-1}). The highest coccolith production rates were observed at stations 14 and 62 (16 – 18 coccoliths cell^{-1} d^{-1}). On Transect 1, coccolith production at stations 3, 11 and 14 was significantly higher than at stations 5 and 8. On Transect 2, coccolith production at station 62 was significantly higher than at stations 69, 72 and 82.

Table 4.2 Statistically significant differences in estimated coccolith production rates (see 4.6C) between stations. Asterisks indicate significant differences (Pairwise Tukey tests, $p < 0.05$).

Station number	3	5	8	11	12	14	17	18	22	26	27	36	41	54	58	62	65	69	72
5	*																		
8	*																		
11		*	*																
12		*																	
14		*	*		*														
17	*			*		*													
18	*			*	*	*													
22	*		*	*	*	*	*												
26	*			*	*	*	*												
27	*		*	*	*	*	*												
36	*	*	*	*	*	*	*	*		*	*								
41	*			*	*	*						*							
54	*	*	*	*	*	*	*	*		*	*		*						
58	*		*	*	*	*	*												
62		*	*		*		*	*	*	*	*	*	*	*	*				
65		*	*				*	*	*	*	*	*	*	*	*				
69	*	*		*		*			*	*	*	*	*	*	*	*			
72		*				*		*	*	*	*	*	*	*	*	*			
82	*	*				*		*	*	*	*	*	*	*	*	*			

4.3.5 Matching abiotic to biotic data

Principal Component Analysis (PCA) of environmental variables (Figure 4.7, Table 4.3) showed that the first principal component (PC1) explained 62.4% of the variation in environmental variables and PC1 and PC2 explained 80.6%. PC1 was a linear combination of mainly temperature, phosphate, nitrate and $\Omega_{calcite}$, with PC1,

nitrate and phosphate being anti-correlated to temperature and $\Omega_{calcite}$ (Figure 4.7, Table 4.3). PC2 was the linear combination of mainly E_{MLD} and pH, with PC2 and pH being anti-correlated to E_{MLD} (Figure 4.7, Table 4.3).

The Subantarctic Zone of both transects was associated with warm, high $\Omega_{calcite}$, and low nutrient conditions. The northern part of the Antarctic Zone on Transect 1 and the Antarctic Zone on Transect 2 were associated with cooler, low $\Omega_{calcite}$, and high nutrient conditions. In particular, the Antarctic Zone of Transect 2 was also associated with high E_{MLD} and low pH. Finally, the Continental Zone and southern part of the Antarctic Zone on Transect 1 were associated with the colder, high nutrient conditions.

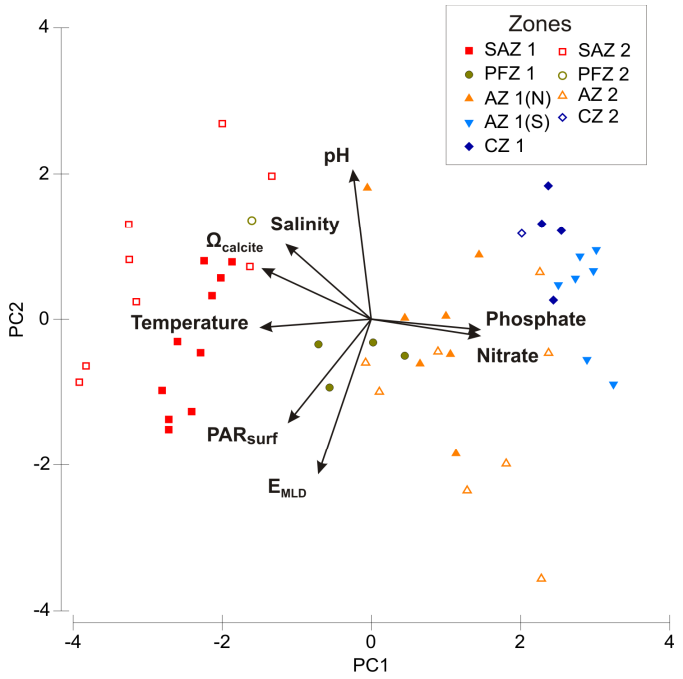

Figure 4.7 PCA plot of environmental variables. Environmental gradients are displayed as arrows pointing in the direction of greatest change. Filled symbols represent samples from the different zones of Transect 1, and empty symbols samples from Transect 2. SAZ = Subantarctic zone, PFZ = Polar Frontal Zone, AZ = Antarctic Zone, CZ = Continental Zone. (N) and (S) denote the northern and southern part of the AZ on Transect 1, as a result of the two branches of the Polar Front.

Table 4.3 Summary of the PCA of environmental data. Eigenvalues and the percentage of variation explained by each principal component (PC) are given. Eigenvectors are coefficients of each variable making up the principal components. The Pearson correlation coefficients between PC scores and environmental variables are given in brackets (values in bold are significant at $p < 0.01$).

	PC1	PC2	PC3	PC4	PC5
Eigenvalues	4.99	1.45	0.839	0.451	0.176
%Variation explained	62.4	18.2	10.5	5.6	2.2
Cum.% Variation	62.4	80.6	91	96.7	98.9
Environmental variables	Eigenvectors				
Temperature	-0.435 **(-0.97)**	-0.032 (-0.04)	0.147 (0.13)	-0.158 (-0.11)	-0.032 (-0.01)
Salinity	-0.334 **(-0.75)**	0.293 (0.35)	0.329 (0.30)	0.639 **(0.43)**	-0.493 (-0.21)
Phosphate	0.427 **(0.95)**	-0.041 (-0.05)	-0.072 (-0.07)	0.378 (0.25)	-0.165 (-0.07)
Nitrate	0.427 **(0.95)**	-0.065 (-0.08)	-0.146 (-0.13)	0.284 (0.19)	-0.073 (-0.03)
pH	-0.072 (-0.16)	0.584 **(0.70)**	-0.751 **(-0.69)**	0.083 (0.06)	0.043 (0.02)
$\Omega_{calcite}$	-0.427 **(-0.95)**	0.198 (0.24)	-0.132 (-0.12)	-0.09 (-0.06)	-0.008 (0.00)
E_{MLD}	-0.206 **(-0.46)**	-0.604 **(-0.73)**	-0.481 **(-0.44)**	-0.067 (-0.05)	-0.589 (-0.25)
$PAR_{surface}$	-0.324 **(-0.72)**	-0.403 **(-0.49)**	-0.176 (-0.16)	0.569 **(0.38)**	0.613 (0.26)

Coccolithophore diversity (species number) was strongly negatively correlated with PC1 (Table 4.5) and so was higher in the Antarctic Zone (warm, high calcite, low nutrients) and lowest in the Continental Zone and southern part of the Antarctic Zone on Transect 1 (Figure 4.8). *E. huxleyi* abundance did not show a clear association with any environmental variables, although it was more abundant in the Polar Frontal Zone on Transect 1, in warmer and higher E_{MLD} conditions (Figure 4.8). *G. muellerae*, *A. quattrospina*, *C. caudatus* and *C. leptoporus* showed preferences for the Subantarctic Zone (Figure 4.8, 4.9) where conditions were warmer. *Wigwamma antarctica* showed a preference for cooler high nutrient waters (Figure 4.8), whereas *Pappomonas* sp. was ubiquitous (Figure 4.9).

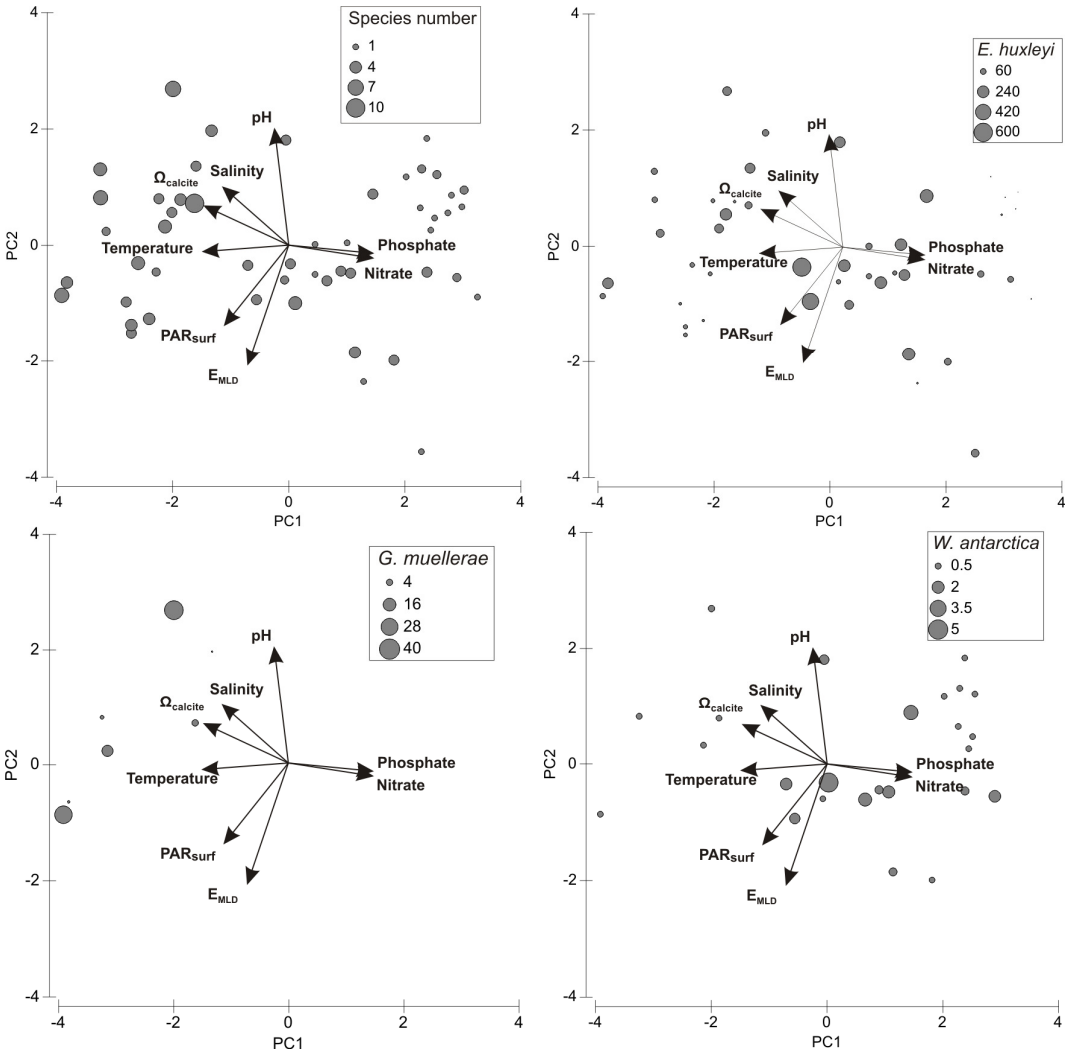

Figure 4.8 PCA plots of environmental variables with superimposed number of species (top left) and abundance (cells mL^{-1}) of *Emiliania huxleyi*, *Gephyrocapsa muellerae* and *Wigwamma antarctica*. Environmental gradients are displayed as arrows pointing in the direction of greatest change.

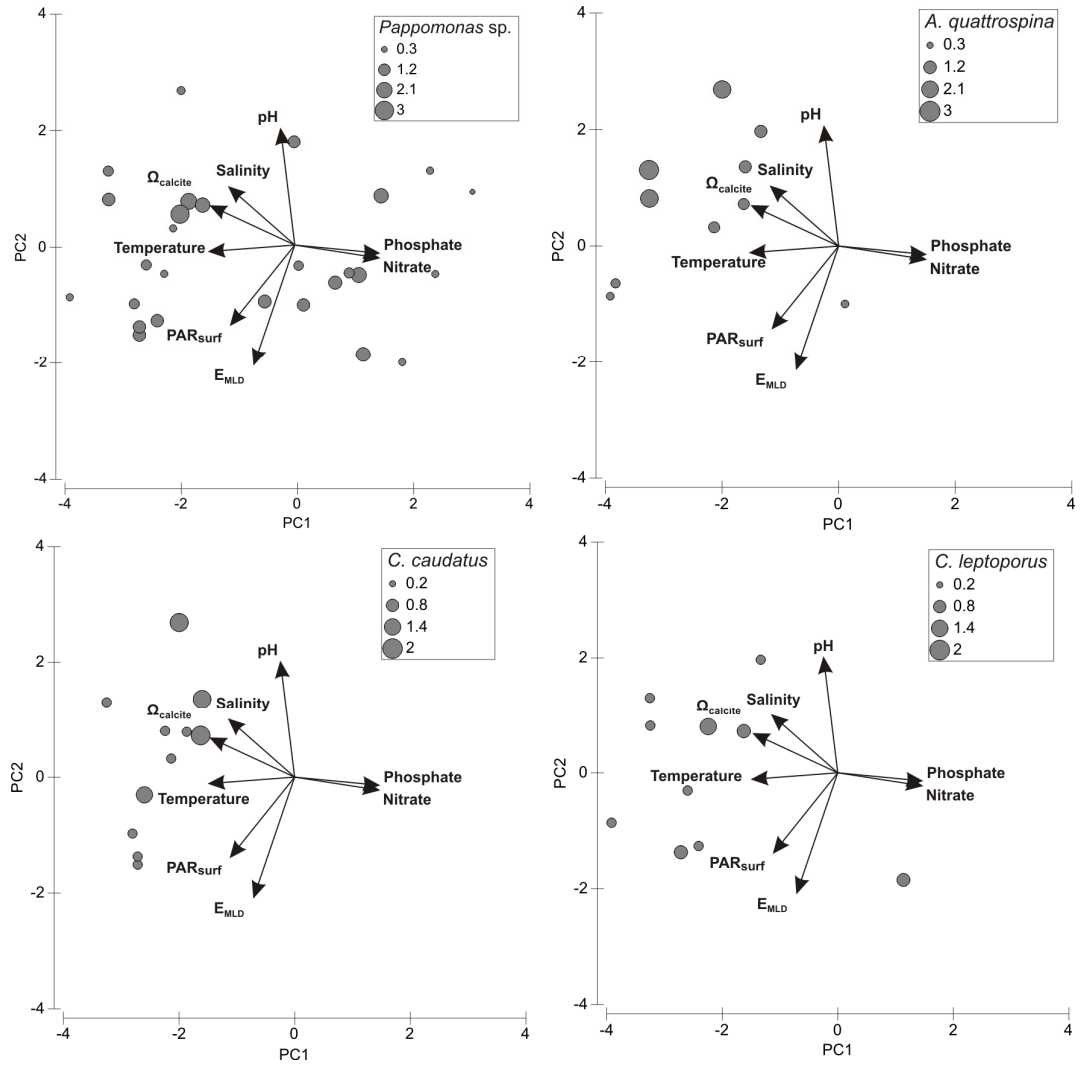

Figure 4.9 PCA plots of environmental variables with superimposed abundance (cells mL^{-1}) of *Pappomonas* sp., *Aqanthoica quattrospina*, *Calciopappus caudatus* and *Calcidiscus leptoporus*. Environmental gradients are displayed as arrows pointing in the direction of greatest change.

The BEST routine showed that a high degree of variation in coccolithophore species distribution and abundance could be explained by a combination of temperature and E_{MLD} ($r_S = 0.393$) (i.e. the variables with the highest correlation with PC1 and PC2, respectively), and the single environmental variable best able to explain this variation was temperature ($r_S = 0.324$), at the 0.1% significance level (Table 4.4).

Spearman's rank correlation showed that coccolith calcite content and coccolith production rates, as well as cell specific and total calcification (cell-CF and total CF) were moderately ($r_s = 0.5 – 0.7$) to strongly ($r_s > 0.7$) negatively correlated with PC1, and hence positively correlated with temperature and $\Omega_{calcite}$, and anti-correlated with phosphate and nitrate concentrations (Table 4.5). Coccolith production rates and cell-CF were also correlated with the light parameters E_{MLD} and $PAR_{above\ surface}$.

Table 4.4 Spearman's Rank correlation of coccolithophore assemblage distribution and environmental variables (values in bold are significant at $p < 0.01$).

Environmental variables	Spearman's Rank correlation
Temperature, E_{MLD}	**0.393**
Temperature	**0.324**
Salinity	-0.054
Phosphate	0.159
Nitrate	0.117
pH	-0.082
$\Omega_{calcite}$	0.197
E_{MLD}	**0.269**
$PAR_{above\ surface}$	0.161

Table 4.5 Spearman's Rank correlations of coccolithophore calcification parameters and environmental variables. Values in bold are significant at $p < 0.05$ and underlined values at $p < 0.01$. SCORES 1 and 2 are the combination of variables for each of the PC1 (temperature, phosphate, nitrate and $\Omega_{calcite}$) and PC2 (E_{MLD} and pH).

	Spearman's Rank correlation				
Environmental variables	Diversity (species number)	Coccolith calcite content	Coccolith production rate	Cell-CF	Total CF
SCORE1	**-0.70**	**-0.57**	**-0.66**	**-0.74**	**-0.64**
SCORE2	0.14	0.07	-0.41	-0.38	-0.18
Temperature	**0.75**	**0.61**	**0.58**	**0.64**	**0.73**
Salinity	**0.64**	0.23	0.18	0.18	**0.57**
Phosphate	**-0.64**	**-0.60**	**-0.72**	**-0.80**	**-0.56**
Nitrate	**-0.63**	**-0.63**	**-0.67**	**-0.75**	**-0.57**
pH	0.06	-0.22	-0.15	-0.16	-0.46
$\Omega_{calcite}$	**0.70**	**0.57**	**0.63**	**0.70**	**0.67**
E_{MLD}	**0.29**	0.10	**0.61**	**0.62**	0.23
$PAR_{above\ surface}$	**0.40**	0.10	**0.49**	**0.50**	0.43

4.4. Discussion

4.4.1 Coccolithophore distribution

In this study, the surface waters of Drake Passage were sampled to assess coccolithophore abundance and species distribution along two latitudinal transects. Total coccolithophore abundance was in agreement with previous observations of maximum abundances between 200 and 500 cells mL^{-1}, in the Atlantic, Pacific, Indian and Australian sectors of the Southern Ocean (Eynaud et al. 1999, Findlay & Giraudeau 2000, Cubillos et al. 2007, Gravalosa et al. 2008, Mohan et al. 2008). A recent study in the Drake Passage, coinciding with the eastern transect (Transect 2), reported similar abundances of up to 600 cells mL^{-1} (Holligan et al. 2010).

Maxima in coccolithophore abundance were associated with oceanic fronts and particularly with the SAF and PF, as was also observed in other studies (Eynaud et al.

1999, Gravalosa et al. 2008, Holligan et al. 2010). It has been suggested that these abundance maxima are related to high productivity due to the dynamics of frontal systems and nutrient availability (Eynaud et al. 1999, Gravalosa et al. 2008). However, iron is the proximate limiting nutrient in the Southern Ocean and iron limitation may be alleviated at fronts due to supply from below.

The southern limit for coccolithophore survival was previously thought to be the Polar Front (PF) (Winter et al. 1999); however low abundances of *E. huxleyi* and other coccolithophores have been recorded well to the south of the PF (Eynaud et al. 1999, Findlay & Giraudeau 2000, Cubillos et al. 2007, Gravalosa et al. 2008, Mohan et al. 2008). These studies suggested that the SACCF was the southern boundary for coccolithophore distribution, at least for *E. huxleyi*. It has also been suggested that temperature controls this distribution, as waters barren of coccolithophores in the Southern Ocean are usually colder than 2ºC (Holligan et al. 2010). In this study, no *E. huxleyi* cells were found south of the SACCF in the surface waters, however detached coccoliths were still present (<20 coccoliths mL^{-1}) and low numbers of this species (<13 cells mL^{-1}) were observed in subsurface waters (>25 m). Moreover, cells of the weakly calcified species *Wigwamma antarctica* were found in very low abundances (1 – 2 cells mL^{-1}) in samples south of the SACCF and the SB. However, the surface water temperature did not drop below 2ºC, even at the most southerly stations. The presence of coccolithophores south of the PF, at temperatures lower than 2ºC, has been attributed to advection within eddies from neighbouring areas (Holligan et al. 2010).

The coccolithophore distribution in the Southern Ocean mainly reflects the distribution of *E. huxleyi* as this is the dominant species both in this and in previous studies in this region. A number of previous studies have reported the succession of *E. huxleyi* morphotypes with latitude in the Southern Ocean, with weakly calcified forms succeeding more heavily calcified ones towards the south in the Australian and Indian sectors (Findlay & Giraudeau 2000, Cubillos et al. 2007, Mohan et al. 2008). In this study only morphotype B/C was observed, from the continental shelves of Chile and the Falkland Islands down to the SACCF. This is not surprising as sea surface temperatures were always <10ºC, conditions which seem to favour dominance of morphotype B/C (Findlay & Giraudeau 2000, Mohan et al. 2008, Holligan et al. 2010). In the Australian sector, morphotype A extends further south and into the Subantarctic Zone (Cubillos et al. 2007). It is possible that type A was transported further south via lateral transport

from the adjacent warmer areas. Moreover, morphotype D coccospheres, also referred to as a malformed or dissolution form of *E. huxleyi* (Findlay & Giraudeau 2000, Cubillos et al. 2007, Mohan et al. 2008), were not observed in this study apart from at one station south of the Falkland Islands (St. 80) where they comprised a high proportion of the *E. huxleyi* assemblage even though both temperature and $\Omega_{calcite}$ were relatively high (8.2ºC and 3.2, respectively). These results suggest that morphotype D cells might not be only associated with the southernmost waters of the Southern Ocean and may not be the direct result of dissolution due to low temperatures or calcite saturation state as has previously been suggested (Findlay & Giraudeau 2000, Mohan et al. 2008).

Coccolithophores other than *E. huxleyi* are scarce in the Southern Ocean, especially polewards of the Subantarctic Zone (Eynaud et al. 1999, Mohan et al. 2008, Holligan et al. 2010). The results of this study are in agreement with this observation, as other species were mainly found only in the Subantarctic and Polar Frontal Zones, at very low densities (<6 cells mL^{-1}). One exception was the species *Gephyrocapsa muellerae*, which was found at moderate abundances (up to 35 cells mL^{-1} and 36% of total abundance) south of the Falklands and close to the SAF. Similar observations by Holligan et al. (2010) in the same area suggest that the occurrence of *G. muellerae* is a characteristic feature of the region south of the Falkland Islands, and is not observed in other sectors of the Southern Ocean. Moreover, *Gephyrocapsa muellerae*, *Acanthoica quattrospina*, *Calciopappus caudatus* and *Calcidiscus leptoporus* were also more abundant south of the Falklands, but were found only occasionally and at lower densities south of Chile. The presence of these species in the warmest (6 – 9°C) and lowest nutrient conditions of both transects, confirms their preference for subpolar regions both in the Southern Ocean (e.g. Eynaud et al. 1999, Findlay & Giraudeau 2000) and in the Northern Hemisphere (e.g. Samtleben et al. 1995, Baumann et al. 2000).

Finally, the weakly calcified species *Pappomonas* sp. and *Wigwamma antarctica* were ubiquitous and the only species recorded in the surface waters of the Continental Zone, albeit at low densities. Species of the family Papposphaeraceae are also characteristic of Arctic waters (Thomsen 1981, and references within) and together with *Wigwamma* spp. they are also characteristic of the Australian Antarctic Zone (Findlay & Giraudeau 2000). There are indications that these polar coccolithophores may be mixotrophic or heterotrophic (Garrison & Thomsen 1993, Marchant & Thomsen 1994),

which could give them an advantage over autotrophic coccolithophores like *E. huxleyi* to survive low light intensities and dark winters in polar waters.

4.4.2 Coccolith size and calcite content

In this study the degree of calcification of *E. huxleyi* morphotype B/C coccoliths was assessed by direct measurements of their distal shield length (DSL), and coccolith calcite content was calculated as a function of volume and a shape dependent constant (k_s) (Young & Ziveri 2000). Even though k_s is subject to errors of ±20%, there are advantages of this method over estimates from regressions between particulate inorganic carbon (PIC) and total coccolith numbers (e.g. Holligan et al. 2010, Poulton et al. 2010): 1) it is species specific, and 2) it is not made less accurate by calcite originating from other material, such as fecal pellets or lithogenic particles. Most importantly, this method reveals spatial patterns in coccolith size and calcite content and allows for more accurate estimates of coccolith production rates, as coccolith calcite values can vary between stations.

The mean distal shield length (DSL) of morphotype B/C detached coccoliths (2.8 μm) was lower than values reported in cultured B/C strains (3.65 μm, Cook et al. 2011), south of Tasmania (3.22 μm, Cook et al. 2011) and on the Patagonian Shelf (3.27 μm, Poulton pers. comm.). However, it was similar to values reported for morphotype C in the Pacific (2.95 μm, Gravalosa et al. 2008) and Australian sectors (2.5 – 3.1 μm, Findlay & Giraudeau 2000) of the Southern Ocean. These two morphotypes of *E. huxleyi* (Type B/C and Type C) are very similar: they both have delicate distal shield elements and a central area that is open or covered with a thin plate (Young et al. 2003). Their only difference seems to be coccolith size, but even this greatly overlaps (B/C: 3 – 4 μm, C: 2.5 – 3.5 μm, Young et al. 2003, C: 1.7 – 4.7 μm, Gravalosa et al. 2008). It is now suggested that morphotype C is not a separate morphotype but is just a small morphotype B/C (J. Young, pers. comm.).

In the present study a spatial pattern was observed where morphotype B/C coccoliths were larger off the Chile shelf (median >3.1 μm) and smaller further south (median <2.9 μm). This can be compared to the north-south trend from overcalcified to weakly calcified *E. huxleyi* morphotypes observed in the Australian and Indian sectors of the Southern Ocean (Findlay & Giraudeau 2000, Cubillos et al. 2007, Mohan et al.

2008), as smaller coccoliths have a lower calcite content. However, a similar trend was not observed south of the Falklands, where DSL was also <2.9 μm, even though the environmental conditions were similar to those off Chile. The slightly lower salinity south of Chile (Figure 4.2) may indicate the presence of a different water mass that favoured the larger coccoliths but not the presence of *Gephyrocapsa muellerae* and other species which were also observed south of the Falklands only. However, Gravalosa et al. (2008) found no trend of DSL with latitude, temperature or salinity in the Pacific sector of the Southern Ocean.

The coccolith calcite content derived from DSL measurements in Drake Passage (mean 0.010 pmol C) is lower than calcite content estimates for the B/C morphotype derived from PIC - total coccolith regression (0.020 pmol C, Holligan et al. 2010) and from DSL measurements (0.014 pmol C, A. Poulton, unpublished data from Patagonian Shelf). Coccolith calcite was between 0.013 – 0.015 pmol C off Chile and ≤0.009 pmol C at the rest of the stations. The wide range of DSL observed within and between different stations (maximum range 1.8 – 4.4 μm), highlights the natural variability found within the same population of *E. huxleyi*.

4.4.3 Calcification and coccolith production rates

This study presents the most southern direct measurements of calcification rates (CF) from ^{14}C uptake. As 97% (88 - 100%) of the surface coccolithophore assemblage at the calcification stations consisted of *E. huxleyi* morphotype B/C, the CF values reported here can be considered as characteristic of this morphotype. Also, the relative influence of rare but high calcite coccolithophore species such as *Acanthoica quattrospina*, *Calcidiscus leptoporus* and *Gephyrocapsa muellerae* is probably small as these only contributed <4% to total coccolithophore abundance at these stations.

Community (total) CF was very low (< 20 μmol C m^{-3} d^{-1}) compared to subarctic regions during both bloom (50 – 1500 μmol C m^{-3} d^{-1}, Fernandez et al. 1993) and non-bloom conditions (100 – 250 μmol C m^{-3} d^{-1}, Lipsen et al. 2007, Poulton et al. 2010). The observed range was very similar to CF measured in the tropics and the oligotrophic subtropical gyres (10 – 50 μmol C m^{-3} d^{-1}, Poulton et al. 2007 and references therein). The CF:PP ratio (0.001 – 0.069) was also similar to subtropical assemblages and much lower than in subarctic regions (0.1 – 0.3, Fernandez et al. 1993; Poulton et al. 2010),

showing that coccolithophores only contributed a small fraction to the total phytoplankton production in Drake Passage.

Cell-CF (0.01 – 0.16 pmol C $cell^{-1}$ d^{-1}) was lower than the estimates of ~0.05 and 0.6 pmol C $cell^{-1}$ d^{-1} at the Patagonian Shelf during December 2008 (Poulton, unpublished). Even though the dominant *E. huxleyi* morphotype was also B/C, Poulton assumed that 50% of the cells (coccospheres) counted were empty, dead or inactive. If all cells were instead assumed to be alive and active, as was assumed also in this study, then the cell-CF rates would be 0.025 – 0.3 pmol C $cell^{-1}$ d^{-1}, much closer to the ones estimated in the present study. Cell-CF was also much lower than in subarctic *E. huxleyi* assemblages (e.g. bloom: 0.72 pmol C $cell^{-1}$ d^{-1}, Fernandez et al. 1993, non-bloom: 0.25 – 0.75 pmol C $cell^{-1}$ d^{-1}, Poulton et al. 2010) and in *E. huxleyi* cultures (0.2 – 0.8 pmol C $cell^{-1}$ d^{-1}, Balch et al. 1996).

These cell-specific rates translate into mean coccolith production rates of 6 (2 – 18) coccoliths d^{-1} or 0.4 (0.1 – 1.2) coccoliths h^{-1} over a 15-h light period, when using the mean coccolith calcite values estimated for morphotype B/C at each station (0.007 – 0.015 pmol C). These are within the range reported for morphotype A in cultures (0 – 3 coccoliths h^{-1}, Balch et al. 1996) and field studies (0.3 – 0.5 coccoliths h^{-1}, Fernandez et al. 1993, 0.4 – 1.8 coccoliths h^{-1}, Poulton et al. 2010). Thus, even though cell-CF rates for morphotype B/C appear to be very low compared to morphotype A, the rate at which coccoliths are produced is fairly similar between the two when coccolith calcite is taken into account. Indeed, the calcite content of the Type A coccoliths in the Iceland Basin was estimated to average 0.033 pmol C (Poulton et al. 2010) which is consistent with higher CF rates.

However, although there is a general similarity in coccolith production rates between northern and southern subpolar environments, between different morphotypes, and between laboratory experiments and field studies, nevertheless the rate appears not to be completely constant. The calculated rates along the two transects (Figure 4.6C) suggest that the environment does impinge on the coccolith production rate across Drake Passage, with a slowing of the coccolith production rate further to the south. It is not known whether the slower rate further to the south, which must delay the time to completion of a complete coccosphere, plays any role in the declining *E. huxleyi* abundance to the south.

In conclusion, *E. huxleyi* morphotype B/C in the Drake Passage produces coccoliths in non-bloom conditions at the same rate as morphotype A in the Northern hemisphere. Cell-CF, however, is much lower and mirrors the low calcite content of the coccoliths produced, resulting in equally low total-CF. Clearly, culturing of this morphotype and extensive laboratory study is essential in order to better understand its role in the Southern Ocean.

4.4.4 Environmental correlations with biotic patterns and parameters

In this study carbonate chemistry parameters (pH and $\Omega_{calcite}$) were used simultaneously with other environmental variables (temperature, salinity, macronutrients and light) to identify relationships with coccolithophore distribution and calcification parameters. Future changes in the ocean (sea surface warming leading to changes in the nutrient and light regimes, ocean acidification) are expected to happen simultaneously. Thus, it is important to consider the effect of these variables on coccolithophores not only in isolation but also to look at how they co-vary in the field and how they relate with natural coccolithophore populations.

The combination of environmental variables best able to explain the coccolithophore species distribution and abundance was temperature and mixed layer irradiance (E_{MLD}) ($r_s = 0.393$). These were also the two variables best correlated with the first and second principal components (PC1 and PC2), respectively, which explained 80% of the variation in environmental data. Coccolithophore diversity in the Drake Passage decreased polewards, in agreement with other studies in the Australian sector of the Southern Ocean and the South Atlantic (Eynaud et al. 1999, Findlay & Giraudeau 2000, Gravalosa et al. 2008). More species were observed in the warmer, lower nutrient waters of the Subantarctic Zone, followed by the cooler, higher nutrient and higher E_{MLD} Antarctic Zone, and the lowest diversity was observed in the coldest, highest nutrient, low E_{MLD} Continental Zone. On the other hand, *E. huxleyi* abundance was higher at the Polar Frontal Zone at relatively warm and high E_{MLD} conditions and decreased with latitude, in contrast with the eurythermal distribution of *E. huxleyi* (Winter et al. 1994), but in agreement with the well-known preference of this species for high light conditions (Paasche 2002, Zondervan 2007).

Mohan et al. (2008) also found that coccolithophore distribution south of Madagascar to Antarctica was controlled by temperature and light, with higher diversity at warmer and higher irradiance conditions, and high abundances of monospecific *E. huxleyi* assemblages corresponding to high nitrate concentrations in the Subantarctic Zone. Similarly, temperature, light availability (upper or lower photic zone) and nutricline depth seem to best explain species distributions in the South Atlantic (Boeckel et al. 2006, Boeckel & Baumann 2008). In the Drake Passage nutrient concentrations were not limiting, whereas E_{MLD} was <3 mol PAR m^{-2} d^{-1} across the Continental Zone and just north of the SAF on Transect 2, a threshold below which light is potentially limiting for Southern Ocean phytoplankton (Venables & Moore 2010). This explains the control of coccolithophore distribution and abundance primarily by temperature and light rather than nutrient concentrations.

Calcification parameters (coccolith calcite content, coccolith production rates, cell-CF and total CF) were negatively correlated with PC1 and so related to the strong latitudinal gradients in environmental variables (Table 4.5). These calcification parameters were higher in warmer, lower nutrient, higher $\Omega_{calcite}$ conditions and decreased towards Antarctica, as the individual correlations show. Additionally, coccolith production rates and cell-CF were positively correlated with E_{MLD} and both of these were higher at stations where both temperature and E_{MLD} were relatively high (mean values of 6.6ºC and 7.4 mol PAR m^{-2} d^{-1}, respectively). The positive correlation of coccolith production rates and cell-CF with E_{MLD} is not surprising as these are strongly light dependent in *E. huxleyi* both in cultures (e.g. Linschooten et al. 1991, Zondervan et al. 2002) and in the field, where both total and cell-CF rates decrease with depth (e.g. Fernandez et al. 1993, Poulton et al. 2010).

However, the correlation of these calcification parameters with phosphate and nitrate is probably the result of strong correlations between nutrients and temperature, as nutrient concentrations were not limiting ($R^2 = 0.89$ and $R^2 = 0.88$, for phosphate and nitrate correlation with temperature, respectively; $n = 50$, $p < 0.01$). The same may be true for $\Omega_{calcite}$. Even though the observed trend of decreasing calcification with decreasing $\Omega_{calcite}$ is in agreement with the negative effects of ocean acidification suggested by various studies (e.g. Riebesell et al. 2000, Zondervan et al. 2001), this variable was also strongly correlated with temperature ($R^2 = 0.86$, $n = 50$, $p < 0.01$). As Cubillos et al. (2007) observed, the succession of heavily to weakly calcified

morphotypes followed the decrease in $\Omega_{calcite}$ but was not caused by it. Unfortunately, in this case, it was not possible to distinguish between the relative influences of these variables (temperature, nutrients and $\Omega_{calcite}$) on coccolithophore dynamics as these were closely coupled.

Even though the approach of this study was quite objective, in that almost all environmental factors thought to affect coccolithophores have been included, there is one important omission and that is iron availability. Given that these variables could only explain some of the variation ($r_s = 0.393$) in coccolithophore species distribution and also their moderate correlation with calcification parameters, it is possible that iron availability might be of greater importance.

The higher chl-*a* values south of the Falklands, despite the equally high macronutrient concentrations south of Chile, point to potential differences in trace metal availability between the two areas. Even though in-situ iron data in the vicinity of the Falklands are sparse, relatively high dissolved iron concentrations have been previously measured at the shelf break east of the Falklands (Bowie et al. 2002). Possible dissolved iron sources may be from resuspended sediments, rivers and glacial discharges, as well as aeolian inputs of dust from the Patagonian deserts (Signorini et al. 2009, and references therein). This might explain the presence of some coccolithophore species in higher densities south of the Falklands. On the other hand, *E. huxleyi* has relatively low iron requirements compared to diatoms and it has been suggested that this is the reason it grows where diatoms are iron-limited (Brand 1991). However, *E. huxleyi* responded to iron enrichment experiments with increased growth rates in the Iceland Basin (Nielsdottir et al. 2009) and increased abundance in the Subarctic Pacific (Crawford et al. 2003), whereas no significant change was observed during the EisenEx experiment in the Southern Ocean (Assmy et al. 2007). Clearly, future coccolithophore research in the Southern Ocean should include iron measurements, in order to account for all possible controlling factors of their distribution.

Finally, biotic controls such as grazing, mortality and competition between coccolithophore species but also with other phytoplankton groups (diatoms in the Southern Ocean) have not been taken into account in the present study. These should also be considered as they could be responsible for short-term dynamics in coccolithophore populations and might be able to explain part of the variability observed.

4.5 Wider implications

Future changes expected in the Southern Ocean include increased sea surface temperatures and stratification, resulting in lower nutrient and higher light conditions (Boyd et al. 2008). However, $\Omega_{calcite}$ is predicted to decrease (Orr et al. 2005). This means that the north-south transects in this study cannot be compared to moving backwards or forwards in time, under global change, because temperature and $\Omega_{calcite}$ rise and fall together along the transects. The results of this study suggest that increased temperature and irradiance conditions will potentially facilitate higher numbers of *E. huxleyi*, causing higher cell and total calcification to extend towards higher latitudes. A poleward migration of this species has already been observed in the Australian sector of the Southern Ocean (Cubillos et al. 2007) and in the Bering Sea (Merico et al. 2003) and Barents Sea (Smyth et al. 2004). Laboratory experiments show that increased CO_2 causes a decrease in *E. huxleyi* calcification under high light conditions (150 µmol photons m^{-2} s^{-1} or 8.6 mol PAR m^{-2} d^{-1} over a 16-h light period), but no sensitivity to CO_2 is observed at low light conditions (<80 µmol photons m^{-2} s^{-1} or 4.6 mol PAR m^{-2} d^{-1} over a 16-h light period) (Zondervan et al. 2002). As E_{MLD} in the Southern Ocean is generally low (mean ~5 mol PAR m^{-2} d^{-1} in this study) and the predicted changes by the year 2100 are not expected to exceed background natural variability (Boyd et al. 2008) it is possible that future ocean acidification will not have an effect on the calcification of *E. huxleyi* in the Southern Ocean. However, the sensitivity of morphotype B/C to ocean acidification and other environmental changes remains to be investigated in laboratory studies.

4.6 Conclusions

In this study, *E. huxleyi* morphotype B/C was found to be the dominant coccolithophore across Drake Passage. A decrease with latitude in coccolith size and calcite content was observed. Coccolith production rates per cell were similar to those of morphotype A in the northern hemisphere. However, total or community calcification was low because of the low calcite content of this morphotype and the low number of cells observed.

Temperature and irradiance were best able to explain variation in coccolithophore distribution and abundance. All calcification parameters were correlated with the strong

latitudinal gradients in temperature, nutrients and calcite saturation state. Additionally, coccolith production rates and cell specific calcification were also correlated with irradiance. However, temperature, nutrients and calcite saturation state were closely coupled and so it was not possible to separate their individual influence on the calcification parameters. The results of this study suggest that future sea surface warming and increased irradiance may result in a poleward advance of *E. huxleyi* and consequently in higher coccolithophore calcification across the Southern Ocean.

Chapter 5: Overall Discussion

The work presented in this thesis aimed to take advantage of latitudinal gradients in carbonate chemistry and other environmental variables (temperature, light, nutrients), in order to provide insights into future coccolithophore responses to ocean acidification and concurrent changes in some of these variables. The individual aims were:

1) To quantify the effect of biotic and abiotic processes on the carbonate chemistry of the North Sea, Norwegian Sea and Svalbard Arctic region.
2) To investigate the distribution of coccolithophore abundance and diversity, and quantify coccolithophore calcification in two high latitude/ polar regions (North Sea – Svalbard and Drake Passage).
3) To try and determine which environmental variables most strongly influence the distribution of coccolithophore abundance, diversity and calcification across these regions.

In this chapter an overarching summary of the three results chapters is presented, including a comparison of the data from the southern and northern hemisphere and the wider implications of the main findings. Finally, the limitations of this study and future directions are discussed.

5.1 Summary

During the ICE-CHASER cruise there were two main processes shaping the carbonate chemistry of the North Sea, the Norwegian Sea and the Svalbard Arctic region: freshwater inputs and primary production. The TA-rich freshwater sources of the Baltic Sea and terrestrial ice melt/ runoff contributed towards high $\Omega_{calcite}$ in the northern North Sea, the Norwegian Sea and in Rijpfjorden. The absence of seasonal stratification caused CO_2 supersaturation and lower $\Omega_{calcite}$ in the southern North Sea, whereas elsewhere along the transect, and especially north of Svalbard, primary production promoted CO_2 undersaturation and higher pH and $\Omega_{calcite}$.

Table 5.1 Summary of coccolithophore distribution between the North Sea and Svalbard and in the Drake Passage. The average abundance (cells mL^{-1}), maximum diversity both as species number (*S*) and Shannon-Wiener diversity index (*H'*), and characteristic species are given for each region. Higher *H'* indicates higher evenness between species abundance.

Region	**Average Abundance**	**Diversity *S* (*H'*)**	**Characteristic species**
Southern/ Central North Sea	High (415)	18 (1.6)	*Emiliania huxleyi* A *Syracosphaera corolla*
Northern North Sea	Moderate (71)	25 (1.7)	*Emiliania huxleyi* A *Syracosphaera corolla* *Acanthoica quattrospina* *Syracosphaera molischii* *Corisphaera gracilis* *Palusphaera vandelii* *Syracosphaera nana*
Norwegian Sea	Low (14)	21 (2.1)	*Emiliania huxleyi* A *Syracosphaera borealis* *Syracosphaera molischii*
Arctic Front	Moderate (111)	20 (0.8)	*Emiliania huxleyi* A *Calciopappus caudatus* *Acanthoica quattrospina*
Svalbard	Low (3)	5 (1.4)	*Pappomonas sp.* *Papposphaera arctica*
<u>*Drake Passage*</u>			
Subantarctic Zone	Moderate (79)	14 (0.8)	*Emiliania huxleyi* B/C *Acanthoica quattrospina* *Gephyrocapsa muellerae* *Pappomonas sp.* *Wigwamma antarctica*
Polar Frontal Zone	High (299)	5 (0.1)	
Antarctic Zone	Moderate (95)	6 (0.7)	*Emiliania huxleyi* B/C *Pappomonas sp.* *Wigwamma antarctica*
Continental Zone	Low (3)	3 (0.7)	

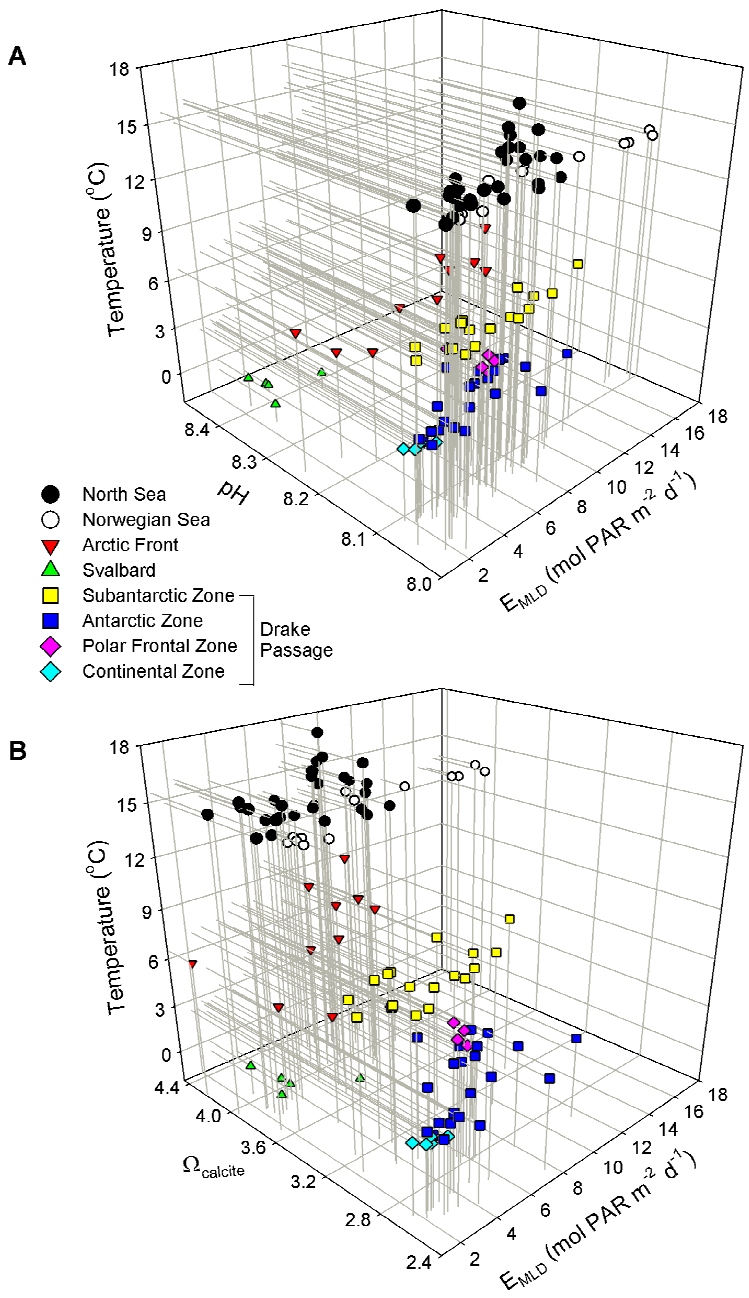

Figure 5.1 Description of the different regions in terms of A) temperature, mixed layer irradiance and pH and B) temperature, mixed layer irradiance and calcite saturation state ($\Omega_{calcite}$)

The high pH, low temperatures and low mixed layer irradiance (E_{MLD}) at Svalbard (Figure 5.1A) were associated with a distinct coccolithophore assemblage of very low abundances dominated by the family Papposphaeraceae (Table 5.1). In the

lower pH, higher temperature North Sea, Norwegian Sea and Arctic influenced waters (Figure 5.1A) variation in E_{MLD} was best able to explain coccolithophore distribution. High coccolithophore diversity was associated with relatively high E_{MLD} in the northern North Sea and southern Norwegian Sea, whereas the high abundance dominated by *Emiliania huxleyi* A in the southern and central North Sea was associated with lower E_{MLD}. However, at a few stations in the Norwegian Sea where E_{MLD} was maximum *E. huxleyi* was the only species contributing to the albeit low abundance. Moreover, even though not revealed through the multivariate analysis, relatively low $\Omega_{calcite}$ in the southern and central North Sea and in the Arctic influenced waters was associated with similar coccolithophore assemblages in these regions (high average coccolithophore abundance, high *Emiliania huxleyi* relative abundance, low diversity and contribution of *Calciopappus caudatus*, *Acanthoica quattrospina* and *Syracosphaera corolla*).

At Drake Passage, the coccolithophore community was dominated by *Emiliania huxleyi* B/C (Table 5.1). Diversity and abundance were highest in the Subantarctic and Polar Frontal Zones, respectively, where temperature and E_{MLD} were high (Table 5.3, Figure 5.1). Moreover, *E. huxleyi* coccolith size was larger off the Chile shelf and lower elsewhere along the two transects. Community and cell specific calcification, as well as coccolith production rates, showed an overall decreasing trend towards Antarctica and were correlated with the strong latitudinal gradients in temperature and $\Omega_{calcite}$ and anti-correlated with nutrient concentrations. Additionally, coccolith production rates and cell specific calcification were also correlated with E_{MLD}.

Coccolithophore calcification rates at Svalbard and at Drake Passage were at the lower end of measurements from other oceanic regions (e.g. Iceland Basin, Arabian Sea, Equatorial Pacific, Subarctic Pacific, Irminger Basin, Patagonian Shelf) and were of similar magnitude to rates from Subtropical assemblages (Figure 5.2). At Svalbard, the low calcification rates were the result of very low coccolithophore abundances of species that have both a low (e.g. Papposphaeraceae) and high (e.g. *Coccolithus pelagicus*) calcite content. At Drake Passage low calcification rates were the result of low to moderate abundances of *E. huxleyi* B/C, which has a low calcite content. The calcification to primary production ratio was also low (<0.01; Figure 5.2) indicating that coccolithophores were contributing little both to the overall productivity of these areas and to export of organic matter.

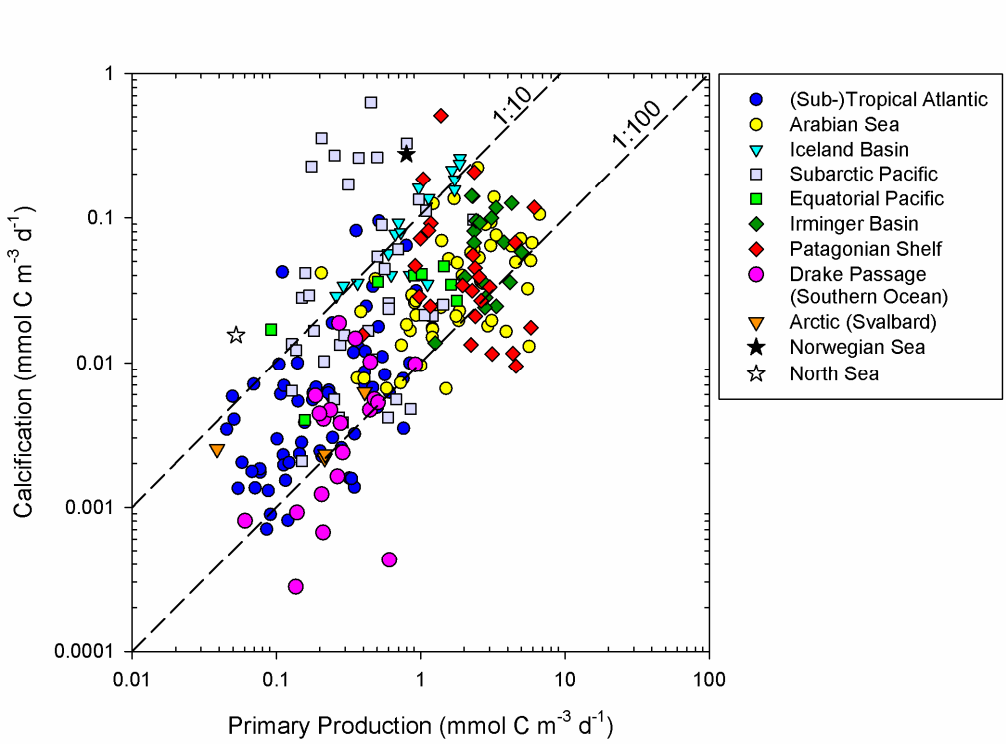

Figure 5.2 The relationship between surface rates of calcification and primary production for the Drake Passage, Arctic, Norwegian Sea and North Sea. Data from other oceanic regions are shown for comparison: Subtropical Atlantic (Poulton et al. 2007), Arabian Sea (Balch et al. 2000), Iceland Basin (Poulton et al. 2010), Subarctic Pacific (Lipsen et al. 2007), Equatorial Pacific (Balch & Kilpatrick 1996), Irminger Basin (Poulton, unpublished), Patagonian Shelf (Poulton et al. in prep.). Adapted from Poulton et al. (2007).

5.2 Comparison of the two study areas

The most striking difference between the North Sea - Svalbard and the Drake Passage coccolithophore assemblages is the observation of two different *E. huxleyi* morphotypes; morphotype A in the northern hemisphere and morphotype B/C in the Southern Ocean (Plate 5.1). The multivariate approach employed in the previous chapters (BEST routine) was repeated to investigate which variables could explain the differences between the northern and southern hemisphere assemblages. This analysis showed that the differences in temperature, $\Omega_{calcite}$ and macronutrient concentrations were best able to explain the differences between the coccolithophore assemblages ($r_S = 0.782$; Table 5.2). Morphotype A was abundant in warm (>10ºC), low nutrient (nitrate <1.5 µM, phosphate 0.4 µM) and high $\Omega_{calcite}$ (3.6 – 4.4) waters, whereas morphotype B/C was abundant in

cooler (<9ºC), high nutrient (nitrate = 16 – 27 µM, phosphate = 1.2 – 1.8 µM), low $\Omega_{calcite}$ (2.5 - 3.2) waters. Similar preferences of the two morphotypes have been observed at the regional level at the Patagonian Shelf (Poulton et al. submitted). In this study, $\Omega_{calcite}$ was the single variable best able to explain these differences ($r_S = 0.717$). This suggests that the low calcite *E. huxleyi* B/C might indeed be a morphotype adapted to the low saturation waters of the Southern Ocean compared to the northern hemisphere. Moreover, a recent photosynthetic pigment study on these two morphotypes suggests differences in their light-harvesting capacity or mechanism, which might be associated with the adaptation of morphotype B/C to iron limitation (Cook et al. 2011).

Table 5.2 Spearman's Rank correlation (BEST routine) of coccolithophore assemblage distribution and environmental variables between all regions. All correlations are significant at $p < 0.01$.

Environmental variable	Spearman's Rank correlation
Temperature, $\Omega_{calcite}$, macronutrients	0.782
$\Omega_{calcite}$	0.717
Nitrate	0.705
Phosphate	0.695
Temperature	0.641
Salinity	0.301
pH	0.186
E_{MLD}	0.165

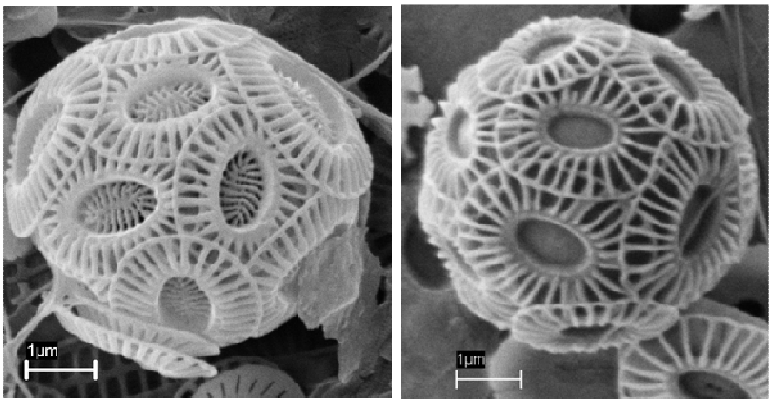

Plate 5.1 *Emiliania huxleyi* from the northern hemisphere (left, morphotype A) and the Southern Ocean (right, morphotype B/C).

Another interesting observation is that species of the family Papposphaeraceae (including the genera *Pappomonas*, *Papposphaera* and *Wigwamma*) were present only in Svalbard in the northern hemisphere transect, whereas they were found across the whole of Drake Passage in the Southern Ocean (Table 5.1). The environmental conditions in these two areas were very different in some regards (Figure 5.1). In Svalbard, temperature was <0ºC, nutrient concentrations were low (both nitrate and phosphate <0.1 μM), pH and $\Omega_{calcite}$ were high (>8.35 and >3.6, respectively) and E_{MLD} was also low (<6 mol PAR m^{-2} d^{-1}). In contrast, in the Drake Passage temperature ranged between 2 and 9ºC, nutrient concentrations were high (nitrate = 16 – 27 μM, phosphate = 1.2 – 1.8 μM), pH and $\Omega_{calcite}$ were low (8.0 – 8.1and 2.5 – 3.2, respectively) and E_{MLD} was also low (mean ~5 mol PAR m^{-2} d^{-1}, range 2 - 12 mol PAR m^{-2} d^{-1}). Epifluorescence microscopy has indicated that the genera of the Papposphaeraceae family possibly lack chloroplasts (Garrison & Thomsen 1993), and feature long haptonemata (Marchant & Thomsen 1994), which suggests that these organisms might be mixotrophic. This would give them an advantage over autotrophic coccolithophores in these two areas in surviving low light intensities and dark winters in polar waters. Moreover, iron limitation in the Southern Ocean would not be as big a problem for mixotrophs as these do not depend entirely on photosynthesis for their energy and they can also acquire iron from their particulate prey. This could potentially explain their wide distribution in the waters of the Drake Passage.

The haploid stage of *Coccolithus pelagicus*, a coccolithophore found in relatively high abundances in Arctic waters (Baumann et al. 2000), is also motile and possibly a mixotroph (Parke & Adams 1960). Thus, it is likely that an alternation between different life stages, that also differ physiologically, might broaden the ecological range of these species and hence help them survive low temperatures and low light conditions at high latitudes. An interesting remark is that the haploid S-cells of *E. huxleyi* are motile too, have two flagella and it is possible that they are also mixotrophic (Paasche 2002), but this hypothesis needs testing. If a similar function to the *C. pelagicus* life cycle is assumed, it is possible that the S-cells might help *E. huxleyi* survive in polar waters. However, not much is known about the distribution of S-cells in nature and it would be interesting to investigate their presence/absence in polar regions. *E. huxleyi* is the main producer of organic compounds called alkenones, which are used as a climatic proxy, and in a Nordic Seas study, coccolith bearing *E. huxleyi* could not be discounted as the biological precursor of alkenones in all water masses (Bendle et al. 2005). This might suggest that

the S-cells or the naked form of this species is indeed present in colder water masses and might be responsible for the production of alkenones in these waters.

5.3 Wider implications

Climate change is already noticeable in the oceans as rising sea surface temperatures (Barnett et al. 2005), which is likely to lead to shallowing of the mixed layer and changes in nutrient and light availability (Bopp et al. 2001, Sarmiento et al. 2004), and also as ocean acidification resulting from rapidly increasing atmospheric CO_2 concentrations (Orr et al. 2005, Bates et al. 2009, Chierici & Fransson 2009). These changes are likely to be most prominent in polar regions. The Arctic is warming up faster than the rest of the world and ice melt becomes more extensive year after year (Polyakov et al. 2010). Moreover, calcite undersaturation has already been observed in the Arctic (Chierici & Fransson 2009). The Southern Ocean is also particularly vulnerable to ocean acidification, and due to the naturally low temperatures and saturation states of this region it is expected to experience aragonite undersaturation of the surface waters by the year 2050, with a calcite undersaturation lag by 50 – 100 years (Orr et al. 2005).

In this context, the results of this study suggest that future climate change might result in a poleward migration of coccolithophore biomes, as has been suggested for the phytoplankton biomes of the marginal ice zones, the subpolar gyres, and the subtropical gyres (Sarmiento et al. 2004). Climate models suggest that the marginal ice zone biomes will contract in both hemispheres, while the subpolar biomes will expand (Sarmiento et al. 2004). An expansion of the subpolar biomes, where *E. huxleyi* is most successful and forms blooms, might suggest increased bloom size and intensity in the future (as has already been observed in the Barents Sea; Smyth et al. 2004) which would enhance export in these areas due to the ballasting effect of calcite, in contrast with the moderate decrease in marine export production some models have predicted for the global ocean (e.g. Bopp et al. 2001). However, the data of Chapter 3 suggest that a poleward migration of subtropical species into the subpolar waters of the Nordic Seas is not evident yet. Comparison of the coccolithophore population observed in the Nordic Seas with studies carried out more than 20 years ago (e.g. Samtleben & Schröder 1992, Samtleben et al. 1995), shows good agreement in terms of species composition and abundance and

absence of low latitude species apart from the occasional presence of two subtropical species (*F. profunda* and *G. oceanica*).

The results of Chapter 2 suggest that Arctic ice melt will have both a direct impact on carbonate chemistry by diluting TA and DIC in the surface waters, and an indirect impact by altering the seasonal pattern in primary production associated with the ice-edge. Ice algae will contribute even less to total primary production as their habitat disappears, whereas pelagic primary production is likely to be facilitated by the absence of ice due to increased light availability (Arrigo et al. 2008). Earlier sea-ice melt and a longer growing season are likely to result in elevated saturation state and pH for a greater proportion of the year. These changes might already be assisting Atlantic species like *Emiliania huxleyi*, which has been blooming with increasing frequency in the Barents Sea (20 years of satellite imagery analysed since 1983 showed a 5-year continuous stretch of blooms between 1999 – 2003; Smyth et al. 2004), to advance further polewards into Arctic waters. Whether these Atlantic species will outcompete weakly calcified Arctic coccolithophore species in the future remains to be determined. Moreover, changing light conditions due to shallower mixed layers (stratification) could also lead to changes in coccolithophore community structure in Subarctic and North Sea assemblages, with a possible increase in species richness, as the results of Chapter 3 suggest.

In the Southern Ocean, increased temperature and irradiance conditions will potentially facilitate higher species richness at higher latitudes and a poleward migration of *E. huxleyi* B/C, as the results of Chapter 4 suggest, a trend that has already been observed in the Australian sector of the Southern Ocean over a few years of sampling (Cubillos et al. 2007). However, $\Omega_{calcite}$ is predicted to decrease (Orr et al. 2005), resulting in conditions opposite to the gradients observed at present in this region. If the future increase in irradiance is not large and the Southern Ocean phytoplankton will still experience overall low light conditions (predicted changes by the year 2100 are not expected to exceed background natural variability; Boyd et al. 2008), it is possible that *E. huxleyi* calcification might not be affected by ocean acidification (lab studies show no sensitivity under low light conditions; Zondervan et al. 2002) and higher calcification may be observed further polewards in the Southern Ocean. This might result in an increased contribution of *E. huxleyi* to export in the Southern Ocean, a region where marine export production is predicted to increase (Bopp et al. 2001). However, the

sensitivity of morphotype B/C to ocean acidification and other environmental changes remains to be investigated in laboratory studies.

Finally, the results presented in this thesis show that calcification rates can change considerably depending on the coccolithophore community composition. In addition to the obvious importance of overall abundance, differences can also stem from species with a high or low calcite content (e.g. *C. pelagicus* vs. Papposharaceae in the Arctic) contributing to the community composition, or from different degrees of calcification of the same species (e.g. *E. huxleyi* A vs *E. huxleyi* B/C, or larger vs. smaller *E. huxleyi* B/C coccoliths in the Southern Ocean). Therefore, it is important to consider the effects of climate change and ocean acidification not only on single coccolithophore species, but on whole communities. Changes in future pelagic calcite production may result from physiological changes acting on single species and/or from shifts in the species composition of coccolithophore assemblages, as well as biome migrations induced by ocean acidification, sea surface warming and stratification.

5.4 Limitations and future directions

This study has employed an observational approach of studying coccolithophore assemblages in their natural environments and taking advantage of the natural variability in carbonate chemistry, temperature, light and nutrients between different regions to investigate how coccolithophores might respond to future changes in the oceans. This has some advantages over laboratory studies that make this approach more realistic; 1) the populations studied are adapted to the in-situ environment, 2) whole community response is investigated, and 3) all factors potentially affecting the *in-situ* populations are taken into account.

However, there are also limitations to this approach. The main weakness of this study was the inability to effectively separate the individual influences of $\Omega_{calcite}$ and nutrient concentrations on the Southern Ocean coccolithophore assemblage, as these were closely coupled with temperature. Future studies should involve a combination of low and high productivity areas (e.g. South Georgia), as the latter tends to cause decoupling between temperature and carbonate chemistry. Another approach would be to study coccolithophores in areas of naturally low/ high $\Omega_{calcite}$, like the Baltic (wintertime calcite undersaturation, summertime supersaturation) and Black Seas (supersaturated

year-round) (Tyrrell et al. 2008). Moreover, it is important to remember that correlation does not necessarily mean causation. Although the approach used is useful to identify possible factors affecting different coccolithophore assemblages and also to determine their relative importance in different regions, it still cannot prove causation which is the advantage of laboratory studies. However, a different approach where diverse coccolithophore populations that have adapted to in-situ conditions are then manipulated to investigate their response to changes in one or more environmental variables would be more beneficial than traditional studies of cultures species or mesocosm experiments. Bioassays are one such type of study and have now started to be used in newly established ocean acidification research programmes (e.g. UK Ocean Acidification Research Programme - UKOARP). However, this approach also has the drawback of dealing with complex ecological interactions and hence the outcomes might not always be clear cut.

The findings presented in this thesis also highlight the need for more laboratory studies on the physiology of a wide range of coccolithophore species. The lack of calcification data for species that can make up a considerable proportion of coccolithophore assemblages hinders our ability to predict the effect of changes in community composition on future pelagic calcite production (or natural variability). Finally, further culturing and research on the physiology and genetic variability of *E. huxleyi* B/C is necessary in order to understand the role of this dominant species in the Southern Ocean and predict the effects of climate change and ocean acidification on the calcite production in this region.

Appendix

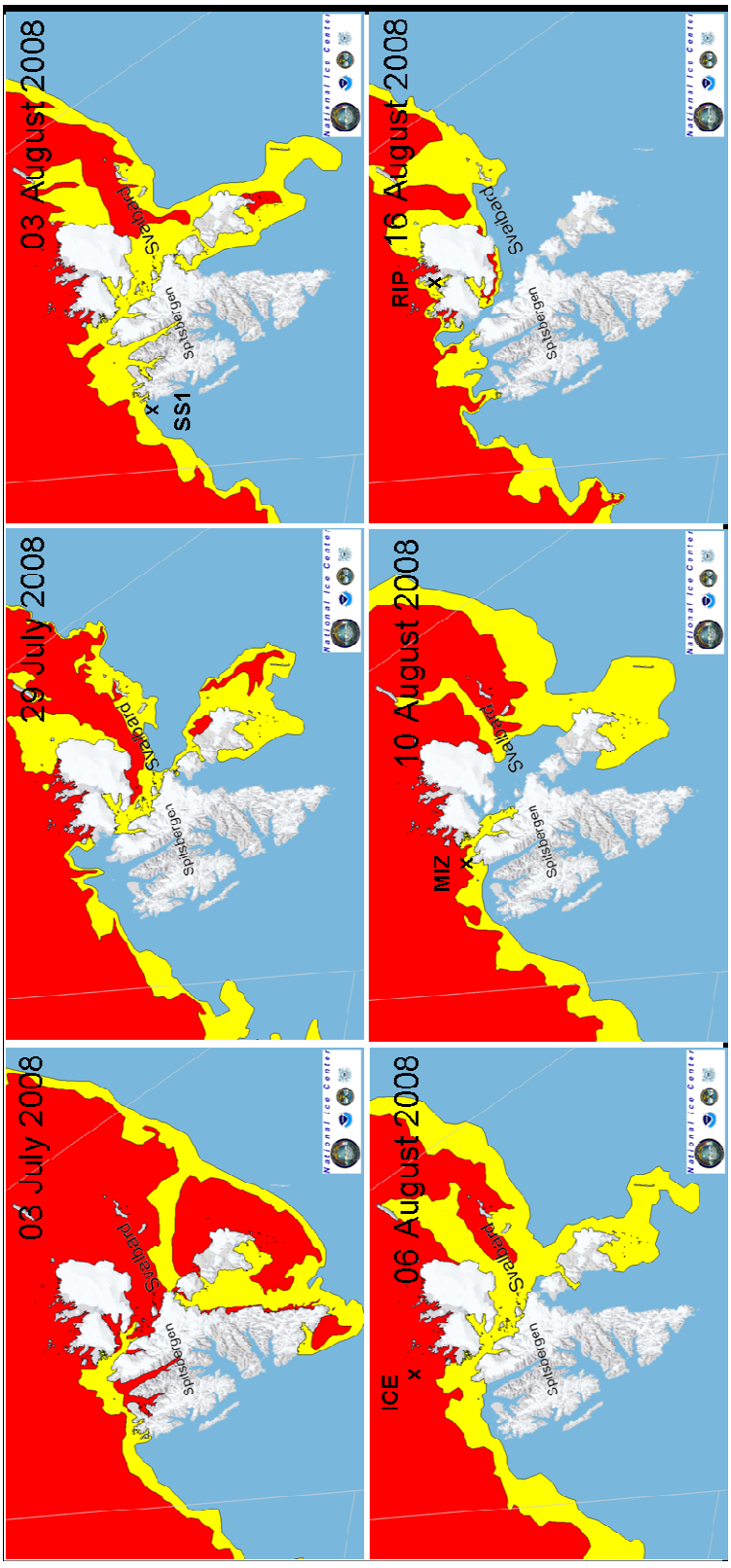

Figure A.1 Ice extent at Svalbard shortly before and during the ICE-CHASER I. The stations SS1, ICE, MIZ and RIP are indicated on the map on the day they were visited. Yellow shading indicates the extent of the marginal ice zone, red indicates 10/10 ice coverage. Maps were obtained from the National Ice Centre of NOAA (http://www.natice.noaa.gov/products/products_on_demand.html).

References

Abramoff MD, Magelhaes PJ, Ram SJ (2004) Image processing with ImageJ. Biophotonics International 11(7):36-42

Anderson LA, Sarmiento JL (1994) Redfield ratios of remineralization determined by nutrient data analysis. Global Biogeochemical Cycles 8(1):65-80

Arrigo KR, van Dijken G, Pabi S (2008) Impact of a shrinking Arctic ice cover on marine primary production. Geophysical Research Letters 35(19), doi:L1960310.1029/2008gl035028

Assmy P, Henjes J, Klaas C, Smetacek V (2007) Mechanisms determining species dominance in a phytoplankton bloom induced by the iron fertilization experiment EisenEx in the Southern Ocean. Deep-Sea Research Part II 54(3):340-362, doi:10.1016/j.dsr.2006.12.005

Azetsu-Scott K, Clarke A, Falkner K, Hamilton J, Jones EP, Lee C, Petrie B, Prinsenberg S, Starr M, Yeats P (2010) Calcium carbonate saturation states in the waters of the Canadian Arctic Archipelago and the Labrador Sea. Journal of Geophysical Research 115(C11021), doi:10.1029/2009jc005917

Bakker D, Jones EM, Riley J (2009) 6. Carbon Parameters. In: Hamersley D, McDonagh E (eds) *Cruise Report No 39, RRS James Cook Cruise JC031, Hydrographic sections of Drake Passage*. National Oceanography Centre, Southampton, p 51-57

Balch WM, Holligan PM, Ackleson SG, Voss KJ (1991) Biological and optical properties of mesoscale coccolithophore blooms in the Gulf of Maine. Limnology and Oceanography 36(4):629-643

Balch WM, Fritz J, Fernandez E (1996) Decoupling of calcification and photosynthesis in the coccolithophore *Emiliania huxleyi* under steady-state light-limited growth. Marine Ecology-Progress Series 142(1-3):87-97

Balch WM, Kilpatrick K (1996) Calcification rates in the equatorial Pacific along 140 degrees W. Deep-Sea Research Part II 43(4-6):971-993

Balch WM, Drapeau DT, Fritz JJ (2000) Monsoonal forcing of calcification in the Arabian Sea. Deep-Sea Research Part II 47(7-8):1301-1337

Barnett TP, Pierce DW, AchutaRao KM, Gleckler PJ, Santer BD, Gregory JM, Washington WM (2005) Penetration of human-induced warming into the world's oceans. Science 309(5732):284-287, doi:10.1126/science.1112418

Bates NR (2006) Air-sea CO_2 fluxes and the continental shelf pump of carbon in the Chukchi Sea adjacent to the Arctic Ocean. Journal of Geophysical Research 111(C10), doi:C1001310.1029/2005jc003083

Bates NR, Mathis JT (2009) The Arctic Ocean marine carbon cycle: evaluation of air-sea CO_2 exchanges, ocean acidification impacts and potential feedbacks. Biogeosciences 6(11):2433-2459

Bates NR, Mathis JT, Cooper LW (2009) Ocean acidification and biologically induced seasonality of carbonate mineral saturation states in the western Arctic Ocean. Journal of Geophysical Research 114(C11), doi:10.1029/2008jc004862

Baumann K, Andruleit H, Schröeder-Ritzrau A, Samtleben C (1997) Spatial and temporal dynamics of coccolithophore communities during low production in the Norwegian-Greenland Sea. In: Hass H, Kaminski M (eds) *Contributions to the micropaleontology and paleoceanography of the northern North Atlantic*. Grzybowski Foundation Special Publication, Krakow, p 227-243

Baumann KH, Andruleit HA, Samtleben C (2000) Coccolithophores in the Nordic Seas: comparison of living communities with surface sediment assemblages. Deep-Sea Research Part II 47(9-11):1743-1772

Beaufort L, Heussner S (1999) Coccolithophorids on the continental slope of the Bay of Biscay - production, transport and contribution to mass fluxes. Deep-Sea Research Part II 46(10):2147-2174

Beaufort L, Couapel M, Buchet N, Claustre H, Goyet C (2008) Calcite production by coccolithophores in the south east Pacific Ocean. Biogeosciences 5(4):1101-1117

Bendle J, Rosell-Mele A, Ziveri P (2005) Variability of unusual distributions of alkenones in the surface waters of the Nordic seas. Paleoceanography 20(2), doi:10.1029/2004pa001025

Boeckel B, Baumann KH, Henrich R, Kinkel H (2006) Coccolith distribution patterns in South Atlantic and Southern Ocean surface sediments in relation to environmental gradients. Deep-Sea Research Part I 53(6):1073-1099, doi:10.1016/j.dsr.2005.11.006

Boeckel B, Baumann KH (2008) Vertical and lateral variations in coccolithophore community structure across the subtropical frontal zone in the South Atlantic Ocean. Marine Micropaleontology 67(3-4):255-273, doi:10.1016/j.marmicro.2008.01.014

Bopp L, Monfray P, Aumont O, Dufresne JL, Le Treut H, Madec G, Terray L, Orr JC (2001) Potential impact of climate change on marine export production. Global Biogeochemical Cycles 15(1):81-99

Borges AV, Frankignoulle M (2002) Distribution and air-water exchange of carbon dioxide in the Scheldt plume off the Belgian coast. Biogeochemistry 59(1-2):41-67

Borges AV, Frankignoulle M (2003) Distribution of surface carbon dioxide and air-sea exchange in the English Channel and adjacent areas. Journal of Geophysical Research 108(C5), doi:10.1029/2000jc000571

Bowie AR, Whitworth DJ, Achterberg EP, Mantoura RFC, Worsfold PJ (2002) Biogeochemistry of Fe and other trace elements (Al, Co, Ni) in the upper Atlantic Ocean. Deep-Sea Research Part I 49(4):605-636

Boyce DG, Lewis MR, Worm B (2010) Global phytoplankton decline over the past century. Nature 466(7306):591-596, doi:10.1038/nature09268

Boyd PW, Doney SC, Strzepek R, Dusenberry J, Lindsay K, Fung I (2008) Climate-mediated changes to mixed-layer properties in the Southern Ocean: assessing the phytoplankton response. Biogeosciences 5(3):847-864

Boyd PW, Strzepek R, Fu FX, Hutchins DA (2010) Environmental control of open-ocean phytoplankton groups: Now and in the future. Limnology and Oceanography 55(3):1353-1376, doi:10.4319/lo.2010.55.3.1353

Bozec Y, Thomas H, Elkalay K, de Baar HJW (2005) The continental shelf pump for CO_2 in the North Sea - evidence from summer observation. Marine Chemistry 93(2-4):131-147, doi:10.1016/j.marchem.2004.07.006

Bozec Y, Thomas H, Schiettecatte LS, Borges AV, Elkalay K, de Baar HJW (2006) Assessment of the processes controlling seasonal variations of dissolved inorganic carbon in the North Sea. Limnology and Oceanography 51(6):2746-2762

Braarud T, Gaarder K, Grontved J (1953) The phytoplankton of the North Sea and adjacent waters in May 1948. Journal du Conseil International pour l'Exploration de la Mer 113:1-87

Brand L (1994) Physiological ecology of marine coccolithophores. In: Winter A, Siesser W (eds) *Coccolithophores*. Cambridge University Press, Cambridge, p 39-49

Brand LE (1991) Minimum iron requirements of marine phytoplankton and the implications for the biogeochemical control of new production. Limnology and Oceanography 36(8):1756-1771

Broecker W, Clark E (2009) Ratio of coccolith $CaCO_3$ to foraminifera $CaCO_3$ in late Holocene deep sea sediments. Paleoceanography 24, doi:10.1029/2009pa001731

Buitenhuis E, vanBleijswijk J, Bakker D, Veldhuis M (1996) Trends in inorganic and organic carbon in a bloom of *Emiliania huxleyi* in the North Sea. Marine Ecology-Progress Series 143(1-3):271-282

Burkill PH, Archer SD, Robinson C, Nightingale PD, Groom SB, Tarran GA, Zubkov MV (2002) Dimethyl sulphide biogeochemistry within a coccolithophore bloom (DISCO): an overview. Deep-Sea Research Part II 49(15):2863-2885

Caldeira K, Wickett ME (2003) Anthropogenic carbon and ocean pH. Nature 425(6956):365-365, doi:10.1038/425365a

Caldeira K, Wickett ME (2005) Ocean model predictions of chemistry changes from carbon dioxide emissions to the atmosphere and ocean. Journal of Geophysical Research 110(C9), doi:10.1029/2004jc002671

Charalampopoulou A, Poulton AJ, Tyrrell T, Lucas MI (2011) Irradiance and pH affect coccolithophore community composition on a transect between the North Sea and the Arctic Ocean. Marine Ecology Progress Series 431:25-43

Chierici M, Fransson A (2009) Calcium carbonate saturation in the surface water of the Arctic Ocean: undersaturation in freshwater influenced shelves. Biogeosciences 6(11):2421-2431

Clarke KR (1993) Non-parametric multivariate analyses of changes in community structure. Australian Journal of Ecology 18:117-143

Clarke KR, Gorley RN (2006) PRIMER v6: user manual/tutorial. PRIMER-E, Plymouth

Cook SS, Whittock L, Wright SW, Hallegraeff G (2011) Photosynthetic pigment and genetic differences between two Southern Ocean morphotypes of *Emiliania*

huxleyi (Haptophyta). Journal of Phycology 47(3):615-626, doi:10.1111/j.1529-8817.2011.00992.x

Cooper LW, McClelland JW, Holmes RM, Raymond PA, Gibson JJ, Guay CK, Peterson BJ (2008) Flow-weighted values of runoff tracers (delta /sup 18/O, DOC, Ba, alkalinity) from the six largest Arctic rivers. Geophysical Research Letters 35(18), doi:10.1029/2008gl035007

Cortés MY, Bollmann J, Thierstein HR (2001) Coccolithophore ecology at the HOT station ALOHA, Hawaii. Deep-Sea Research Part II 48(8-9):1957-1981

Crawford DW, Lipsen MS, Purdie DA, Lohan MC, Statham PJ, Whitney FA, Putland JN, Johnson WK, Sutherland N, Peterson TD, Harrison PJ, Wong CS (2003) Influence of zinc and iron enrichments on phytoplankton growth in the northeastern subarctic Pacific. Limnology and Oceanography 48(4):1583-1600

Cubillos JC, Wright SW, Nash G, de Salas MF, Griffiths B, Tilbrook B, Poisson A, Hallegraeff GM (2007) Calcification morphotypes of the coccolithophorid *Emiliania huxleyi* in the Southern Ocean: changes in 2001 to 2006 compared to historical data. Marine Ecology-Progress Series 348:47-54, doi:10.3354/meps07058

Dallmann WK, Ohta Y, Elvevold S, Blomeier DE (2002) Bedrock map of Svalbard and Jan Mayen. In: Dallmann WK, Ohta Y, Elvevold S, Blomeier D (eds), Norsk Polarinstitutt Temakart No.33

Delille B, Harlay J, Zondervan I, Jacquet S, Chou L, Wollast R, Bellerby RGJ, Frankignoulle M, Borges AV, Riebesell U, Gattuso JP (2005) Response of primary production and calcification to changes of pCO_2 during experimental blooms of the coccolithophorid *Emiliania huxleyi*. Global Biogeochemical Cycles 19(2), doi:10.1029/2004gb002318

Dickson AG (1981) An exact definition of total alkalinity and a procedure for the estimation of alkalinity and total inorganic carbon from titration data. Deep-Sea Research 28:609-623

Dickson AG, Millero FJ (1987) A comparison of the equilibrium-constants for the dissociation of carbonic-acid in seawater media. Deep-Sea Research I 34(10):1733-1743

Dickson AG, Sabine CL, Christian JR (2007) Guide to best practices for ocean CO_2 measurements. PICES Special Publication 3, p 191

Dieckmann GS, Nehrke G, Papadimitriou S, Gottlicher J, Steininger R, Kennedy H, Wolf-Gladrow D, Thomas DN (2008) Calcium carbonate as ikaite crystals in Antarctic sea ice. Geophysical Research Letters 35(8), doi:10.1029/2008gl033540

Doney SC, Fabry VJ, Feely RA, Kleypas JA (2009) Ocean Acidification: The Other CO_2 Problem. Annual Review of Marine Science 1:169-192, doi:10.1146/annurev.marine.010908.163834

Dong S, Sprintall J, Gille ST, Talley L (2008) Southern Ocean mixed-layer depth from Argo float profiles. Journal of Geophysical Research 113(C6), doi:10.1029/2006jc004051

Engel A, Zondervan I, Aerts K, Beaufort L, Benthien A, Chou L, Delille B, Gattuso JP, Harlay J, Heemann C, Hoffmann L, Jacquet S, Nejstgaard J, Pizay MD, Rochelle-Newall E, Schneider U, Terbrueggen A, Riebesell U (2005) Testing the direct effect of CO_2 concentration on a bloom of the coccolithophorid *Emiliania huxleyi* in mesocosm experiments. Limnology and Oceanography 50(2):493-507

Eynaud F, Giraudeau J, Pichon JJ, Pudsey CJ (1999) Sea-surface distribution of coccolithophores, diatoms, silicoflagellates and dinoflagellates in the South Atlantic Ocean during the late austral summer 1995. Deep-Sea Research Part I 46(3):451-482

Fabry VJ, Seibel BA, Feely RA, Orr JC (2008) Impacts of ocean acidification on marine fauna and ecosystem processes. Ices Journal of Marine Science 65(3):414-432, doi:10.1093/icesjms/fsn048

Feely RA, Sabine CL, Lee K, Berelson W, Kleypas J, Fabry VJ, Millero FJ (2004) Impact of anthropogenic CO_2 on the $CaCO_3$ system in the oceans. Science 305(5682):362-366

Feng Y, Warner ME, Zhang Y, Sun J, Fu FX, Rose JM, Hutchins DA (2008) Interactive effects of increased pCO_2, temperature and irradiance on the marine coccolithophore *Emiliania huxleyi* (Prymnesiophyceae). European Journal of Phycology 43(1):87-98

Fernandez E, Boyd P, Holligan PM, Harbour DS (1993) Production of organic and inorganic carbon within a large-scale coccolithophore bloom in the northeast Atlantic Ocean. Marine Ecology-Progress Series 97(3):271-285

Findlay CS, Giraudeau J (2000) Extant calcareous nannoplankton in the Australian Sector of the Southern Ocean (austral summers 1994 and 1995). Marine Micropaleontology 40(4):417-439

Findlay HS, Calosi P, Crawfurd K (2011) Determinants of the PIC:POC response in the coccolithophore *Emiliania huxleyi* under future ocean acidification scenarios. Limnology and Oceanography 56(3):1168-1178, doi:10.4319/lo.2011.56.3.1168

Fowler J, Cohen L, Jarvis P (1998) Practical statistic for field biology. John WIley & Sons Ltd., Chichester, England, p 257

Frankignoulle M, Borges AV (2001) European continental shelf as a significant sink for atmospheric carbon dioxide. Global Biogeochemical Cycles 15(3):569-576

Fransson A, Chierici M, Nojiri Y (2009) New insights into the spatial variability of the surface water carbon dioxide in varying sea ice conditions in the Arctic Ocean. Continental Shelf Research 29(10):1317-1328, doi:10.1016/j.csr.2009.03.008

Friis K, Kortzinger A, Wallace DWR (2003) The salinity normalization of marine inorganic carbon chemistry data. Geophysical Research Letters 30(2), doi:10.1029/2002gl015898

Garrison D, Thomsen H (1993) Ecology and biology of ice biota. Berichte Zur Polarforschung 121:68-74

Gravalosa JM, Flores JA, Sierro FJ, Gersonde R (2008) Sea surface distribution of coccolithophores in the eastern Pacific sector of the Southern Ocean (Bellingshausen and Amundsen Seas) during the late austral summer of 2001. Marine Micropaleontology 69(1):16-25, doi:10.1016/j.marmicro.2007.11.006

Gypens N, Lancelot C, Borges AV (2004) Carbon dynamics and CO_2 air-sea exchanges in the eutrophied coastal waters of the Southern Bight of the North Sea: a modelling study. Biogeosciences 1(2):147-157

Gypens N, Borges AV, Lancelot C (2009) Effect of eutrophication on air-sea CO_2 fluxes in the coastal Southern North Sea: a model study of the past 50 years. Global Change Biology 15(4):1040-1056, doi:10.1111/j.1365-2486.2008.01773.x

Haidar AT, Thierstein HR (2001) Coccolithophore dynamics off Bermuda (N. Atlantic). Deep-Sea Research Part II 48(8-9):1925-1956

Harland WB (1997) The Geology of Svalbard. The Geological Society, London, p 529

Hegseth EN (1992) Sub-ice algal assemblages of the Barents sea: species composition, chemical composition, and growth rates. Polar Biology 12(5):485-496

Hegseth EN (1998) Primary production of the northern Barents Sea. Polar Research 17(2):113-123

Hegseth EN, Sundfjord A (2008) Intrusion and blooming of Atlantic phytoplankton species in the high Arctic. Journal of Marine Systems 74(1-2):108-119, doi:10.1016/j.jmarsys.2007.11.011

Heimdal BR (1983) Phytoplankton and nutrients in the waters northwest of Spitsbergen in the autumn of 1979. Journal of Plankton Research 5(6):901-918

Hjalmarsson S, Wesslander K, Anderson LG, Omstedt A, Perttila M, Mintrop L (2008) Distribution, long-term development and mass balance calculation of total alkalinity in the Baltic Sea. Continental Shelf Research 28(4-5):593-601, doi:10.1016/j.csr.2007.11.010

Holligan PM, Fernandez E, Aiken J, Balch WM, Boyd P, Burkill PH, Finch M, Groom SB, Malin G, Muller K, Purdie DA, Robinson C, Trees CC, Turner SM, Vanderwal P (1993a) A biogeochemical study of the coccolithophore, *Emiliania huxleyi*, in the North Atlantic. Global Biogeochemical Cycles 7(4):879-900

Holligan PM, Groom S, Harbour DS (1993b) What controls the distribution of the coccolithophore, *Emiliania huxleyi,* in the North Sea? Fisheries Oceanography 2:175-183

Holligan PM, Charalampopoulou A, Hutson R (2010) Seasonal distributions of the coccolithophore, *Emiliania huxleyi*, and of particulate inorganic carbon in surface waters of the Scotia Sea. Journal of Marine Systems 82(4):195-205, doi:10.1016/j.jmarsys.2010.05.007

Houdan A, Probert I, Zatylny C, Veron B, Billard C (2006) Ecology of oceanic coccolithophores. I. Nutritional preferences of the two stages in the life cycle of *Coccolithus braarudii* and *Calcidiscus leptoporus*. Aquatic Microbial Ecology 44(3):291-301

Houghton SD (1991) Coccolith sedimentation and transport in the North Sea. Marine Geology 99(1-2):267-274

Iglesias-Rodriguez MD, Halloran PR, Rickaby REM, Hall IR, Colmenero-Hidalgo E, Gittins JR, Green DRH, Tyrrell T, Gibbs SJ, von Dassow P, Rehm E, Armbrust EV, Boessenkool KP (2008) Phytoplankton calcification in a high-CO_2 world. Science 320(5874):336-340, doi:10.1126/science.1154122

IPCC (2007) Climate Change 2007: The Physical Science Basis. Contribution of Working Group I to the Fourth Assessment Report of the Intergovernmental Panel on Climate Change, Cambridge University Press, Cambridge, UK

Johnson KM, Williams PJL, Brändström L, Sieburth JM (1987) Coulometric total carbon dioxide analysis for marine studies: automatization and calibration. Marine Chemistry 21:117-133

Jones EM, Bakker DCE, Venables HJ, Whitehouse MJ, Korb RE, Watson AJ (2010) Rapid changes in surface water carbonate chemistry during Antarctic sea ice melt. Tellus Series B-Chemical and Physical Meteorology 62(5):621-635, doi:10.1111/j.1600-0889.2010.00496.x

Kempe S, Pegler K (1991) Sinks and sources of CO_2 in coastal seas - The North Sea. Tellus Series B-Chemical and Physical Meteorology 43(2):224-235

Kinkel H, Baumann KH, Cepek M (2000) Coccolithophores in the equatorial Atlantic Ocean: response to seasonal and Late Quaternary surface water variability. Marine Micropaleontology 39(1-4):87-112

Kirk JTO (1983) Light and photosynthesis in aquatic ecosystems. Cambridge University Press, Cambridge, p 401 pp

Kirkwood D (1996) Nutrients: Practical notes on their determination in seawater. ICES Techniques in marine environmental sciences, International Council for the Exploration of the Sea, Copenhagen

Klaas C, Archer DE (2002) Association of sinking organic matter with various types of mineral ballast in the deep sea: Implications for the rain ratio. Global Biogeochemical Cycles 16(4), doi:10.1029/2001gb001765

Langdon C, Takahashi T, Sweeney C, Chipman D, Goddard J, Marubini F, Aceves H, Barnett H, Atkinson MJ (2000) Effect of calcium carbonate saturation state on the calcification rate of an experimental coral reef. Global Biogeochemical Cycles 14(2):639-654, doi:10.1029/1999gb001195

Langer G, Geisen M, Baumann KH, Klas J, Riebesell U, Thoms S, Young JR (2006) Species-specific responses of calcifying algae to changing seawater carbonate chemistry. Geochemistry Geophysics Geosystems 7(9), doi:10.1029/2005gc001227

Langer G, Nehrke G, Probert I, Ly J, Ziveri P (2009) Strain-specific responses of *Emiliania huxleyi* to changing seawater carbonate chemistry. Biogeosciences 6(11):2637-2646

Leakey RJG (2008) Oceans 2025 Arctic Cruise Report. ICE CHASER, RRS James Clark Ross, 23 July to 21 August 2008, Natural Environment Research Council

Levitus S, Antonov JI, Boyer TP, Stephens C (2000) Warming of the world ocean. Science 287(5461):2225-2229

Linschooten C, Vanbleijswijk JDL, Vanemburg PR, Devrind JPM, Kempers ES, Westbroek P, Devrinddejong EW (1991) Role of the light-dark cycle and medium composition on the production of coccoliths by *Emiliania huxleyi* (Haptophyceae). Journal of Phycology 27(1):82-86

Lipsen MS, Crawford DW, Gower J, Harrison PJ (2007) Spatial and temporal variability in coccolithophore abundance and production of PIC and POC in the NE subarctic Pacific during El Nino (1998), La Nina (1999) and 2000. Progress in Oceanography 75(2):304-325, doi:10.1016/j.pocean.2007.08.004

Mackinder L, Wheeler G, Schroeder D, Riebesell U, Brownlee C (2010) Molecular mechanisms underlying calcification in coccolithophores. Geomicrobiology Journal 27(6-7):585-595, doi:10.1080/01490451003703014

Manton I, Sutherland J, McCully M (1976a) Fine-structural observations on coccolithophorids from South Alaska in the genera *Papposphaera* Tangen and *Pappomonas* Manton and Oates. British Phycological Journal 11:225-238

Manton I, Sutherland J, Oates K (1976b) Arctic coccolithophorids - two species of *Turrisphaera* gen-nov from West Greenland, Alaska, and Northwest Passage. Proceedings of the Royal Society of London Series B-Biological Sciences 194(1115):179-194

Manton I, Sutherland J, Oates K (1977) Arctic coccolithophorids: *Wigwamma arctica* gen et sp. nov. from Greenland and Arctic Canada, *Wigwamma annulifera* sp. nov. from South Africa and S Alaska and *Calciarcus alaskensis* gen. et sp. nov. from S Alaska. Proceedings of the Royal Society of London Series B-Biological Sciences 197(1127):145-168

Marañón E, González N (1997) Primary production, calcification and macromolecular synthesis in a bloom of the coccolithophore *Emiliania huxleyi* in the North Sea. Marine Ecology-Progress Series 157:61-77

Marchant H, Thomsen H (1994) Haptophytes in polar waters. In: Green J, Leadbeater B (eds) *The Haptophyte Algae Systematics Association Special* Vol 51. Oxford University Press, Oxford, p 209-228

Mathis JT, Cross JN, Bates NR (2011) Coupling primary production and terrestrial runoff to ocean acidification and carbonate mineral suppression in the eastern Bering Sea. Journal of Geophysical Research 116(C02030), doi:10.1029/2010jc006453

Mehrbach C, Culberso C, Hawley J, Pytkowic R (1973) Measurement of apparent dissociation-constants of carbonic-acid in seawater at atmospheric-pressure. Limnology and Oceanography 18(6):897-907

Merico A, Tyrrell T, Brown CW, Groom SB, Miller PI (2003) Analysis of satellite imagery for *Emiliania huxleyi* blooms in the Bering Sea before 1997. Geophysical Research Letters 30(6), doi:10.1029/2002gl016648

Merico A, Tyrrell T, Lessard EJ, Oguz T, Stabeno PJ, Zeeman SI, Whitledge TE (2004) Modelling phytoplankton succession on the Bering Sea shelf: role of climate influences and trophic interactions in generating *Emiliania huxleyi* blooms 1997-2000. Deep-Sea Research Part II 51(12):1803-1826, doi:10.1016/j.dsr.2004.07.003

Merico A, Tyrrell T, Cokacar T (2006) Is there any relationship between phytoplankton seasonal dynamics and the carbonate system? Journal of Marine Systems 59(1-2):120-142, doi:10.1016/j.jmarsys.2005.11.004

Milliman JD (1993) Production and accumulation of calcium carbonate in the ocean: budget of a non-steady state. Global Biogeochemical Cycles 7(4):927-957

Mohan R, Mergulhao LP, Guptha MVS, Rajakurnar A, Thamban M, AnilKurnar N, Sudhakar M, Ravindra R (2008) Ecology of coccolithophores in the Indian sector of the Southern Ocean. Marine Micropaleontology 67(1-2):30-45, doi:10.1016/j.marmicro.2007.08.005

Monterey G, Levitus S (1997) Seasonal variability of mixed layer depth for the world ocean. NOAA Atlas, NESDIS 14, Washington D.C.

Nielsdottir MC, Moore CM, Sanders R, Hinz DJ, Achterberg EP (2009) Iron limitation of the postbloom phytoplankton communities in the Iceland Basin. Global Biogeochemical Cycles 23, doi:10.1029/2008gb003410

Olsson K, Anderson LG (1997) Input and biogeochemical transformation of dissolved carbon in the Siberian shelf seas. Continental Shelf Research 17(7):819-833

Orr JC, Fabry VJ, Aumont O, Bopp L, Doney SC, Feely RA, Gnanadesikan A, Gruber N, Ishida A, Joos F, Key RM, Lindsay K, Maier-Reimer E, Matear R, Monfray P, Mouchet A, Najjar RG, Plattner GK, Rodgers KB, Sabine CL, Sarmiento JL, Schlitzer R, Slater RD, Totterdell IJ, Weirig MF, Yamanaka Y, Yool A (2005) Anthropogenic ocean acidification over the twenty-first century and its impact on calcifying organisms. Nature 437(7059):681-686, doi:10.1038/nature04095

Orsi AH, Whitworth T, Nowlin WD (1995) On the meridional extent and fronts of the Antarctic Circumpolar Current. Deep-Sea Research Part I 42(5):641-673

Paasche E, Brubak S (1994) Enhanced calcification in the coccolithophorid *Emiliania huxleyi* (Haptophyceae) under phosphorus limitation. Phycologia 33(5):324-330

Paasche E, Brubak S, Skattebol S, Young JR, Green JC (1996) Growth and calcification in the coccolithophorid *Emiliania huxleyi* (Haptophyceae) at low salinities. Phycologia 35(5):394-403

Paasche E (1998) Roles of nitrogen and phosphorus in coccolith formation in *Emiliania huxleyi* (Prymnesiophyceae). European Journal of Phycology 33(1):33-42

Paasche E (2002) A review of the coccolithophorid *Emiliania huxleyi* (Prymnesiophyceae), with particular reference to growth, coccolith formation, and calcification-photosynthesis interactions. Phycologia 40(6):503-529

Parke M, Adams I (1960) The motile (*Crystallolithus hyalinus* Gaarder & Markali) and non-motile phases in the life history of *Coccolithus pelagicus* (Wallich) Schiller. Journal of the Marine Biological Association of the United Kingdom 39(02):263-274, doi:doi:10.1017/S002531540001331X

Pierrot DE, Lewis E, Wallace DWR (2006) MS Excel Program Developed for CO2 System Calculations. ORNL/CDIAC-105a. Carbon Dioxide Information Analysis Centre, Oak Ridge National Laboratory, U.S. Department of Energy, Oak Ridge, Tennessee.

Polyakov IV, Timokhov LA, Alexeev VA, Bacon S, Dmitrenko IA, Fortier L, Frolov IE, Gascard JC, Hansen E, Ivanov VV, Laxon S, Mauritzen C, Perovich D, Shimada K, Simmons HL, Sokolov VT, Steele M, Toolen J (2010) Arctic Ocean warming contributes to reduced polar ice cap. Journal of Physical Oceanography 40(12):2743-2756, doi:10.1175/2010jpo4339.1

Poulton AJ, Adey TR, Balch WM, Holligan PM (2007) Relating coccolithophore calcification rates to phytoplankton community dynamics: Regional differences and implications for carbon export. Deep-Sea Research Part II 54(5-7):538-557, doi:10.1016/j.dsr2.2006.12.003

Poulton AJ, Charalampopoulou A, Young JR, Tarran GA, Lucas MI, Quartly GD (2010) Coccolithophore dynamics in non-bloom conditions during late summer in the central Iceland Basin (July-August 2007). Limnology and Oceanography 55(4):1601-1613, doi:10.4319/lo.2010.55.4.1601

Purdie DA, Finch MS (1994) Impact of a coccolithophorid bloom on dissolved carbon dioxide in seawater enclosures in a Norwegian fjord. Sarsia 79(4):379-387

Raitsos DE, Lavender SJ, Pradhan Y, Tyrrell T, Reid PC, Edwards M (2006) Coccolithophore bloom size variation in response to the regional environment of the subarctic North Atlantic. Limnology and Oceanography 51(5):2122-2130

Rickaby REM, Henderiks J, Young JN (2010) Perturbing phytoplankton: response and isotopic fractionation with changing carbonate chemistry in two coccolithophore species. Climate of the Past 6(6):771-785, doi:10.5194/cp-6-771-2010

Riebesell U, Zondervan I, Rost B, Tortell PD, Zeebe RE, Morel FMM (2000) Reduced calcification of marine plankton in response to increased atmospheric CO_2. Nature 407(6802):364-367

Riegman R, Stolte W, Noordeloos AAM, Slezak D (2000) Nutrient uptake, and alkaline phosphate (EC 3:1:3:1) activity of *Emiliania huxleyi* (Prymnesiophyceae) during growth under N and P limitation in continuous cultures. Journal of Phycology 36(1):87-96

Robinson C, Williams PJL (1992) Development and assessment of an analytical system for the accurate and continual measurement of total dissolved inorganic carbon. Marine Chemistry 34:157-175

Rochford PA, Kara AB, Wallcraft AJ, Arnone RA (2001) Importance of solar subsurface heating in ocean general circulation models. Journal of Geophysical Research-Oceans 106(C12):30923-30938

Rysgaard S, Glud RN, Sejr MK, Bendtsen J, Christensen PB (2007) Inorganic carbon transport during sea ice growth and decay: A carbon pump in polar seas. Journal of Geophysical Research 112(C3), doi:10.1029/2006jc003572

Rysgaard S, Bendtsen J, Pedersen LT, Ramlov H, Glud RN (2009) Increased CO_2 uptake due to sea ice growth and decay in the Nordic Seas. Journal of Geophysical Research 114(C9), doi:10.1029/2008jc005088

Samtleben C, Schröder A (1992) Living coccolithophore communities in the Norwegian - Greenland Sea and their record in sediments. Marine Micropaleontology 19(4):333-354

Samtleben C, Schafer P, Andruleit H, Baumann A, Baumann KH, Kohly A, Matthiessen J, Schroderritzrau A (1995) Plankton in the Norwegian - Greenland Sea: from living communities to sediment assemblages - an actualistic approach. Geologische Rundschau 84(1):108-136

Sarmiento JL, Slater R, Barber R, Bopp L, Doney SC, Hirst AC, Kleypas J, Matear R, Mikolajewicz U, Monfray P, Soldatov V, Spall SA, Stouffer R (2004) Response of ocean ecosystems to climate warming. Global Biogeochemical Cycles 18(3), doi:10.1029/2003gb002134

Schei B (1975) Coccolithophorid distribution and ecology in the coastal waters of North Norway. Nordic Journal of Botany 22:217-225

Sciandra A, Harlay J, Lefevre D, Lemee R, Rimmelin P, Denis M, Gattuso JP (2003) Response of coccolithophorid *Emiliania huxleyi* to elevated partial pressure of CO_2 under nitrogen limitation. Marine Ecology-Progress Series 261:111-122

Shi D, Xu Y, Morel FMM (2009) Effects of the pH/pCO_2 control method on medium chemistry and phytoplankton growth. Biogeosciences 6(7):1199-1207

Signorini SR, Garcia VMT, Piola AR, Evangelista H, McClain CR, Garcia CAE, Mata MM (2009) Further studies on the physical and biogeochemical causes for large interannual changes in the Patagonian Shelf spring–summer phytoplankton bloom biomass, NASA/TM-2009-214176

Smyth TJ, Tyrrell T, Tarrant B (2004) Time series of coccolithophore activity in the Barents Sea, from twenty years of satellite imagery. Geophysical Research Letters 31(11), doi:10.1029/2004gl019735

Steinacher M, Joos F, Frolicher TL, Plattner GK, Doney SC (2009) Imminent ocean acidification in the Arctic projected with the NCAR global coupled carbon cycle-climate model. Biogeosciences 6(4):515-533

Stroeve J, Holland MM, Meier W, Scambos T, Serreze M (2007) Arctic sea ice decline: Faster than forecast. Geophysical Research Letters 34(9):5, doi:10.1029/2007gl029703

Sun C, Watts DR (2001) A circumpolar gravest empirical mode for the Southern Ocean hydrography. Journal of Geophysical Research 106(C2):2833-2855

Swift JH (1986) The Arctic waters. In: BG H (ed) *The Nordic Seas*. Springer, New York

Taylor J, R (1982) An introduction to error analysis. University Science Books, Sausalito, California, p 327

Thomas H, Bozec Y, Elkalay K, de Baar HJW (2004) Enhanced open ocean storage of CO_2 from shelf sea pumping. Science 304(5673):1005-1008

Thomas H, Bozec Y, de Baar HJW, Elkalay K, Frankignoulle M, Schiettecatte LS, Kattner G, Borges AV (2005a) The carbon budget of the North Sea. Biogeosciences 2(1):87-96

Thomas H, Bozec Y, Elkalay K, de Baar HJW, Borges AV, Schiettecatte LS (2005b) Controls of the surface water partial pressure of CO_2 in the North Sea. Biogeosciences 2(4):323-334

Thomsen HA (1981) Identification by electron-microscopy of nanoplanktonic coccolithophorids (Prymnesiophyceae) from West Greenland, including the description of *Papposphaera sarion* sp. nov. British Phycological Journal 16(1):77-94

Thomsen HA, Ostergaard JB, Hansen LE (1991) Heteromorphic life histories in Arctic coccolithophorids (Prymnesiophyceae). Journal of Phycology 27(5):634-642

Tyrrell T, Merico A (2004) *Emiliania huxleyi*: bloom observations and the conditions that induce them. In: Thierstein HR, Young JR (eds) *Coccolithophores: from Molecular Processes to Global Impact*, p 75-97

Tyrrell T, Schneider B, Charalampopoulou A, Riebesell U (2008) Coccolithophores and calcite saturation state in the Baltic and Black Seas. Biogeosciences 5(2):485-494

Van Bleijswijk J, Van der Wal P, Kempers R, Veldhuis M, Young J, Muyzer G, de Vrind-de Jong E, Westbroek P (1991) Distribution of two types of *Emiliania huxleyi* (Prymnesiophyceae) in the Northeast Atlantic region as determined by immunofluorescence and coccolith morphology. Journal of Phycology 27:566 - 570

Van der Wal P, Kempers RS, Veldhuis MJW (1995) Production and downward flux of organic matter and calcite in a North Sea bloom of the coccolithophore *Emiliania huxleyi*. Marine Ecology Progress Series 126(1-3):247-265

Van Lenning K, Probert I, Latasa M, Estrada M, Young JR (2004) Pigment diversity of coccolithophores in relation to taxonomy, phylogeny and ecological preferences. In: Thierstein HR, Young JR (eds) *Coccolithophores: From Molecular Processes to Global Impact*. Springer, Berlin, p 51-73

Venables H, Moore CM (2010) Phytoplankton and light limitation in the Southern Ocean: Learning from high-nutrient, high-chlorophyll areas. Journal of Geophysical Research 115, doi:10.1029/2009jc005361

Welschmeyer NA (1994) Fluorometric analysis of chlorophyll-*a* in the presence of chlorophyll-*b* and pheopigments. Limnology and Oceanography 39(8):1985-1992

Whitworth T (1980) Zonation and geostrophic flow of the Antarctic Circumpolar Current at Drake Passage. Deep-Sea Research 21:497-507

Winter A, Jordan R, Roth P (1994) Biogeography of living coccolithophores in ocean waters. In: Winter A, Siesser W (eds) *Coccolithophores*. Cambridge University Press, Cambridge, p 161-177

Winter A, Elbrachter M, Krause G (1999) Subtropical coccolithophores in the Weddell Sea. Deep-Sea Research Part I 46(3):439-449

Young JR, Ziveri P (2000) Calculation of coccolith volume and its use in calibration of carbonate flux estimates. Deep-Sea Research Part II 47(9-11):1679-1700

Young JR, Geisen M, Cros L, Kleijne A, Sprengel C, Probert I, Østergaard J (2003) A guide to extant coccolithophore taxonomy. Journal of Nannoplankton Research 1(Special Issue):1-132

Zeebe RE, Wolf-Gladrow D (2001) CO_2 in seawater: Equilibrium, kinetics, isotopes Elsevier, Amsterdam, p 346

Zeebe RE, Zachos JC, Caldeira K, Tyrrell T (2008) Oceans - Carbon emissions and acidification. Science 321(5885):51-52, doi:10.1126/science.1159124

Zondervan I, Zeebe RE, Rost B, Riebesell U (2001) Decreasing marine biogenic calcification: A negative feedback on rising atmospheric pCO_2. Global Biogeochemical Cycles 15(2):507-516

Zondervan I, Rost B, Riebesell U (2002) Effect of CO_2 concentration on the PIC/POC ratio in the coccolithophore *Emiliania huxleyi* grown under light-limiting conditions and different daylengths. Journal of Experimental Marine Biology and Ecology 272(1):55-70

Zondervan I (2007) The effects of light, macronutrients, trace metals and CO_2 on the production of calcium carbonate and organic carbon in coccolithophores - A review. Deep-Sea Research Part II 54(5-7):521-537, doi:10.1016/j.dsr2.2006.12.004